

Harvard-Smithsonian Center 1
60 Garden Street, MS 78, Cambridge
Telephone 617 495 7294, FAX 6

Email: jzhao@cfa.harvar

P. Ho
C. Masson
K. Menthen
M. Reid
E. S. Verburg

To: SMA Project
From: Jun-Hui Zhao
Subject: Technical Memorandum no. 77
Date: December 31, 1993

SMA Synthesis Beams of Tangential versus Concentric Configurations

1. Introduction

Previous designs of the Submillimeter Array were based on concentric configurations consisting of a four fold of triangular configuration with a scaling factor of 2.65. Each configuration of 6 antennas represents a triangular polygon of rotation which gives an aperture synthesis array providing uniform uv coverage (Keto 1993). Recently, the STAG committee pointed out that without losing image quality, tangential configurations of 6 antennas could have advantages of closer to the control building and therefore easy for operations. In addition, it is likely that the SMA will be expanded from 6 antennas to more antennas; the immediate expansion of the SMA without a further contract will be to 8 antennas, and therefore, a comprehensive design of configuration for optimal uv coverage is needed considering 2 additional antennas. There are a few designs suggested recently. In this memo, I will show numerical simulations of the synthesis beams produced from these proposed configurations. A quantitative comparison between these designs in terms of image quality can be made by measuring the shape of beam and both maximum and r.m.s. of beam sidelobes. In this memo, A, B, C and D are referred to as each triangular configuration from large to small scale.

2. Simulations

A setup of beam simulations has been discussed in details in SMA Technical Memo no. 76. In this memo, I show the simulations of synthesis beam using two declinations of

-29° (close to the Galactic center) and 45° (a typical declination in the northern sky). The observing frequency of 230 GHz is assumed.

Case 1: an original SMA design with a four fold of concentric configuration (each configuration has 6 pads). There are a total of 15 hybrid configurations of 8 antennas on 2 adjacent concentric configurations, where the inner configuration (D) is fully loaded and the other 2 antennas are on the next larger configuration (C). Figs. 1-1, 1-2, ...1-29,1-30 show layout of configuration, uv-tracks, and synthesis beam. Table 1 gives major and minor sizes of FWHP beam, position angle and both maximum and rms of beam sidelobes. The distribution of uv points is not circularly uniform. The typical maximum of beam sidelobes is in a range of 10% to 15% for a source at $\delta = 45^\circ$ and 19% to 33% at $\delta = -29^\circ$. The typical r.m.s. is 2% at $\delta = 45^\circ$ and 3% at $\delta = -29^\circ$.

Case 2: tangential configurations where 2 adjacent configurations share 2 common pads. Simulations of synthesis beam are made for a total of 6 hybrid configurations of 6 antennas loaded on the D configuration and 2 on the C configuration. The layout of configuration, uv-tracks and synthesis beam are presented in Figs. 2. Relevant parameters are given in Table 2. The configurations of 8 antennas are not optimal and the distribution of uv points is far from circular uniform. The typical maximum of beam sidelobes is in a range of 15% to 19% for a source at $\delta = 45^\circ$ and 22% to 26% at $\delta = -29^\circ$. The typical r.m.s. is 2% at $\delta = 45^\circ$ and 3% at $\delta = -29^\circ$.

Case 3: tangential configurations suggested by Keto (1994). A draft of Keto's desgin is shown in Fig. 3. The configurations are optimized not only for 6 antennas but also for 8. In a case of 6 antennas, there is a common pad shared by each configuration of different scale so that 21 pads are needed to fill out the four configurations. In a case of 8 antennas, 2 additional pads are added into each triangular configuration and one of the two pads can be shared by two adjacent configurations. The baseline between the two new antennas is east-west. A total of 26 pads are required for the four configurations of 8 antennas. The uv coverage obtained from the D-configuration of 8 antennas appears nearly uniform and the amplitude of sidelobes is greatly reduced. The maximum of sidelobes becomes 9% in the D-configuration at $\delta = 45^\circ$, and 18% at a low declination ($\delta = -29^\circ$) (see Table 3).

Case 4: tangential configurations suggested by Masson (1994) based on Keto's triangular polygon (see Fig. 5). There are a few differences between *Case 3* and *Case 4*: 1) in a case of 6 antennas, *Case 4* allows sharing two common pads in two adjacent configurations so

that only needs 18 antennas to fill out the 4 configurations; a total of 26 pads are needed for configurations of 6 antennas. 2) The orientation of the baseline between two additional pads in a case of 8 antennas is off from east-west; The position angle of this baseline is -30° in the D configuration and -60° in the C-configuration. Simulations for both the D and C configurations are shown in Fig. 6. The beam parameters are given in Table 4. There appears to be no significant difference in terms of the beam quality between *Case 3* and *Case 4* in the C configuration at $\delta = 45^\circ$ and $\delta = -29^\circ$, and in the D configuration at $\delta = 45^\circ$. In the D configuration at $\delta = -29^\circ$, the maximum beam-sidelobe in *Case 4* tends to be 9% greater than that in *Case 3*.

Case 5: a combination of the uv points obtained in two adjacent configurations of 6 antennas (for example D and C). Combining visibility data obtained from configurations of different scale is very useful technique to image complex of source structure. A good design needs avoiding baseline redundancy between configurations of different scale as the redundant baselines give no direct contributions to image quality. Avoiding redundancy becomes particularly important at the time when only a few antennas are available. In addition, an apparent trade-off for sharing more pads between configurations of different scale is use of more redundant baselines. Keto's design for 6 antennas (See *Case 3*) avoids redundancy of baselines requiring total 21 pads while Masson's design saves 3 pads but gives unavoidable redundancy (for example 3 pairs of redundant baselines when combining the C and D configurations). Synthesis beams are calculated by combining the C and D configurations for both Keto and Masson's designs. The parameters of the synthesis beam are given in Table 5. A quantitative comparison between the two designs can be made. The maximum sidelobe of the beams in Masson's design appears 14% greater than that in Keto's design at $\delta = 45^\circ$ while 7% greater at $\delta = -29^\circ$.

3. Summary

Based on the simulations of synthesis beams discussed above, it has been shown that Keto's design for tangential configurations provides a nearly uniform uv coverage and substantially reduces amplitudes of beam-sidelobes. In addition, in Keto's design for 6 antennas, there is no baseline redundancy when combining the configurations of different scale. Redundancy of baselines can significantly enhance beam-sidelobe level and may reduce the quality of synthesis image.

Table 1: Synthesis Beams of Concentric Configurations (*Case 1*)
with Natural Weighting

$\nu = 230 \text{ GHz}$ Configuration	Decl	Bmaj	Bmin	Bpa	Beam parameters	Sidelobes
					Max	Rms
D+7+8	+45°	6."9	6."3	-70°.4	14.9%	2.0%
	-29	9.4	5.1	-5.2	32.9	3.2
D+7+9	+45	9.2	5.8	-80.5	12.2	2.1
	-29	6.7	6.6	-44.7	23.3	3.3
D+7+10	+45	8.5	6.0	-64.7	11.7	2.0
	-29	5.8	5.0	-36.0	23.8	3.2
D+7+11	+45	7.4	6.4	-83.6	14.9	2.0
	-29	9.4	5.5	-3.5	32.8	3.2
D+7+12	+45	8.0	5.4	+84.6	11.8	2.1
	-29	7.1	6.2	+21.7	22.6	3.2
D+8+9	+45	7.7	5.8	+84.8	10.9	2.1
	-29	8.3	5.6	+4.7	25.6	3.2
D+8+10	+45	6.6	5.7	-65.2	12.4	2.0
	-29	7.6	4.8	-14.2	22.8	3.1
D+8+11	+45	5.8	5.7	+44.4	15.2	2.0
	-29	9.2	4.6	+10.7	33.0	3.1
D+8+12	+45	7.0	5.4	+67.3	11.3	2.0
	-29	6.3	4.7	+24.2	25.1	3.1
D+9+10	+45	9.0	5.6	-81.0	10.4	2.1
	-29	8.6	8.4	-47.2	19.0	3.2
D+9+11	+45	8.8	6.0	+75.7	15.2	2.1
	-29	7.0	6.2	+33.2	25.5	3.2
D+9+12	+45	9.7	5.1	+78.9	11.3	2.1
	-29	9.5	6.9	+59.4	20.0	3.3
D+10+11	+45	7.7	5.6	-83.1	13.4	2.0
	-29	7.3	5.9	-16.9	25.2	3.2
D+10+12	+45	8.1	4.8	-88.6	11.1	2.0
	-29	6.9	6.0	-77.7	19.8	3.2
D+11+12	+45	8.5	5.7	+73.2	12.6	2.1
	-29	6.1	5.6	+37.5	25.9	3.2

Table 2: Synthesis Beams of Tangential Configurations (*Case 2*)
with Natural Weighting

$\nu = 230 \text{ GHz}$ Configuration	Decl	Beam parameters			Sidelobes	
		Bmaj	Bmin	Bpa	Max	Rms
D+9+10	+45°	5."3	5."1	-13°.6	18.7%	2.1%
	-29	9.4	3.6	-2.0	26.4	3.1
D+9+11	+45	6.0	4.8	+69.7	17.2	2.1
	-29	6.5	4.5	+15.5	24.5	3.0
D+9+12	+45	6.6	4.3	+85.3	13.9	2.1
	-29	5.6	5.3	+10.4	21.9	3.0
D+10+11	+45	5.5	4.4	+63.8	17.4	2.1
	-29	5.8	3.4	+16.9	23.8	3.0
D+10+12	+45	5.9	3.9	+77.7	14.5	2.1
	-29	5.4	3.9	+12.2	23.0	3.0
D+11+12	+45	7.4	4.0	+72.6	14.8	2.1
	-29	8.4	7.0	+49.0	21.6	3.0

Table 3: Synthesis Beams of Tangential Configurations (*Case 3*)
with Natural Weighting, Optimized for 8 Antennas (E. Keto)

$\nu = 230 \text{ GHz}$ Configuration	Decl	Bmaj	Bmin	Bpa	Max	Sidelobes Rms
D8	+45°	8.''6	7.''3	-89°3	9.1%	2.0%
	-29	10	6.9	-2.4	16.6	3.0
C8	+45°	3.6	3.0	83.8	10.7	2.4
	-29	4.3	2.7	3.1	21.0	3.9

Table 4: Synthesis Beams of Tangential Configuration (*Case 4*)
with Natural Weighting (C. Masson)

$\nu = 230 \text{ GHz}$ Configuration	Decl	Bmaj	Bmin	Bpa	Max	Sidelobes Rms
D8	+45°	9.''2	7.''6	81°0	9.1%	2.0%
	-29	11	6.9	5.1	18.2	3.1
C8	+45	4.2	2.8	82.6	10.8	2.5
	-29	3.5	3.2	28.0	20.8	3.9

Table 5: Comparison between Keto and Masson's Designs
for Tangential Configurations of 6 Antennas

$\nu = 230 \text{ GHz}$ Configuration	Decl	Bmaj	Bmin	Bpa	Max	Sidelobes Rms
D6+C6(Keto)	+45°	6.''3	4.''2	89°0	10.3%	2.2%
	-29	5.9	4.7	2.6	16.1	3.5
D6+C6(Masson)	+45	6.3	4.2	89.9	11.9	2.2
	-29	5.9	4.7	-2.2	17.3	3.6

Figure Caption

Fig. 1: A total of 15 concentric configurations of 8 antennas where the D configuration is fully loaded and the other 2 antennas are on the C configurations. Simulations of synthesis beams obtained from these configurations are made for the two declinations of $\delta = 45^\circ$ and $\delta = -29^\circ$. Left panel: uv-tracks; top-right panel: layout of configurations; bottom-right panel: contours of synthesis beam.

Fig. 2: A total of 6 tangential configurations, where 2 adjacent triangular configurations shared 2 common pads. Simulations of synthesis beams of these configurations are made for the two declinations of $\delta = 45^\circ$ and $\delta = -29^\circ$. Left panel: uv-tracks; top-right panel: layout of configurations; bottom-right panel: contours of synthesis beam.

Fig. 3: A layout of tangential configurations suggested by Keto.

Fig. 4: Simulations of synthesis beams obtained from the D and C configurations based on Keto's design. Calculations are made for the two declinations of $\delta = 45^\circ$ and $\delta = -29^\circ$. Left panel: uv-tracks; top-right panel: layout of configurations; bottom-right panel: contours of synthesis beam.

Fig. 5: A layout of tangential configurations suggested by Masson.

Fig. 6: Simulations of synthesis beams obtained from the D and C configurations based on Masson's design. Calculations are made for the two declinations of $\delta = 45^\circ$ and $\delta = -29^\circ$. Left panel: uv-tracks; top-right panel: layout of configurations; bottom-right panel: contours of synthesis beam.

$\delta = 45^\circ$

UvTrack: csma78dp45.uv

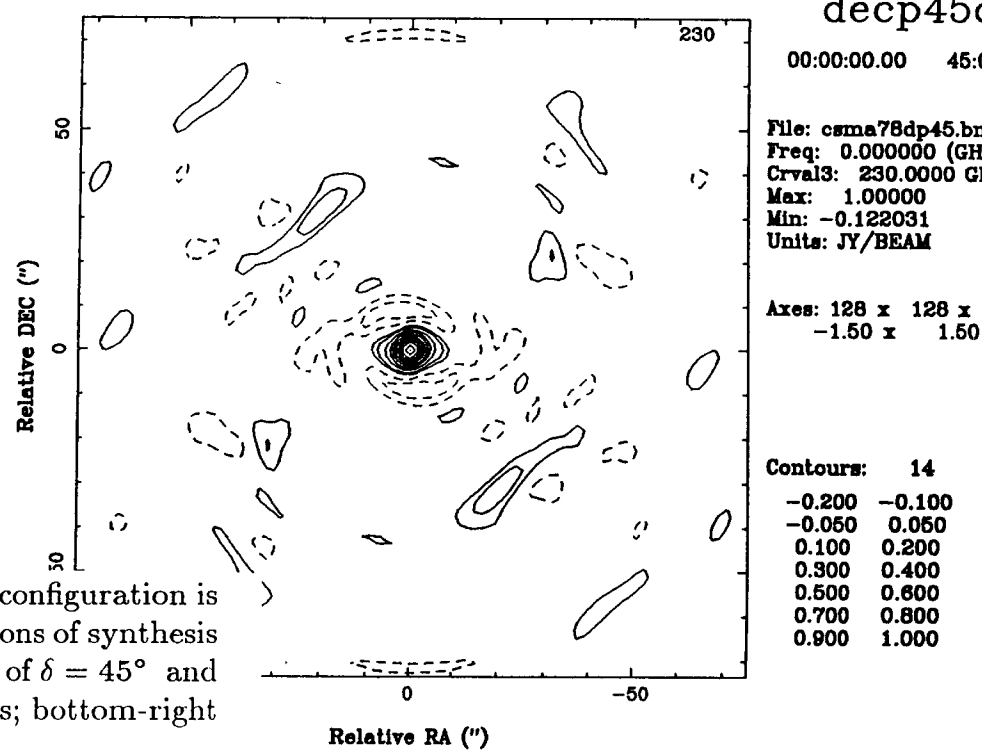
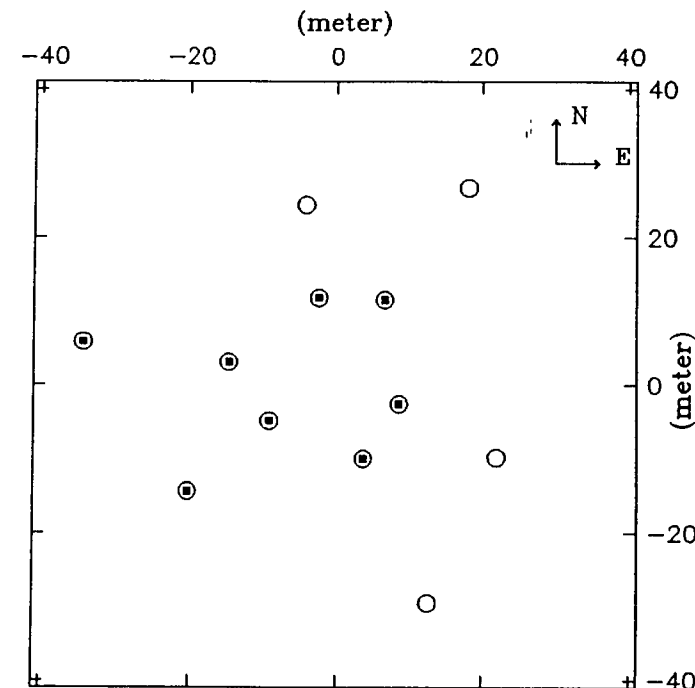
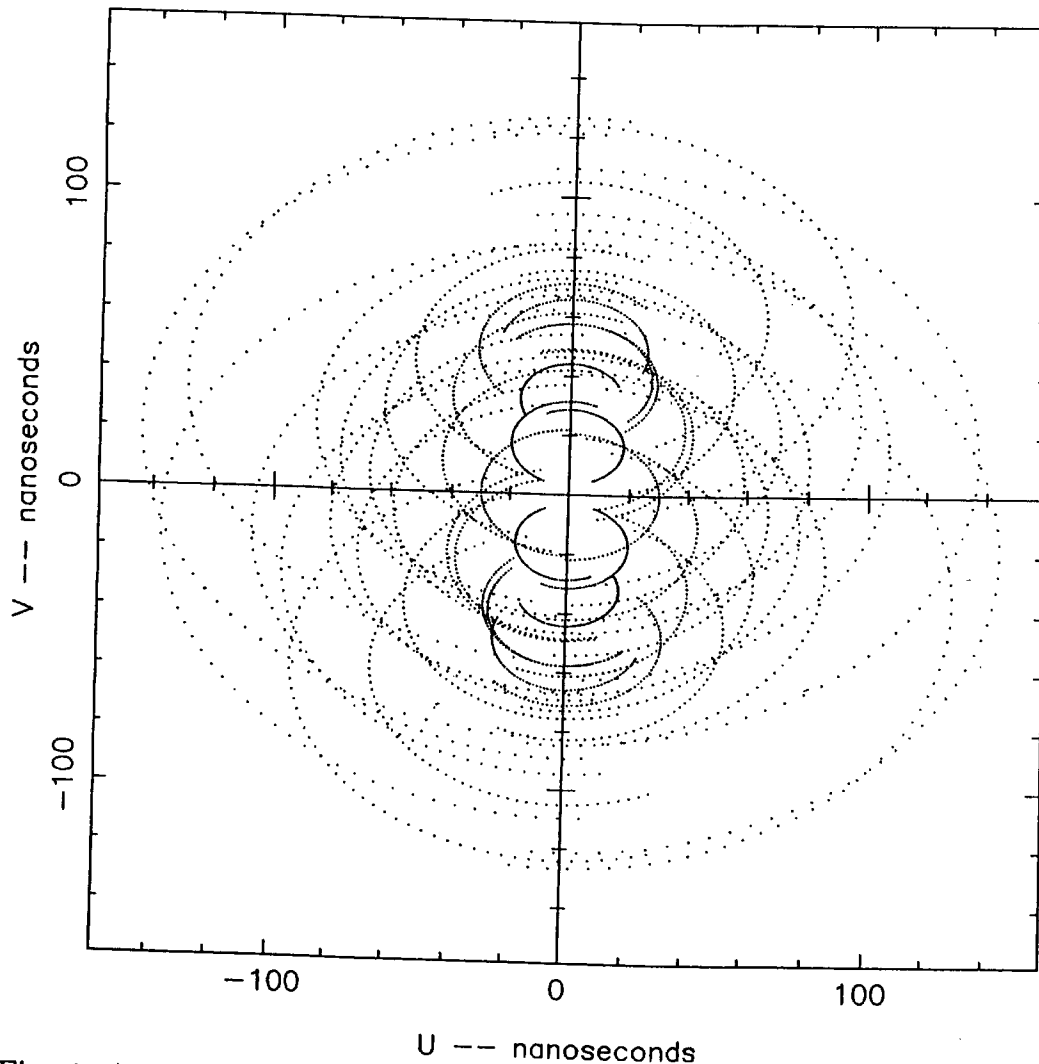
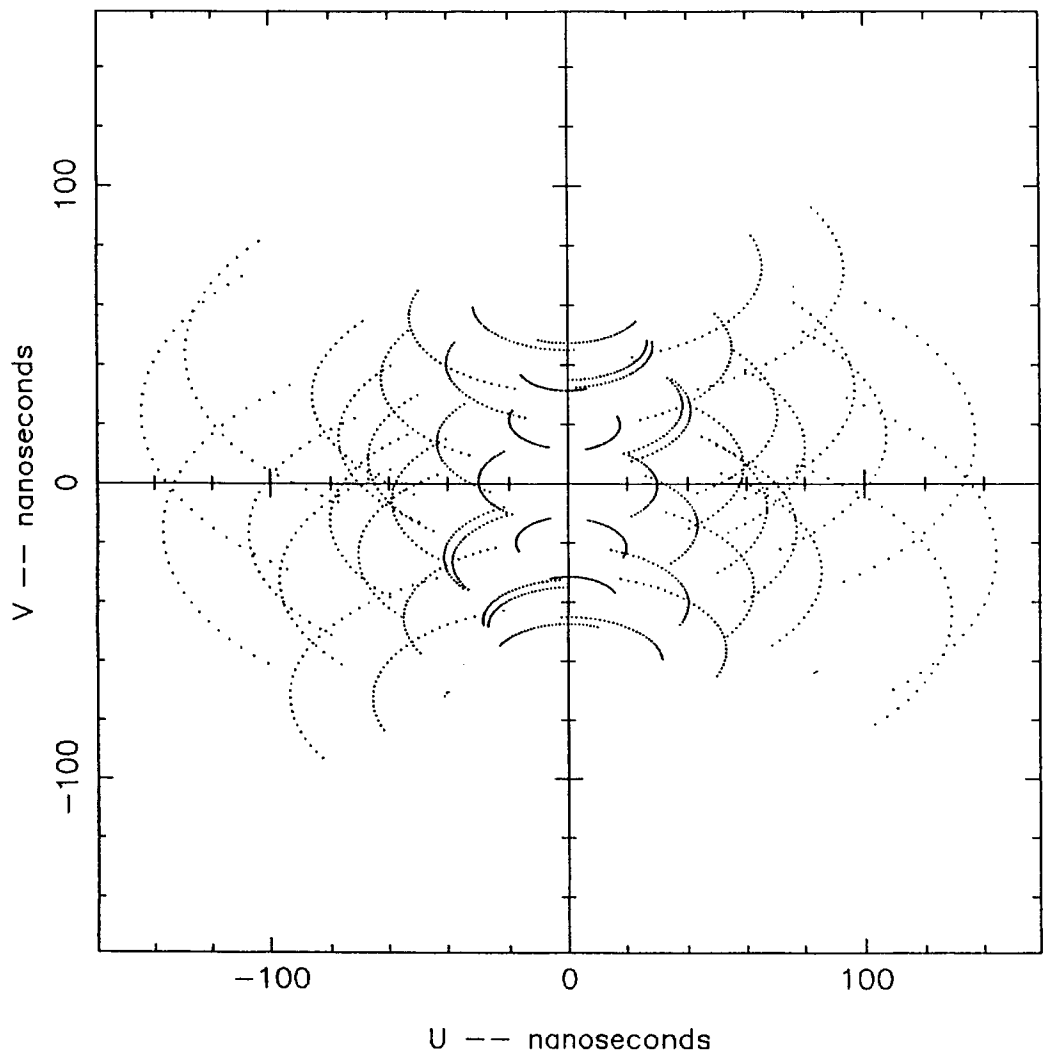


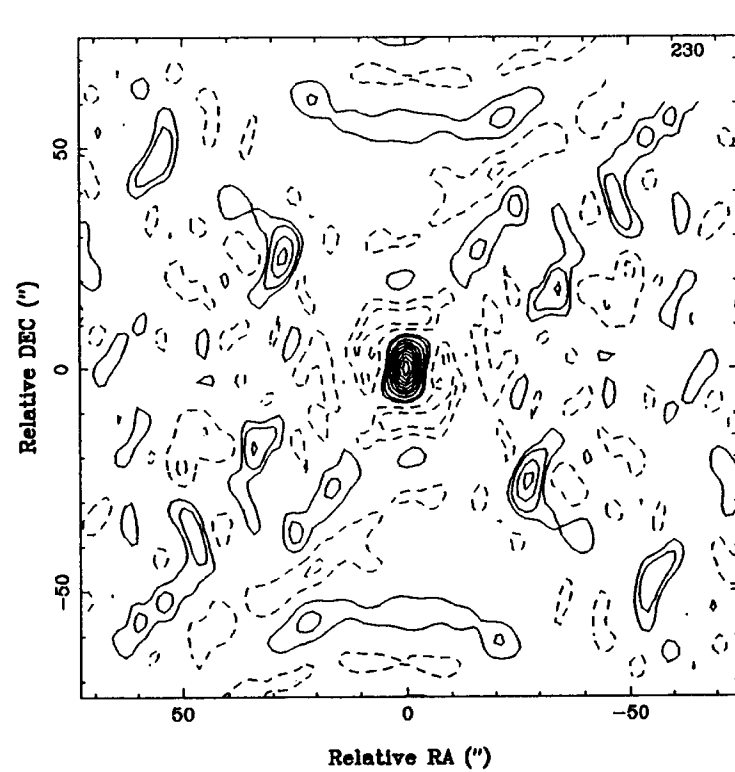
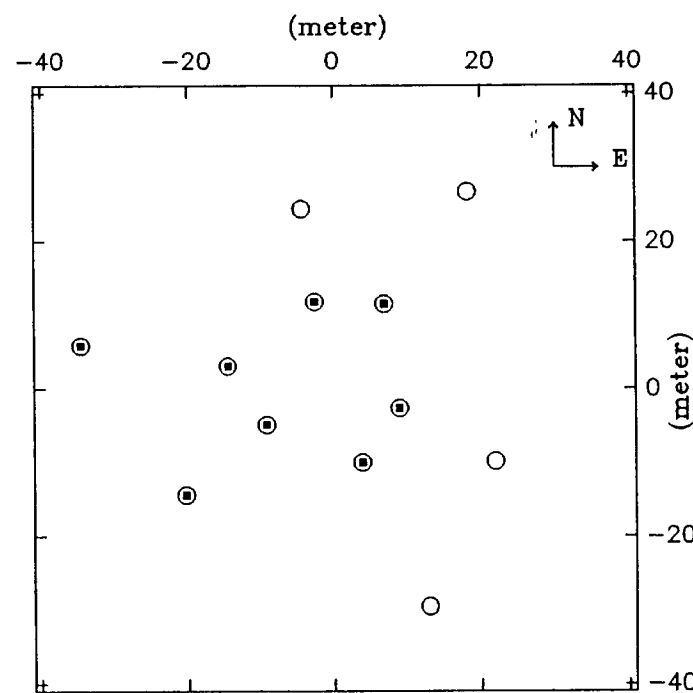
Fig. 1: A total of 15 concentric configurations of 8 antennas where the D configuration is fully loaded and the other 2 antennas are on the C configurations. Simulations of synthesis beams obtained from these configurations are made for the two declinations of $\delta = 45^\circ$ and $\delta = -29^\circ$. Left panel: uv-tracks; top-right panel: layout of configurations; bottom-right panel: contours of synthesis beam.

$\delta = -29^\circ$

UvTrack: csma78dn29.uv



1-2



$\delta = 45^\circ$

UvTrack: csma79dp45.uv

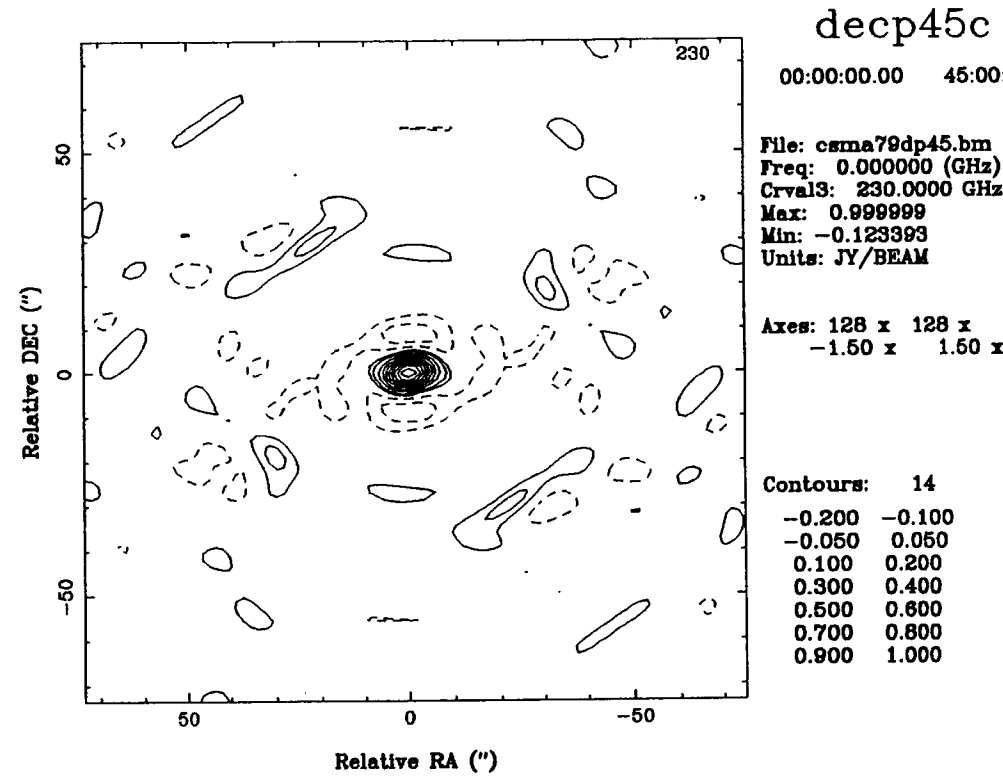
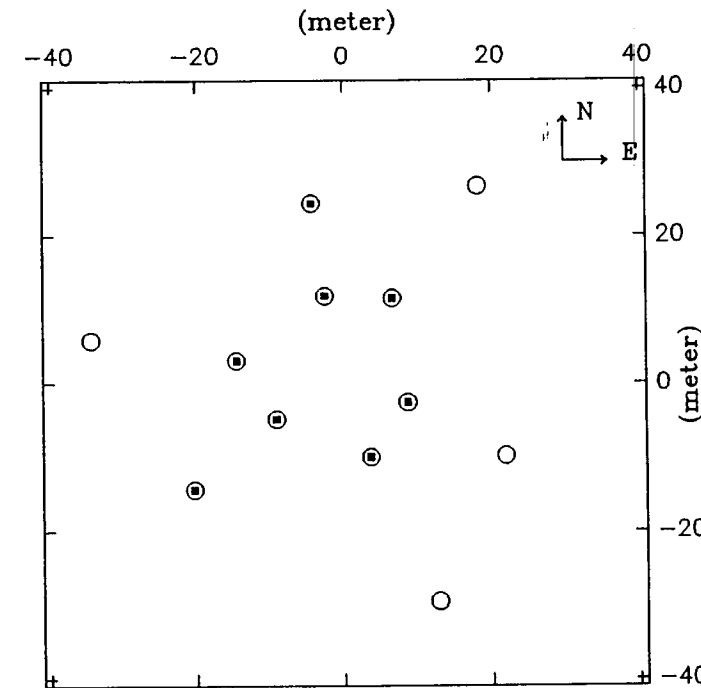
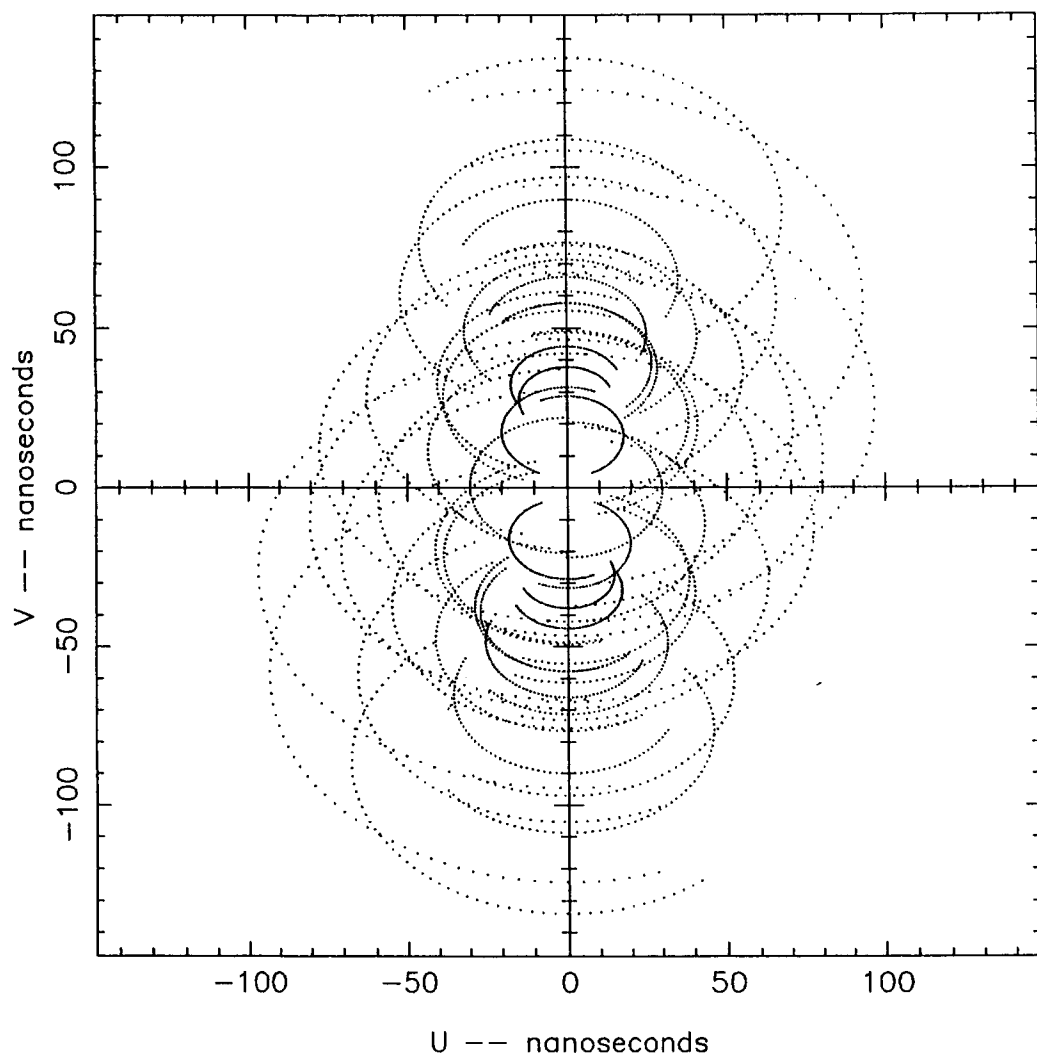
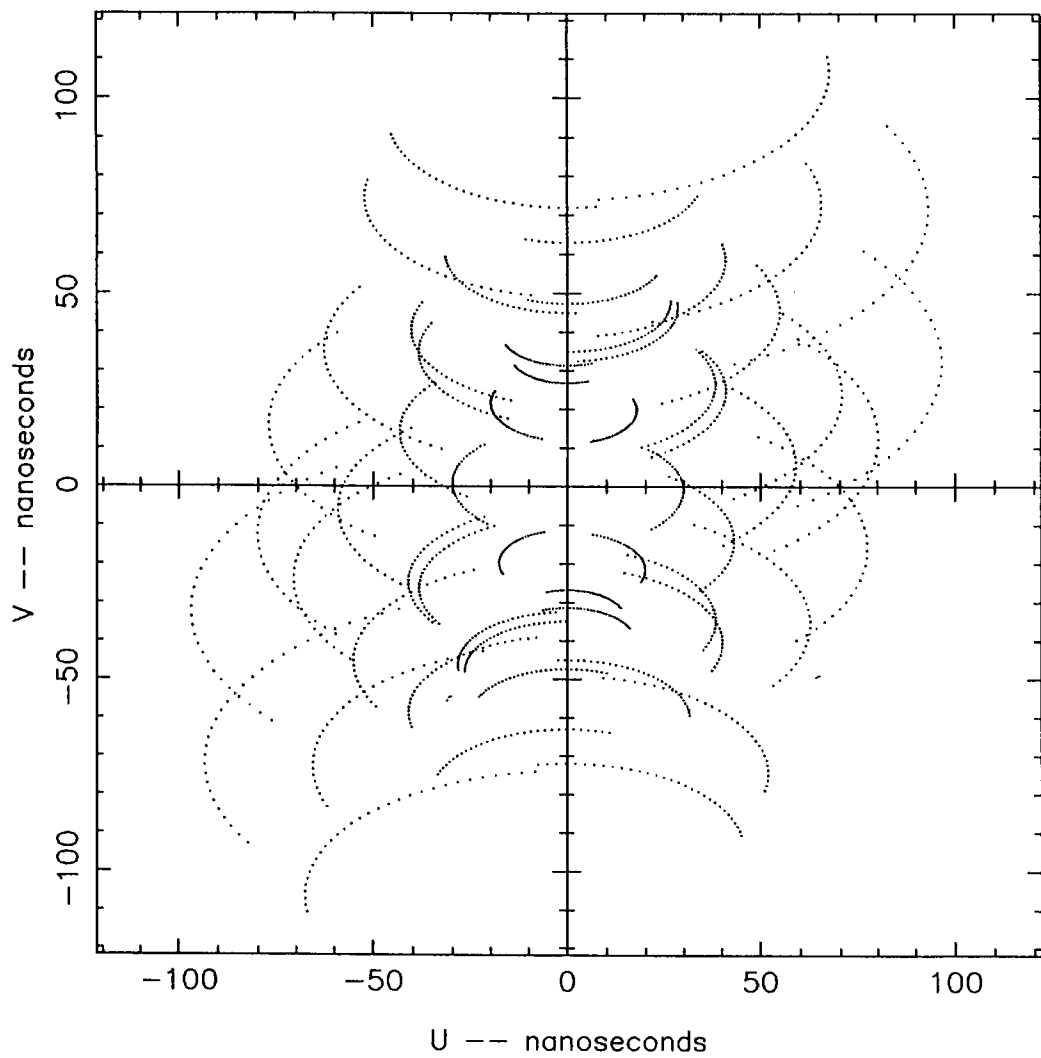


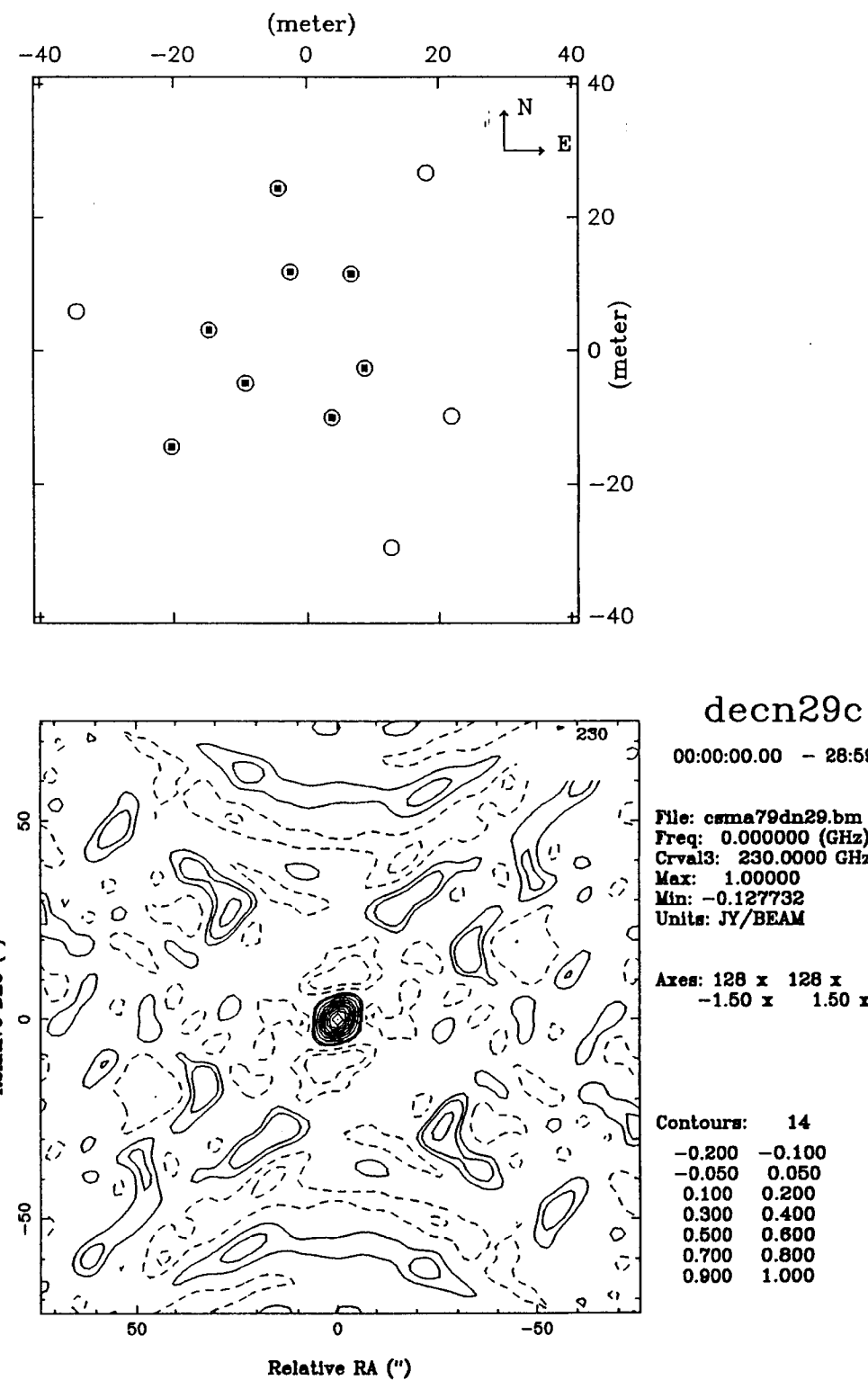
Fig 1-3

$$\delta = -29^\circ$$

UvTrack: csma79dn29.uv



| - 4



$$\delta = 45^\circ$$

UvTrack: csma710dp45.uv

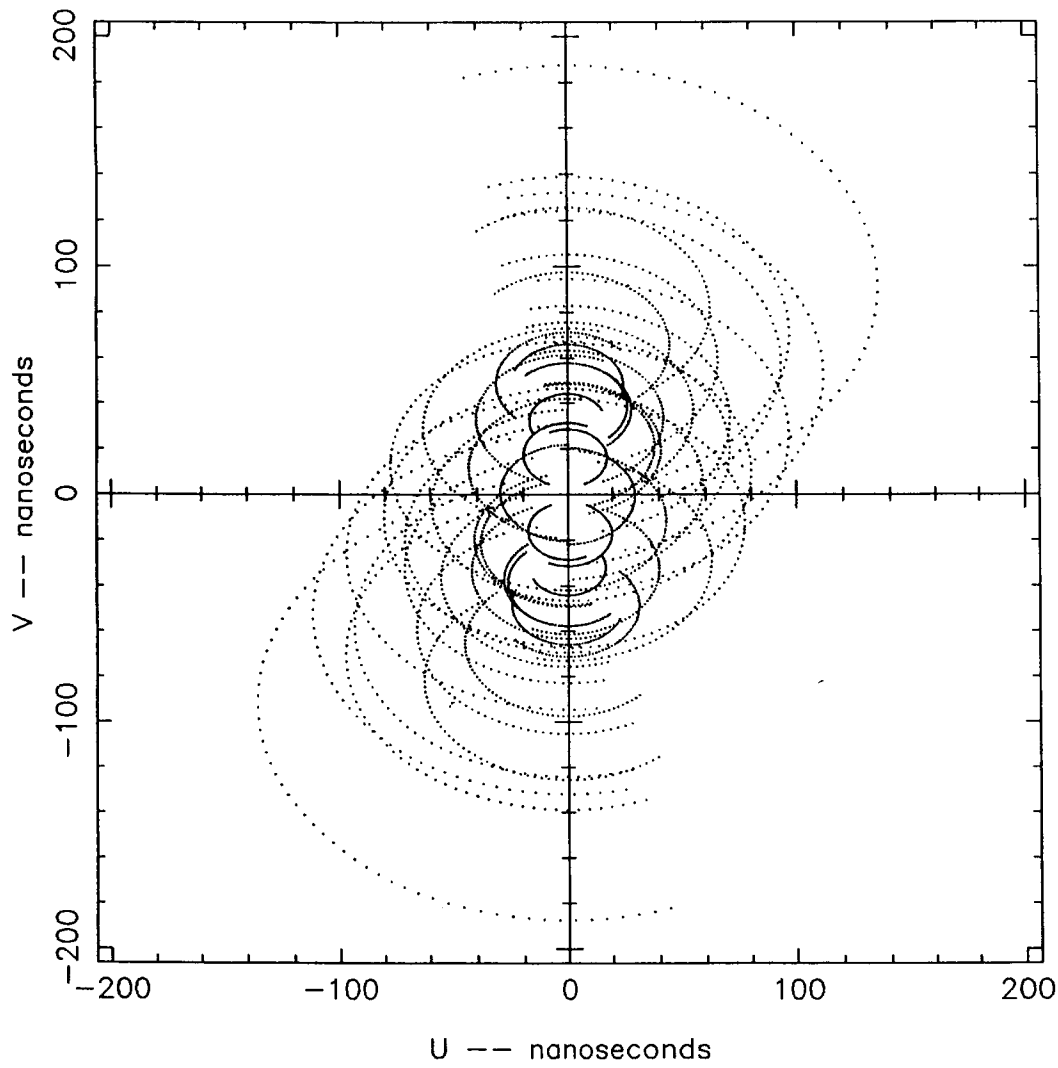
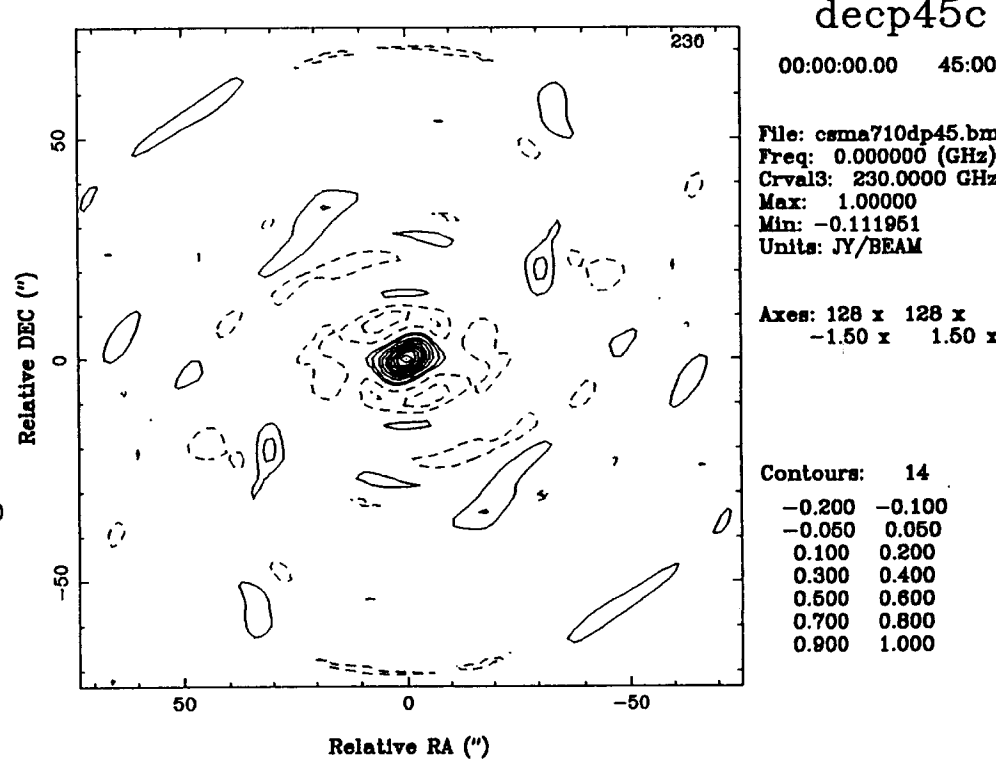
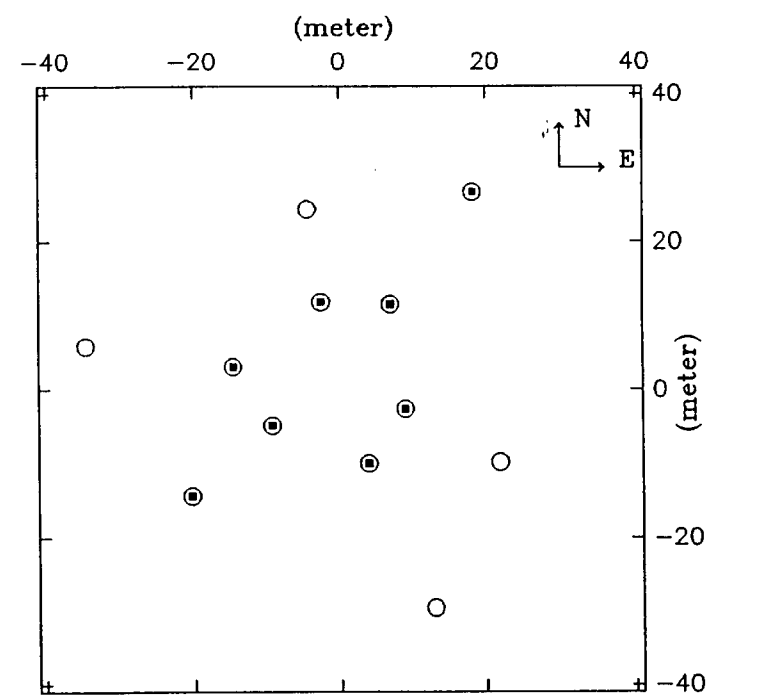


Fig. 1-5



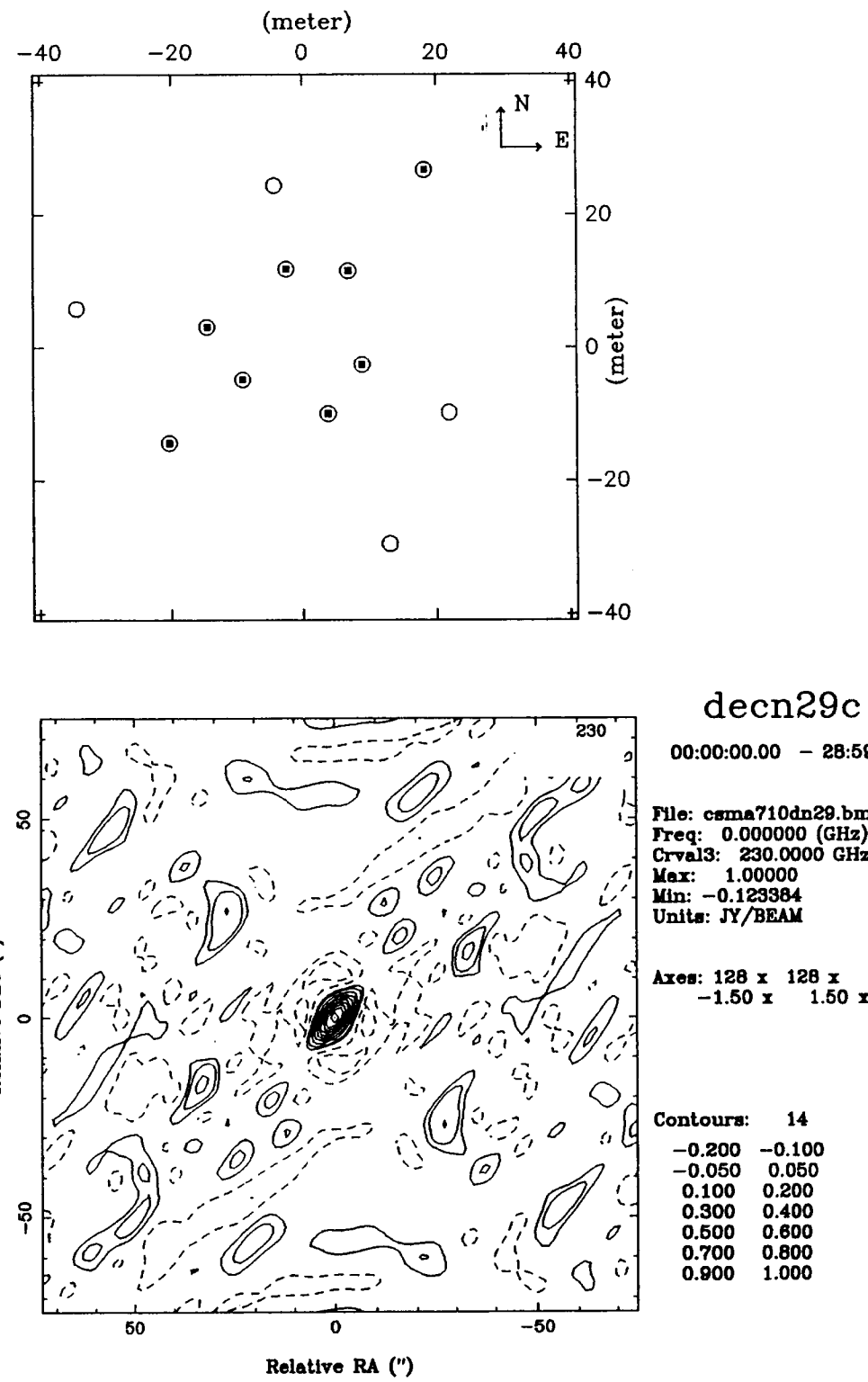
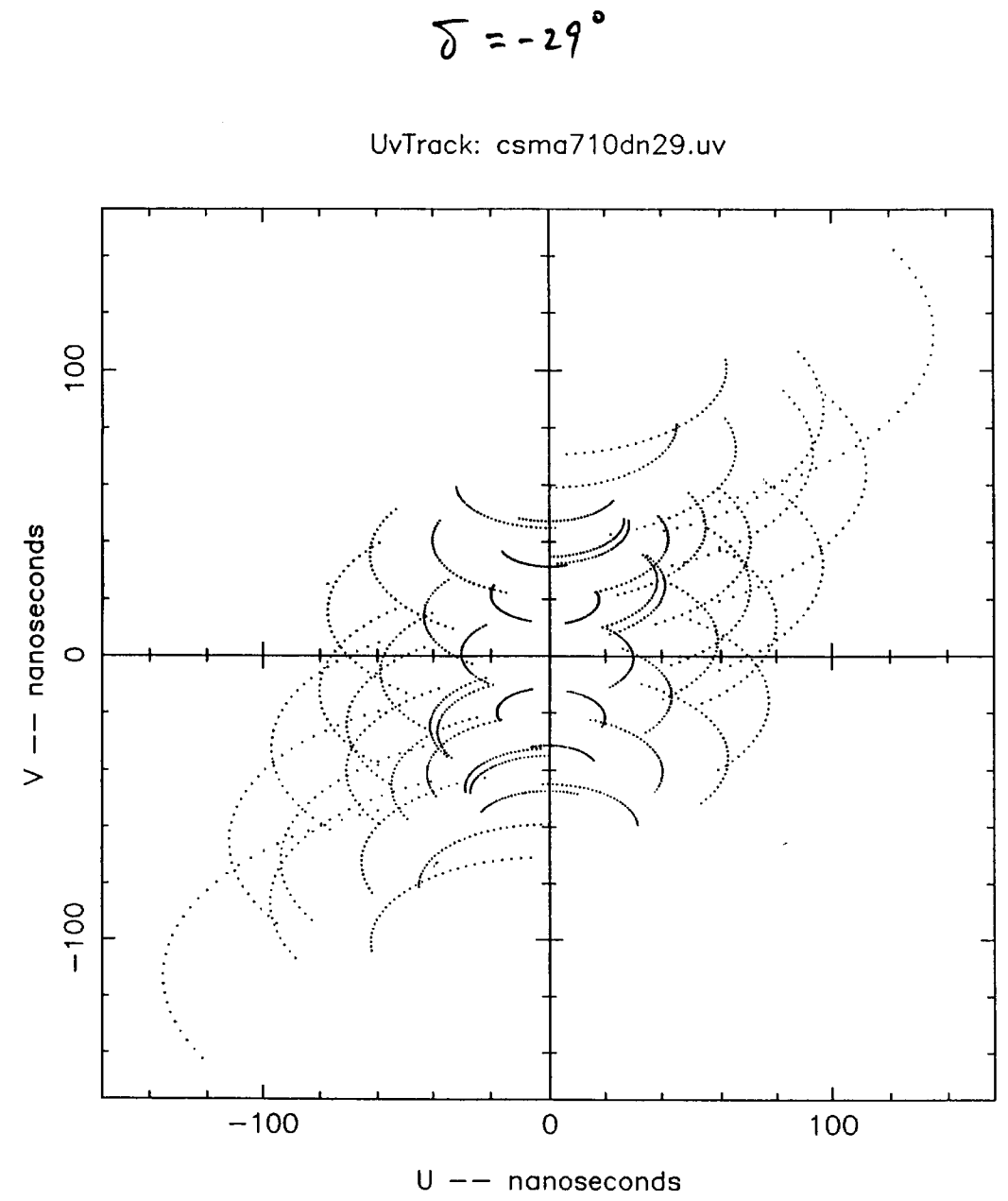


Fig. 1-6

$$\delta = 45^\circ$$

UvTrack: csma711dp45.uv

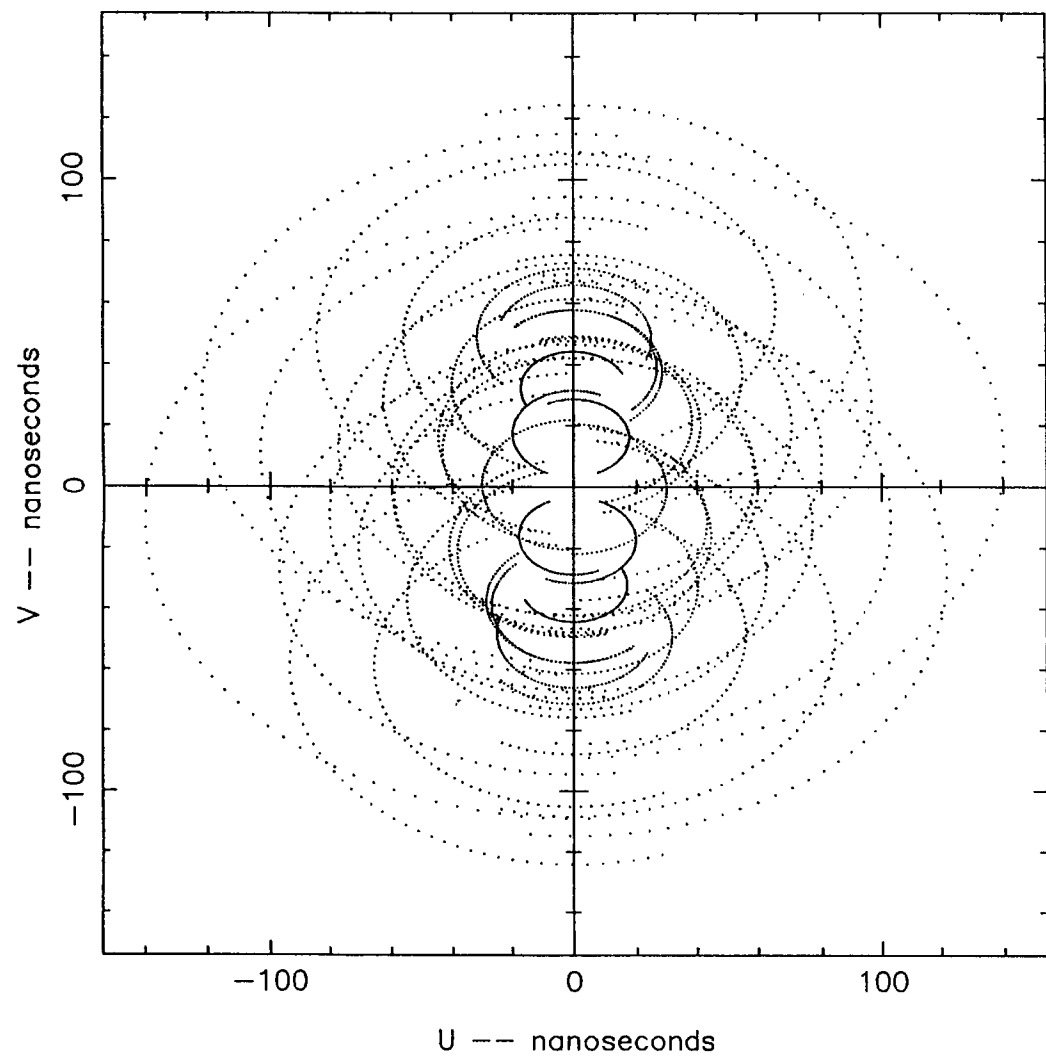
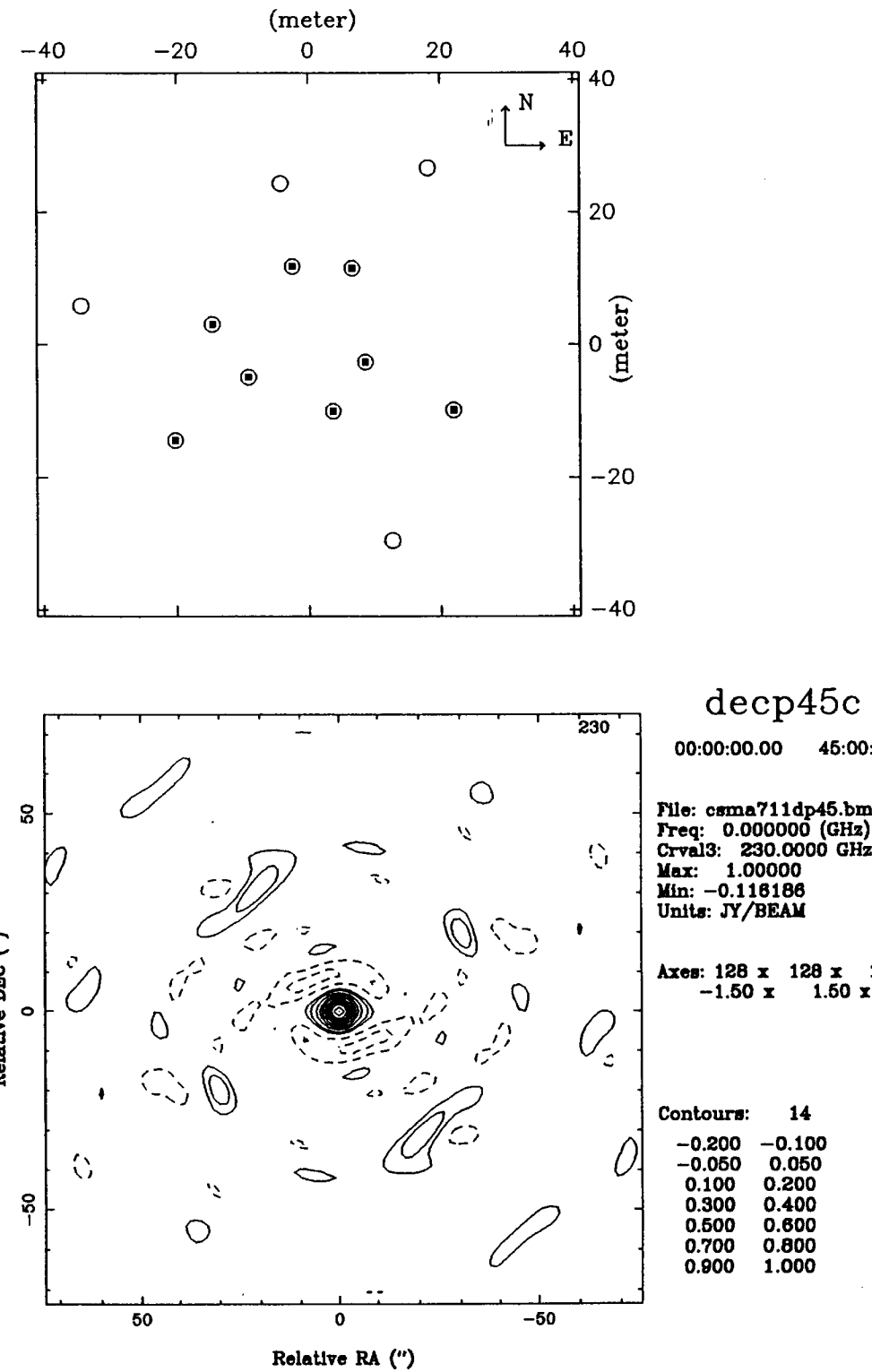


Fig. 1-7



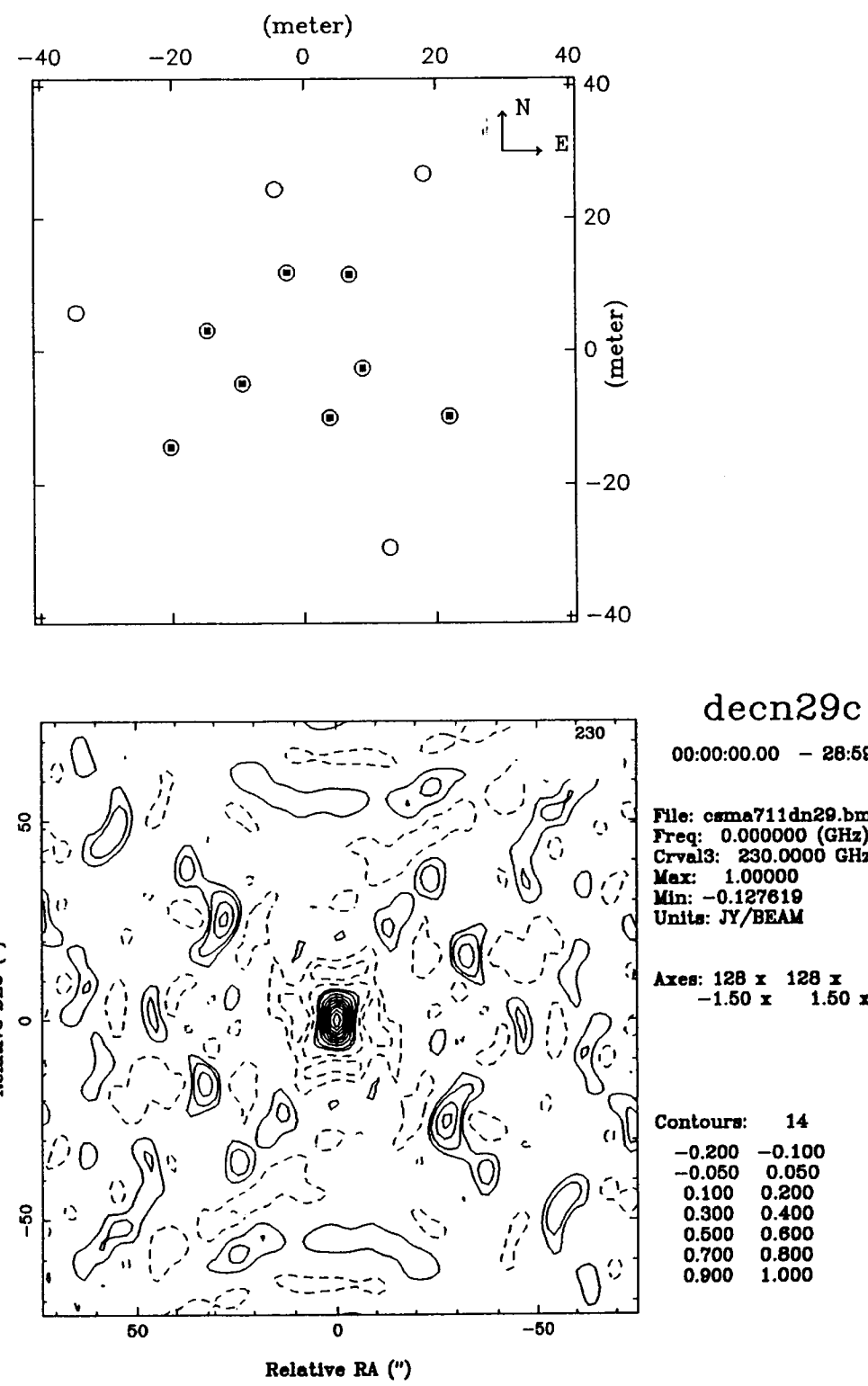
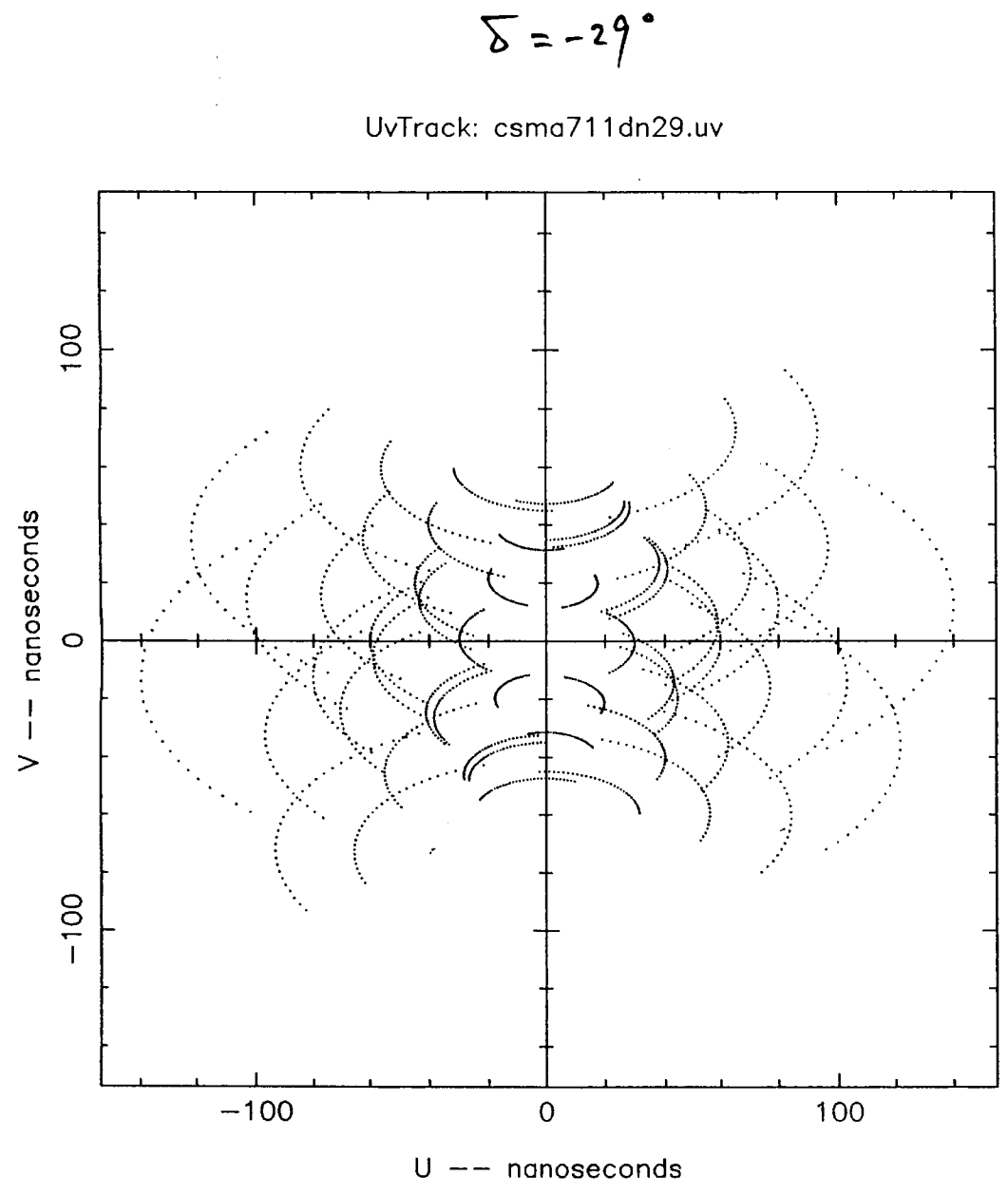


Fig. 1-8

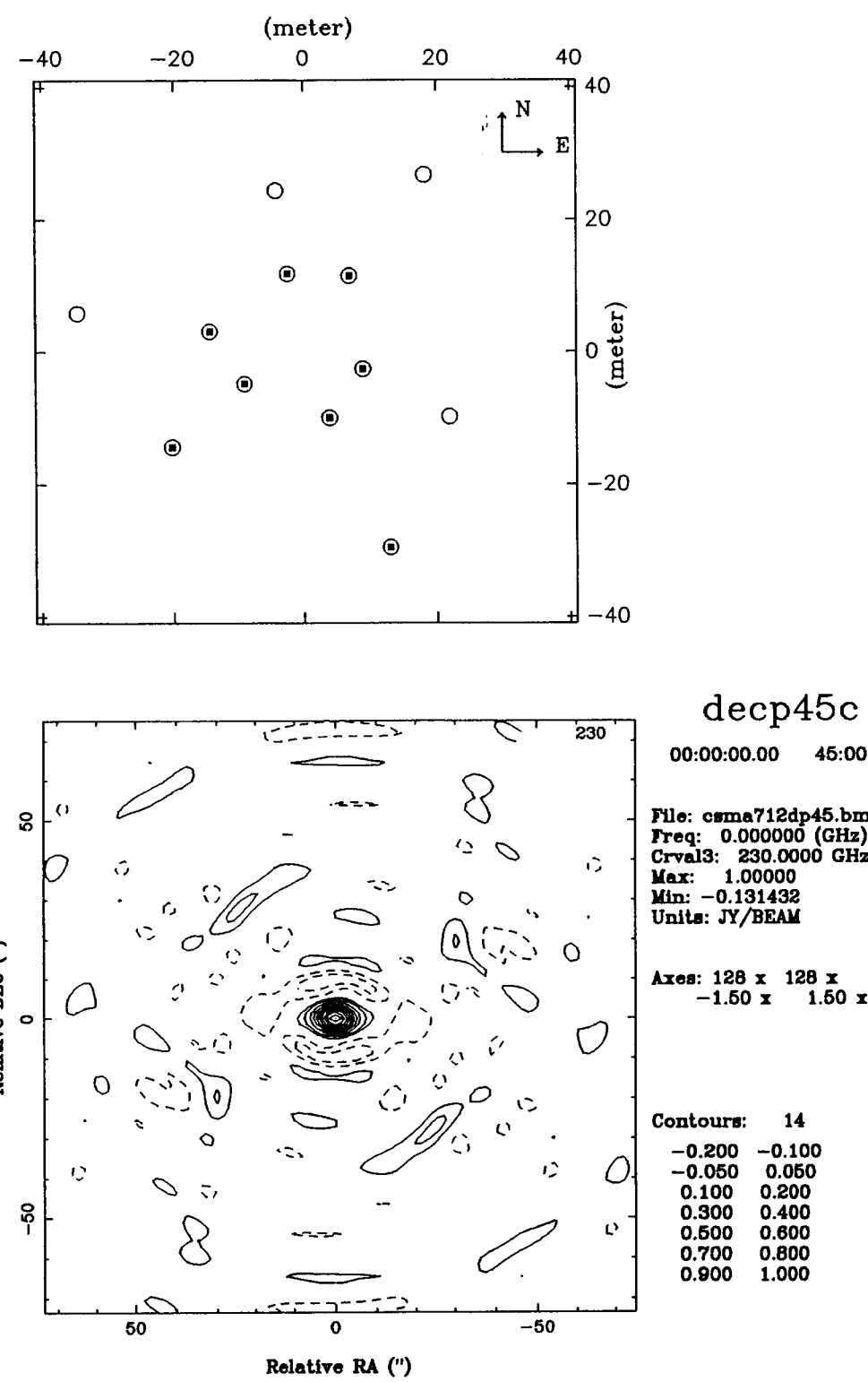
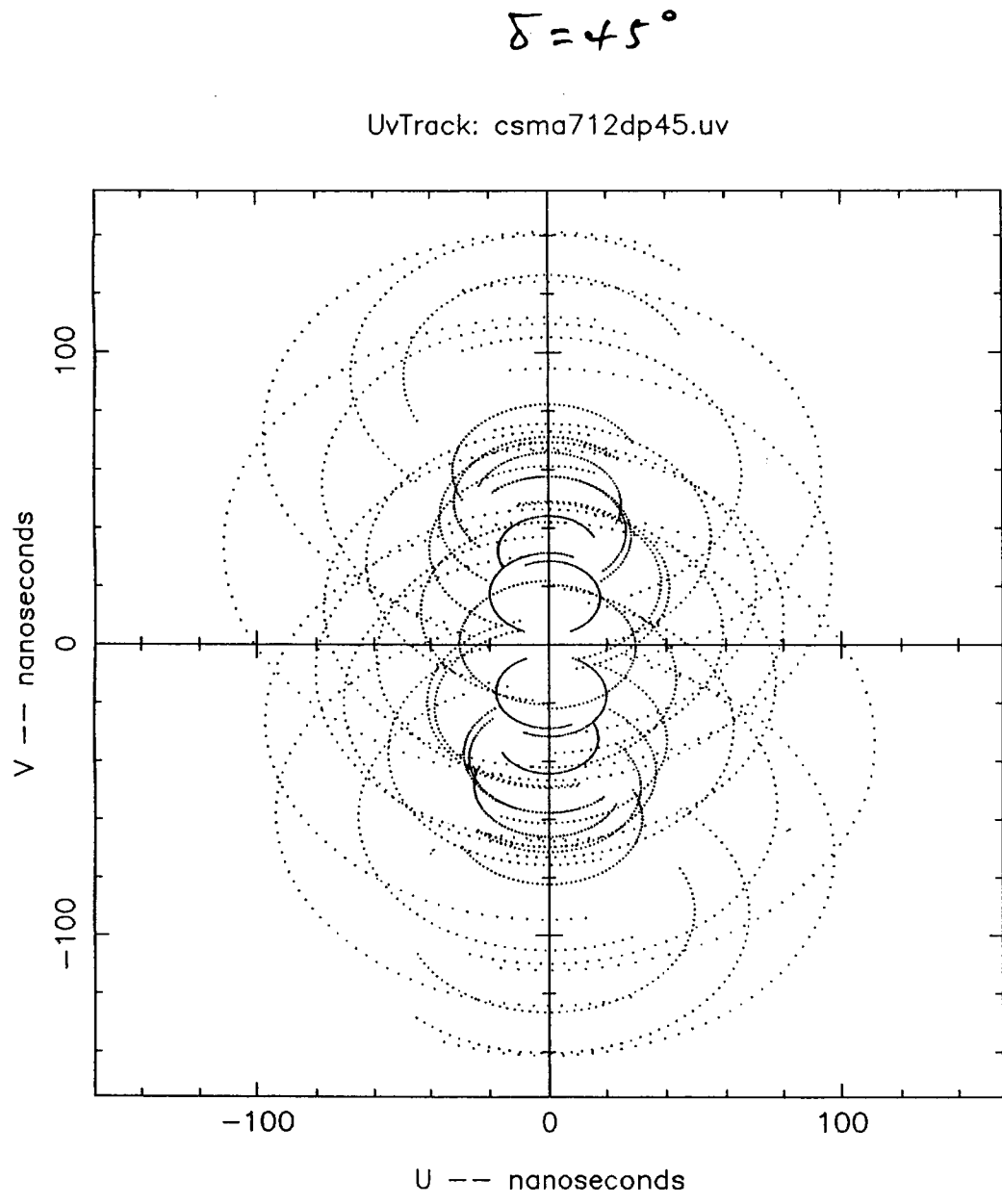


Fig. 1-9

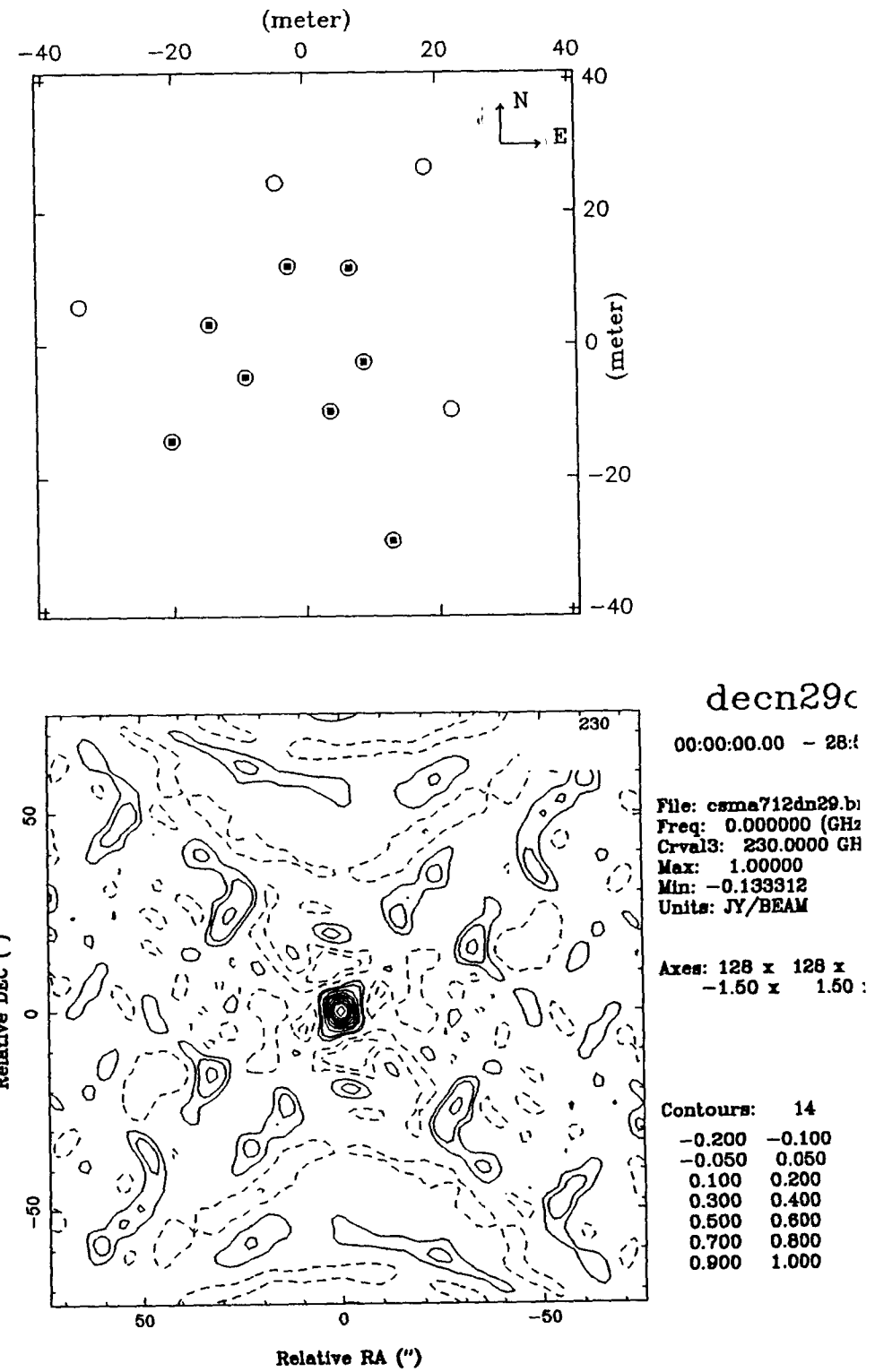
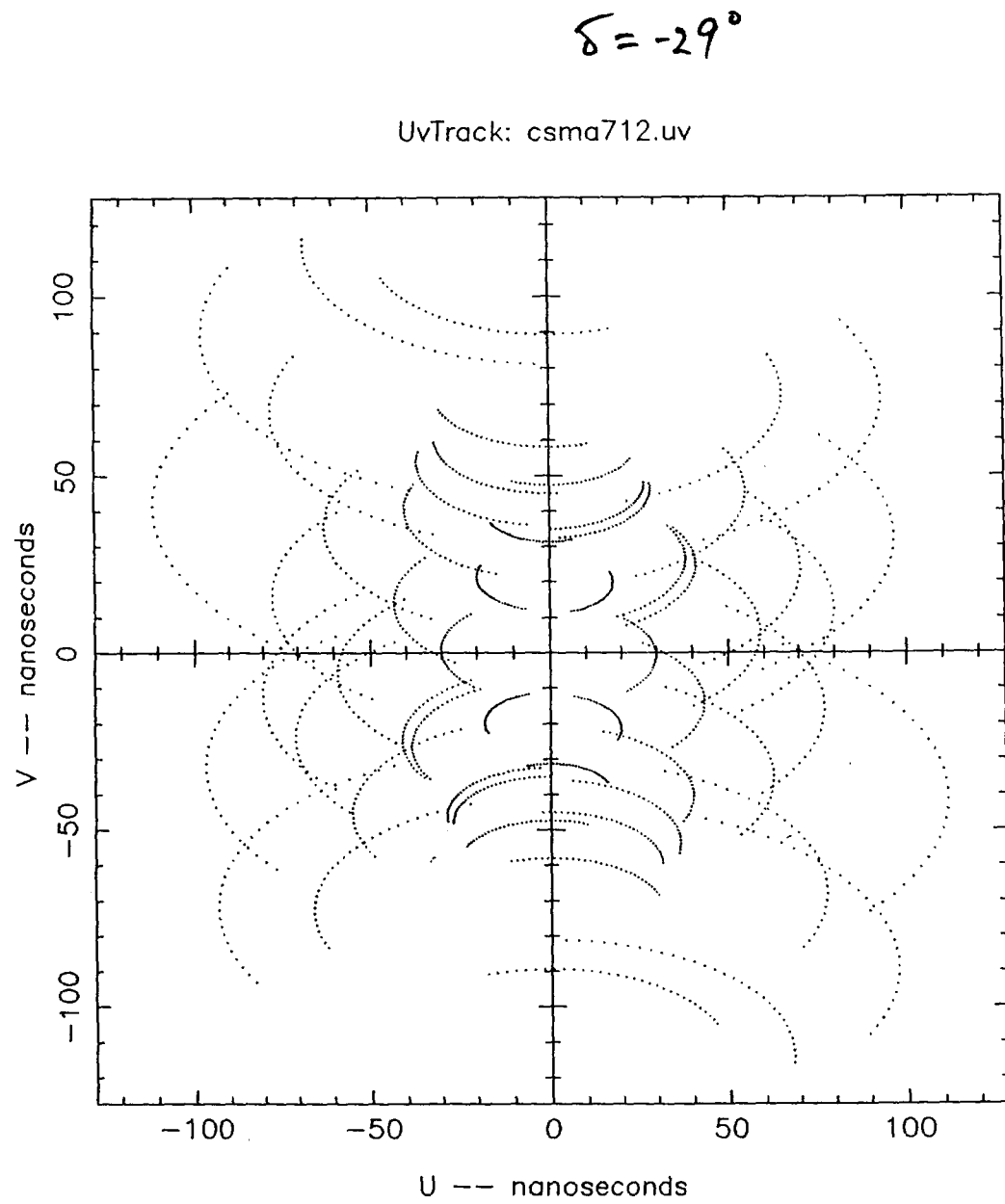


Fig. 1-10

$\delta = 45^\circ$

UvTrack: csma89dp45.uv

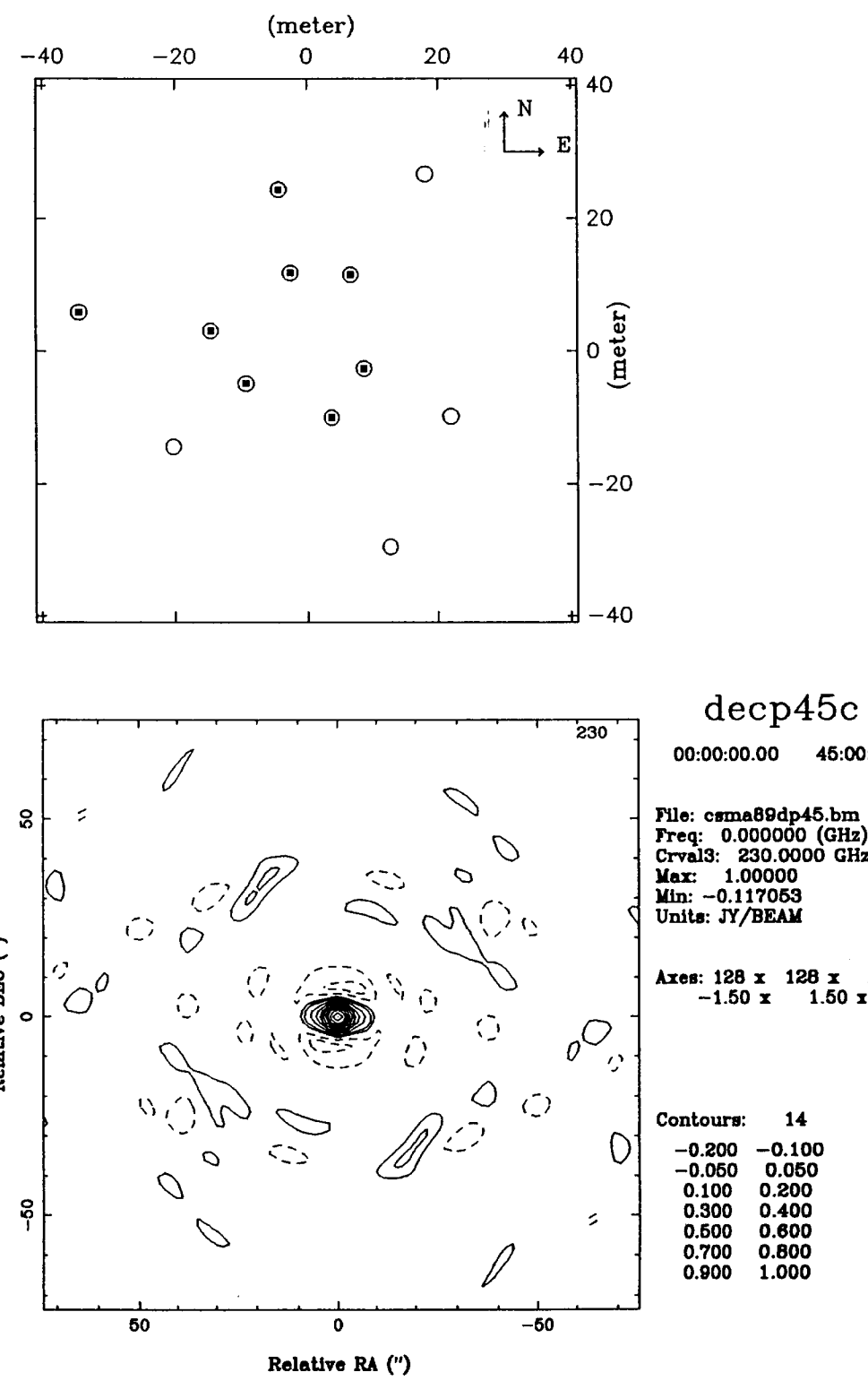
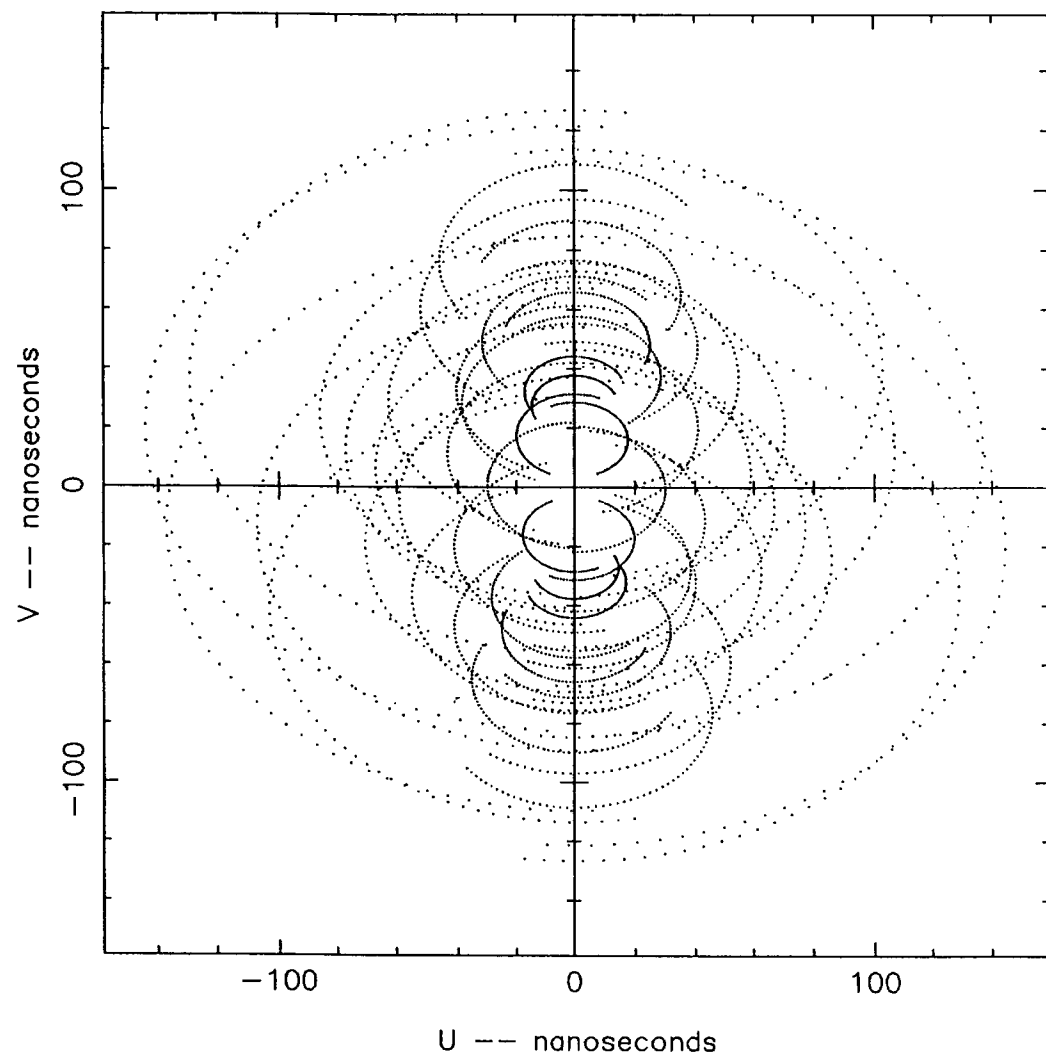


Fig. 1-11

$\delta = -29^\circ$

UvTrack: csma89dn29.uv

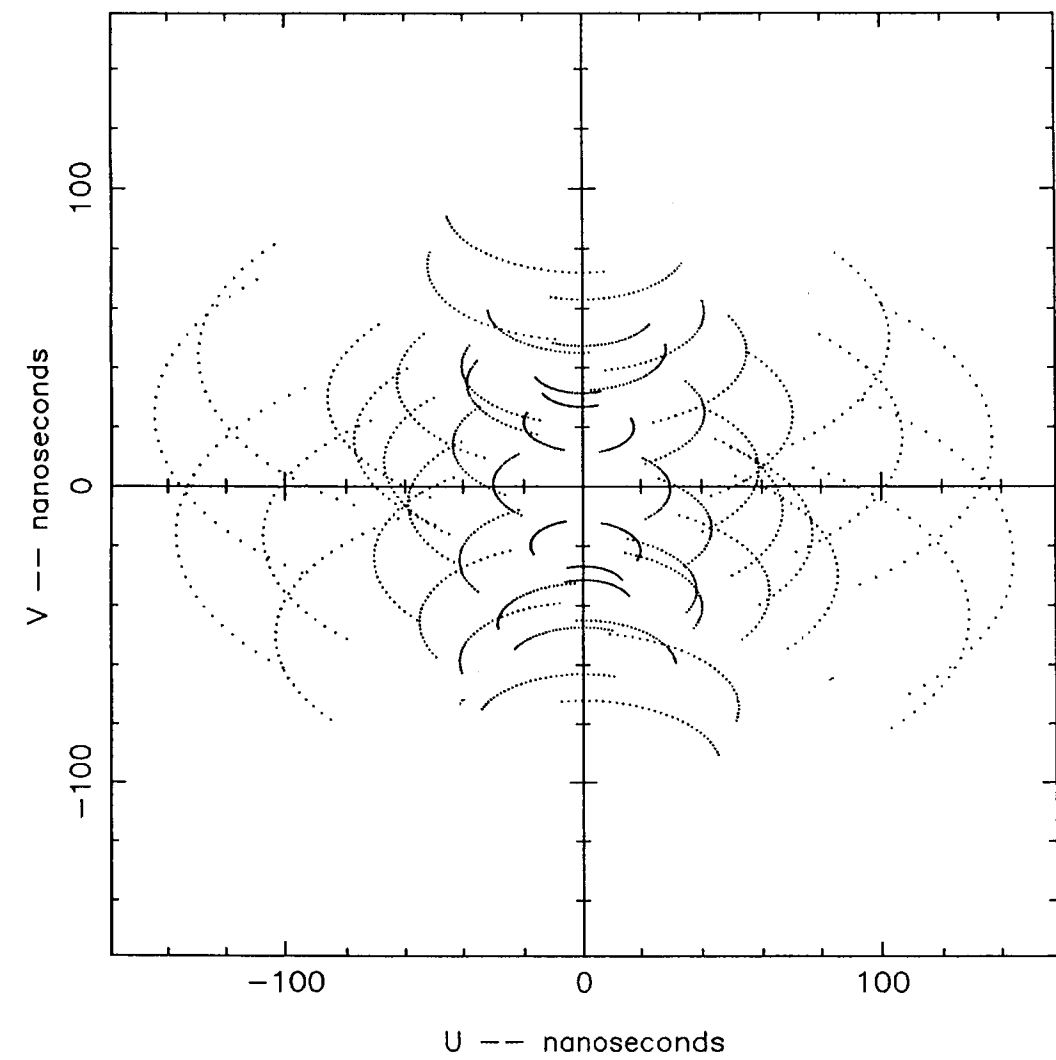
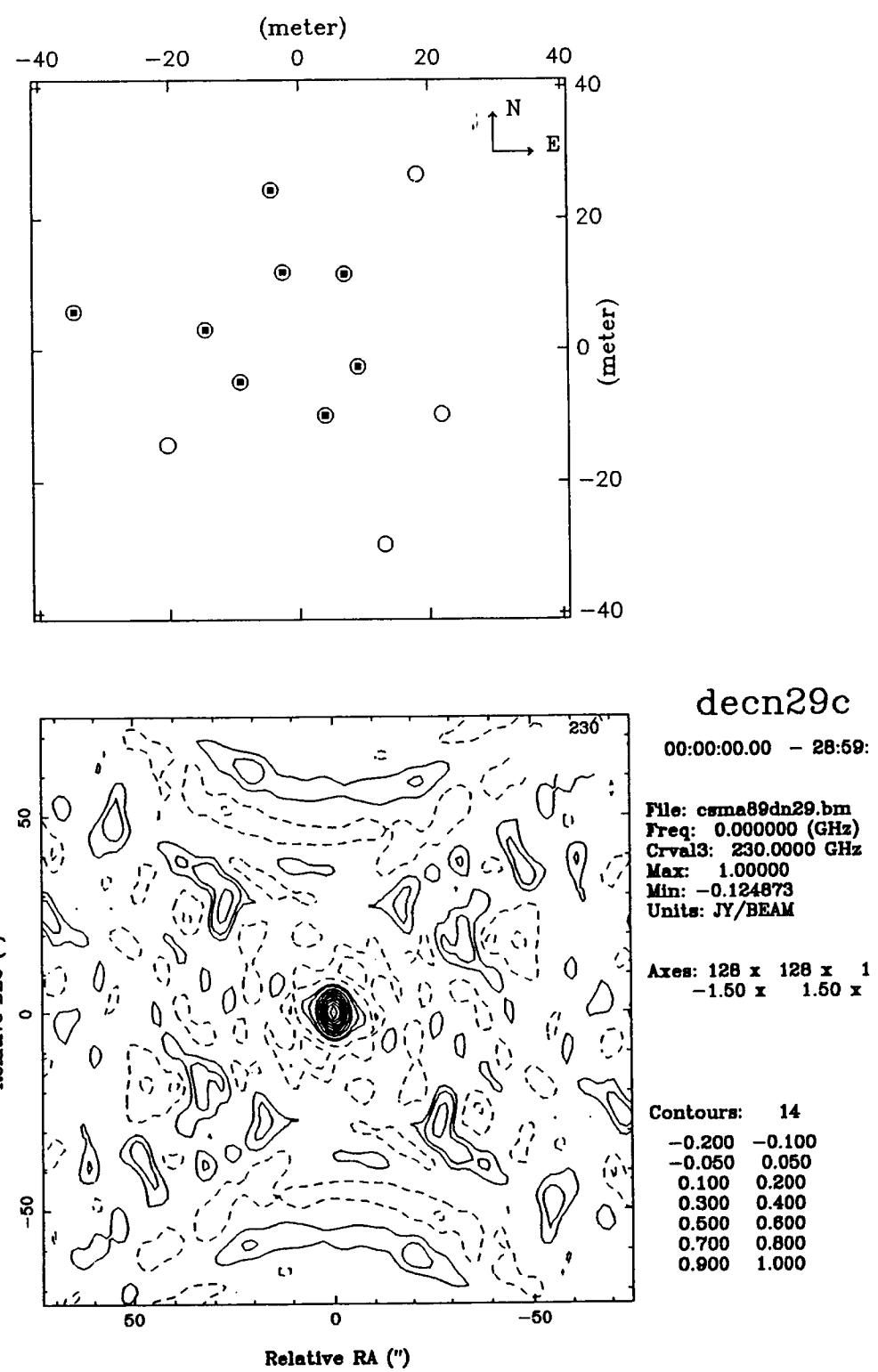
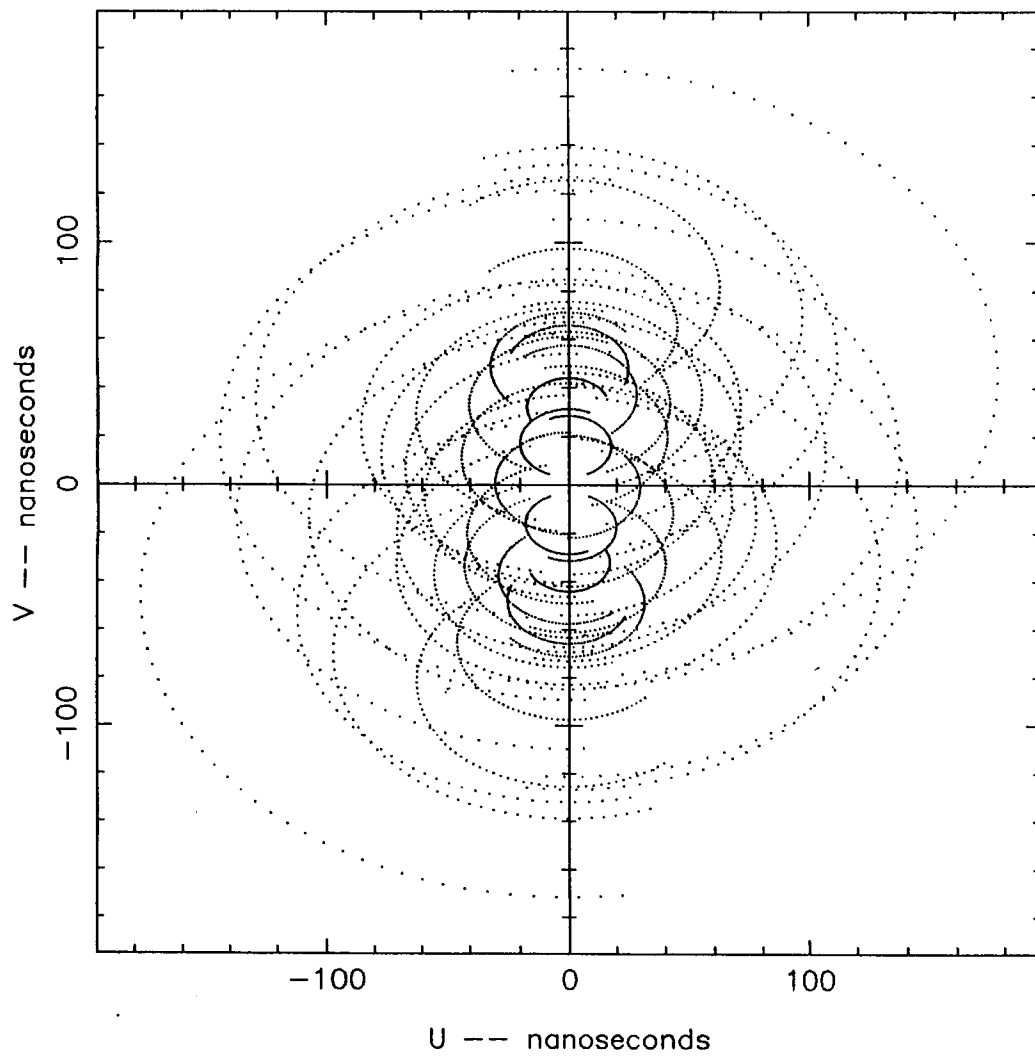


Fig. 1-12



1

UvTrack: csma810dp45.uv



$$\delta = 45^\circ$$

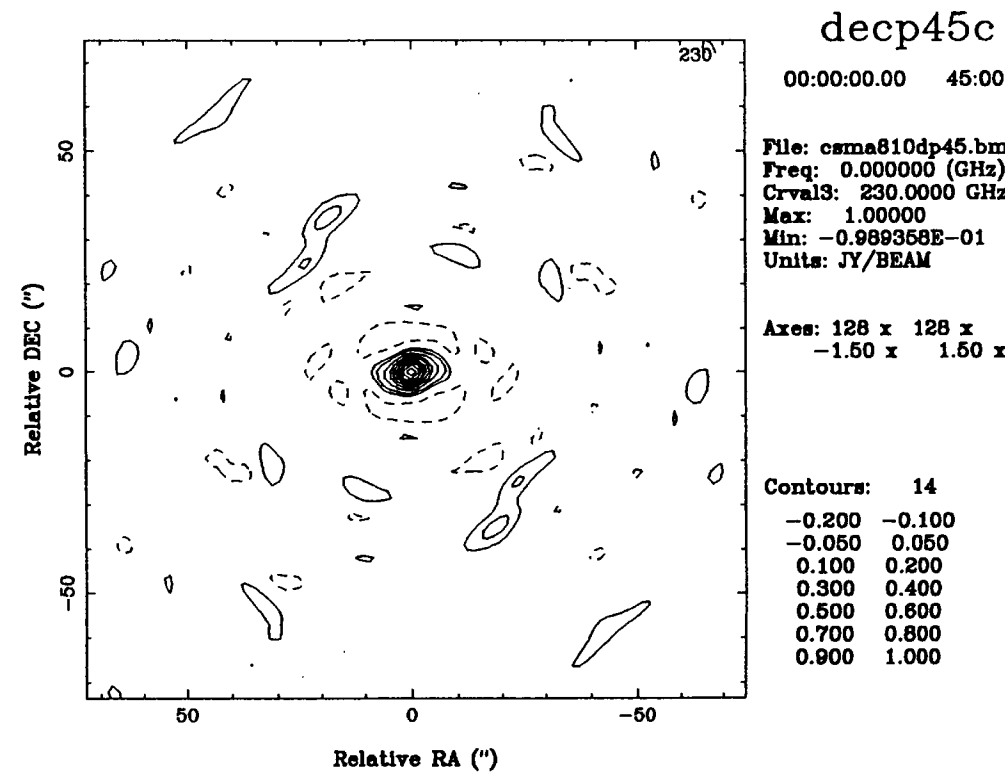
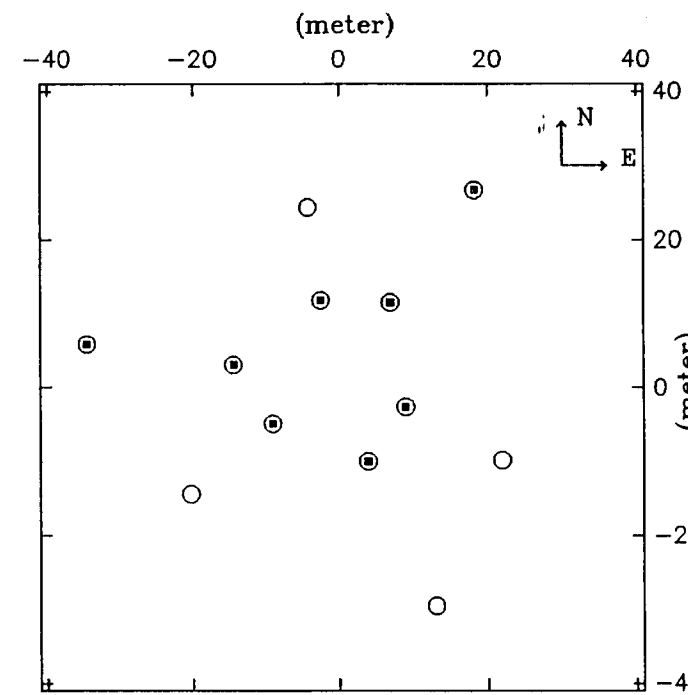


Fig. 1-13

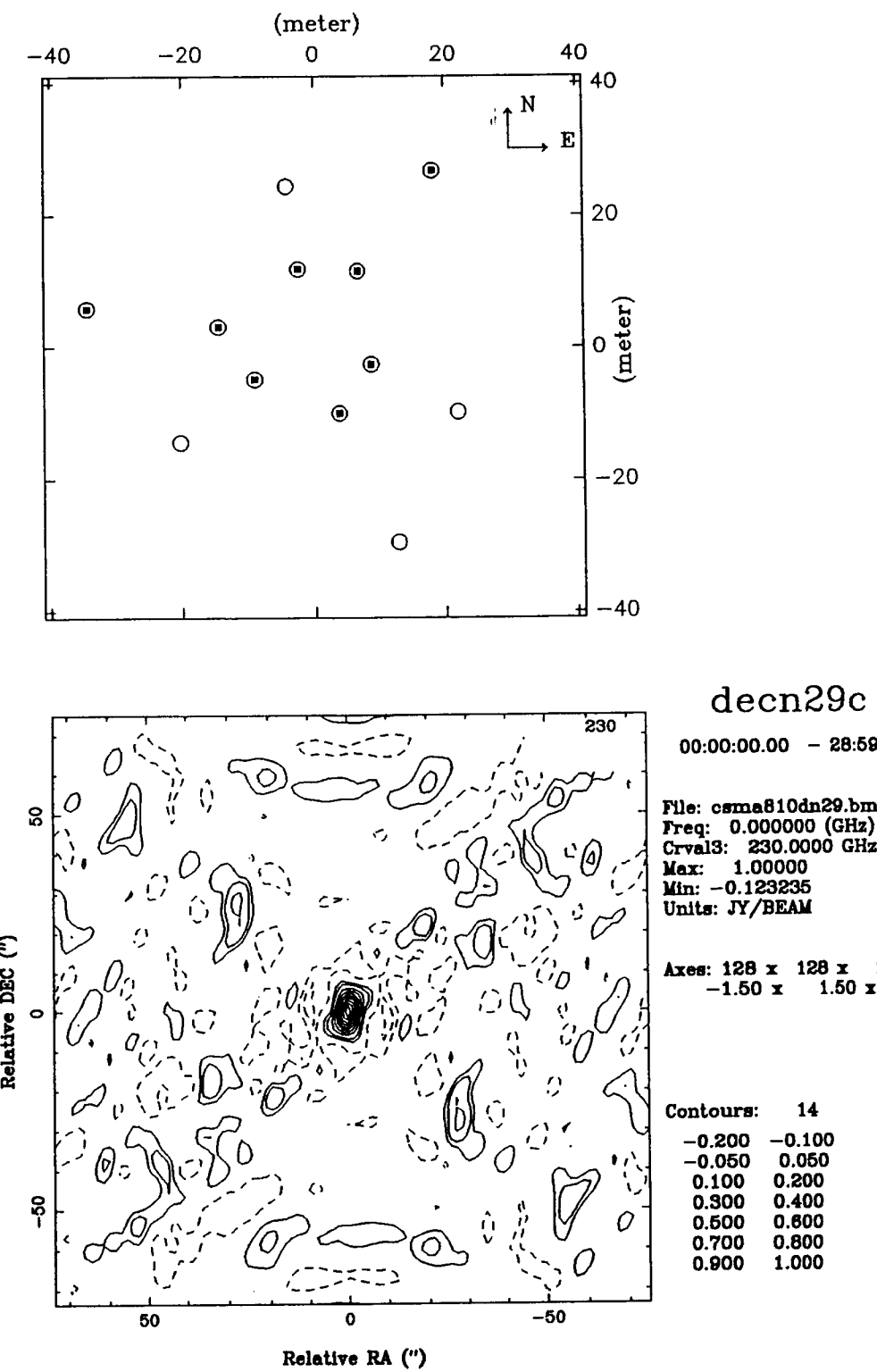
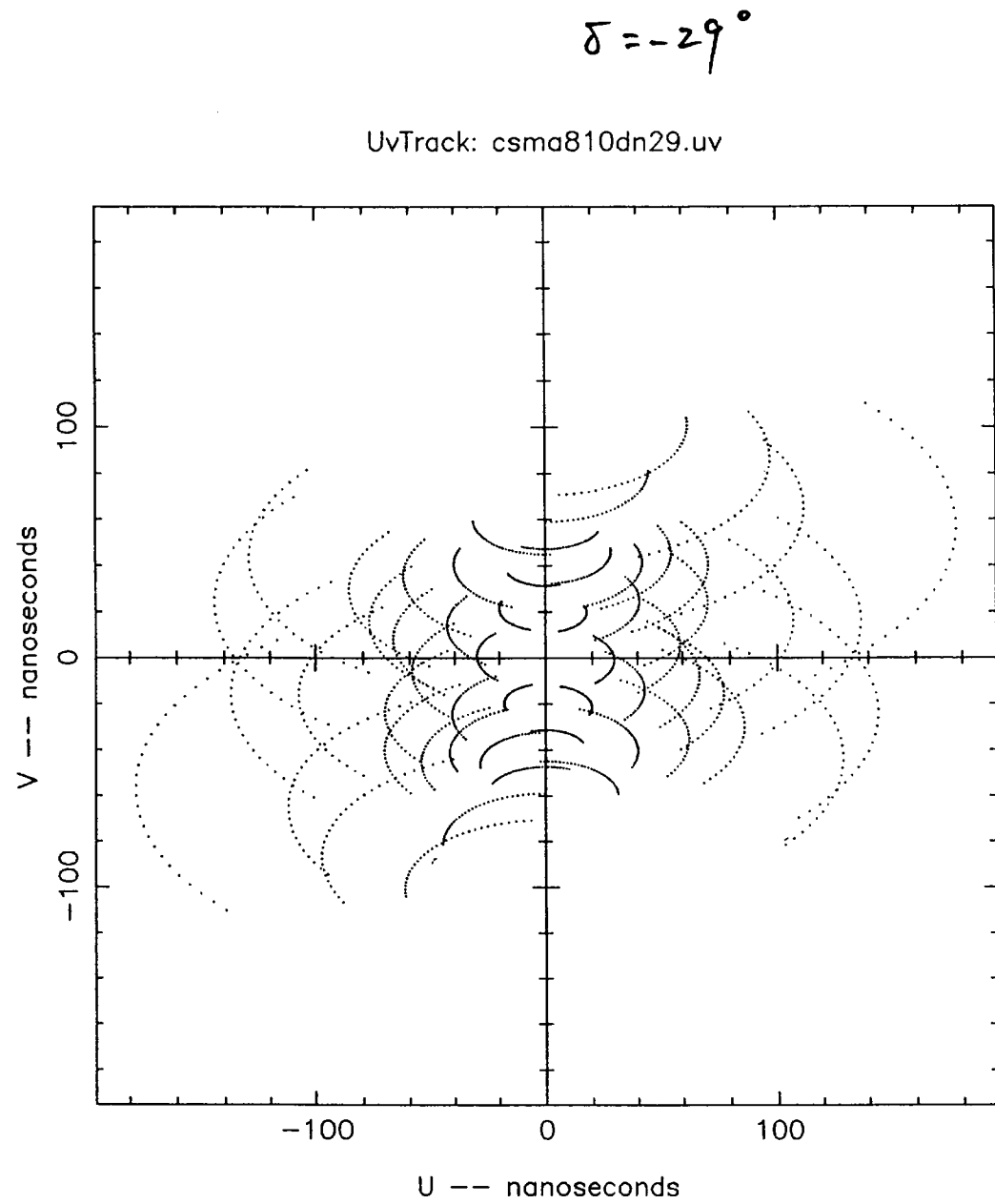


Fig. 1-14

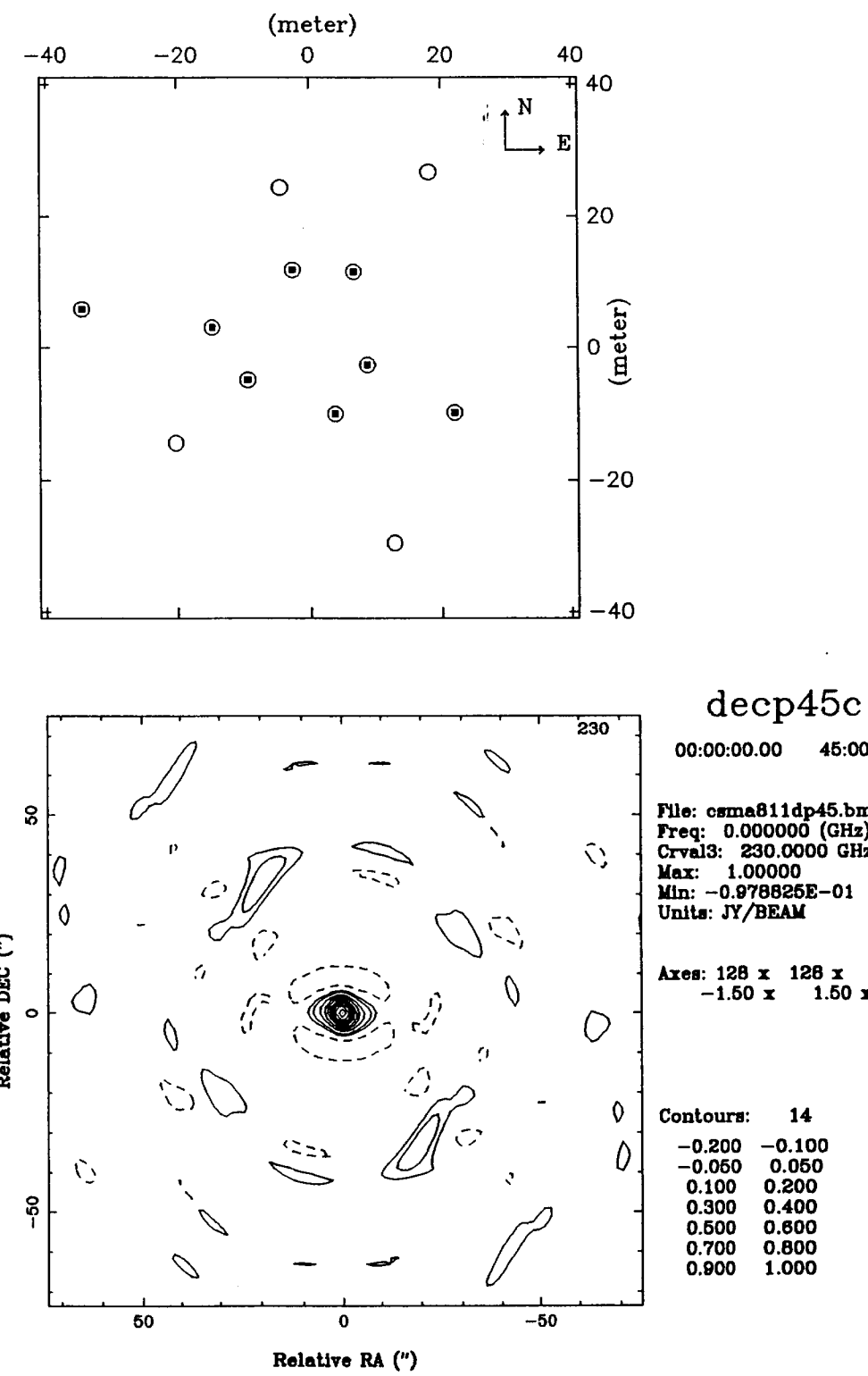
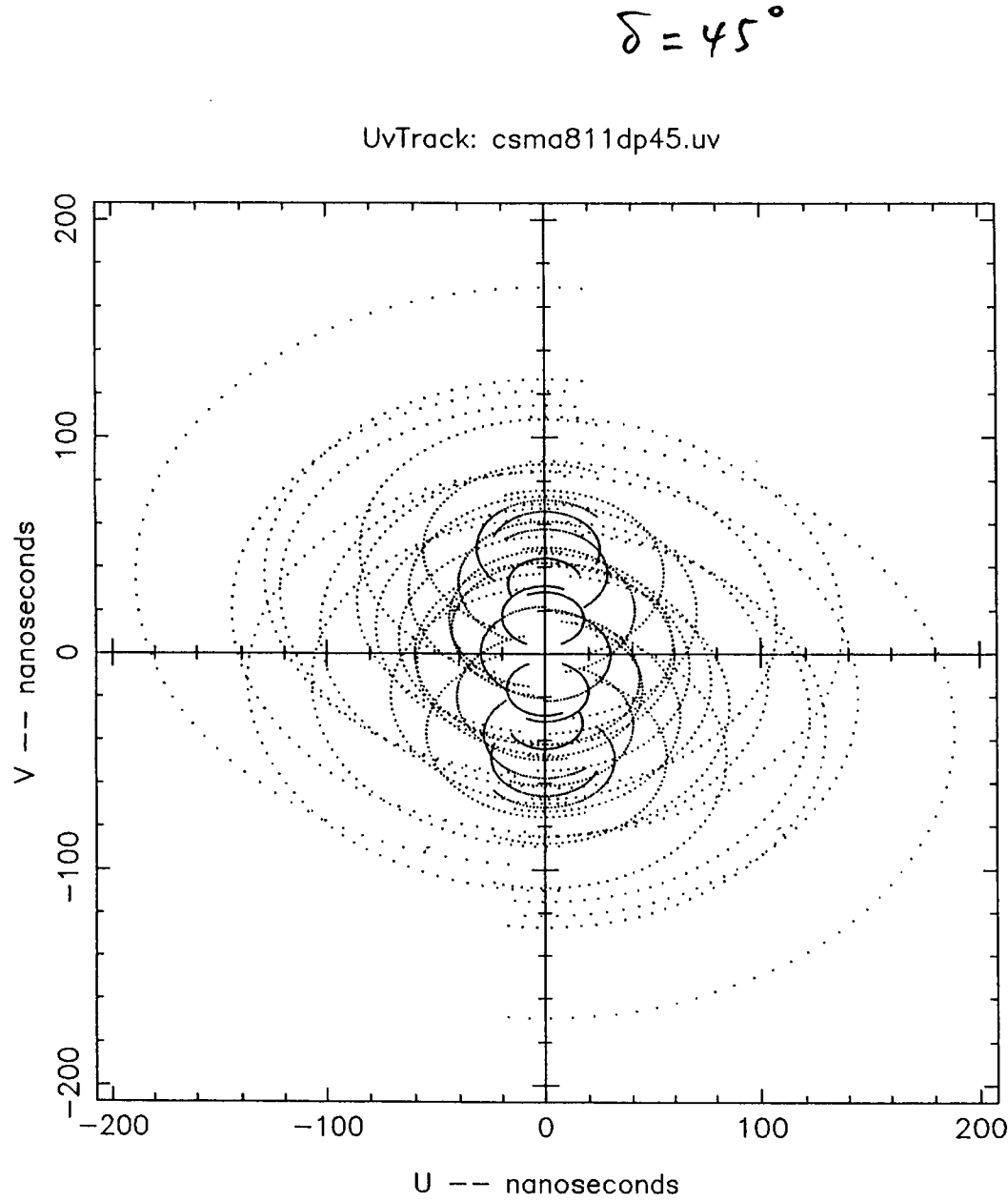


Fig.1-15

$$\delta = -29^\circ$$

UvTrack: csma811dn29.uv

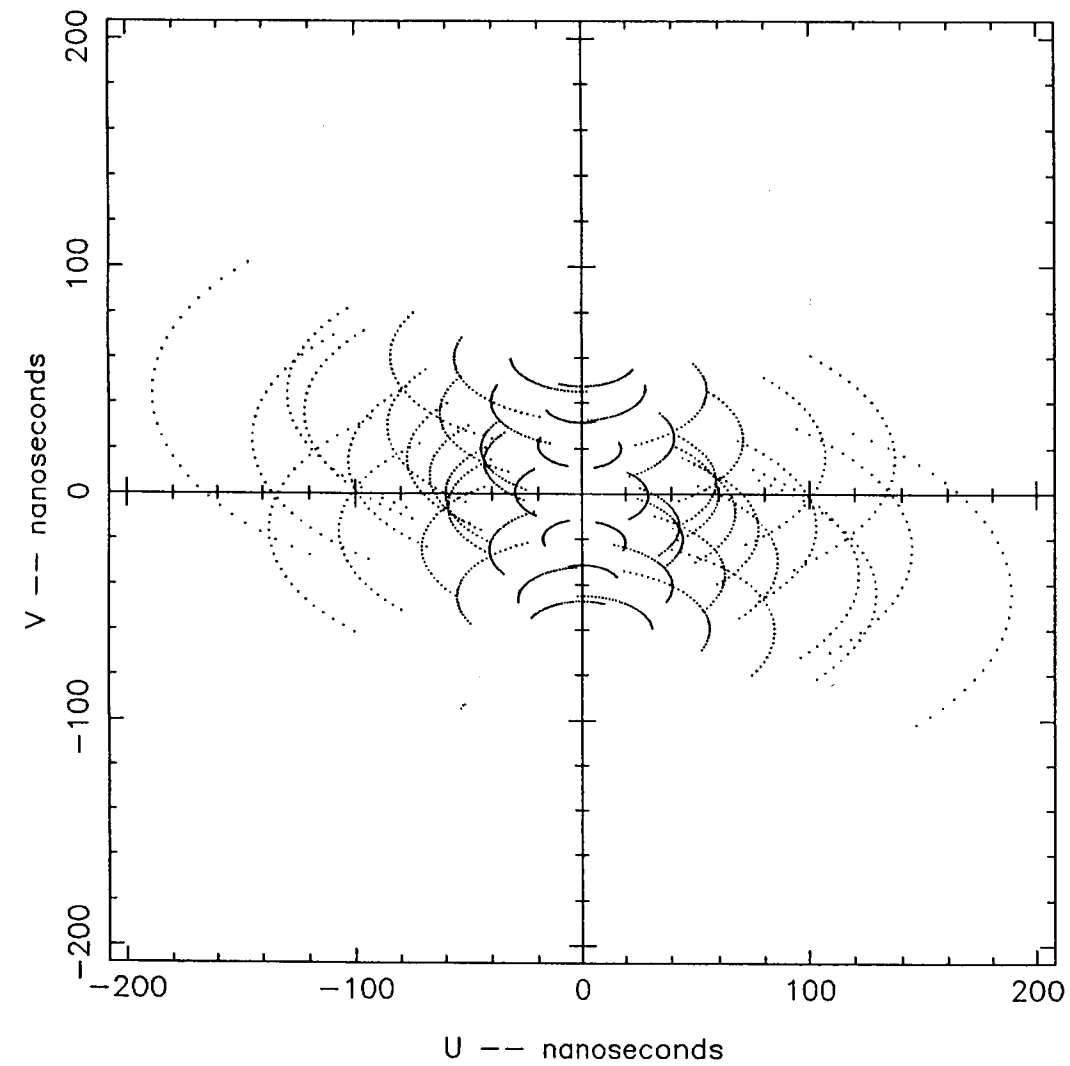
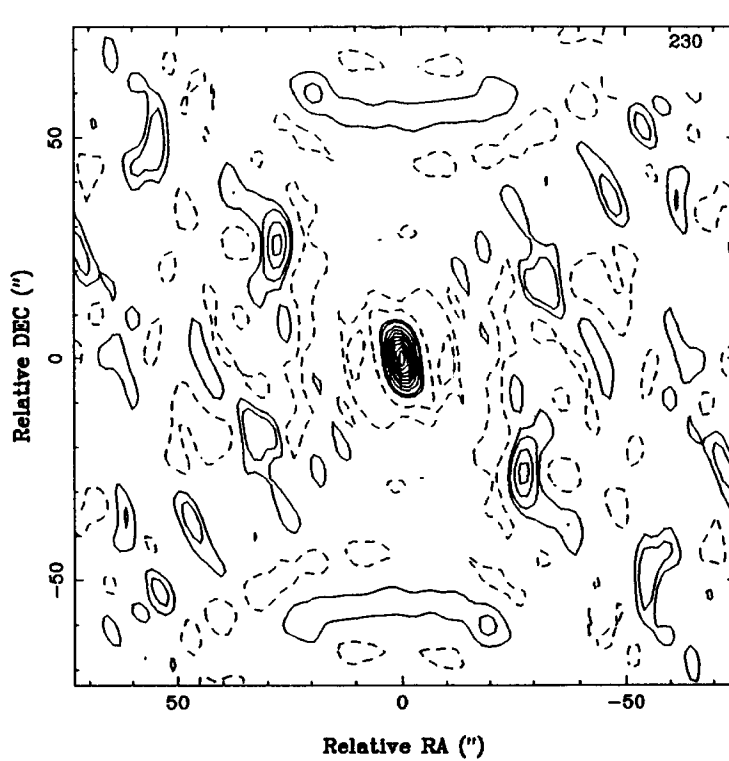
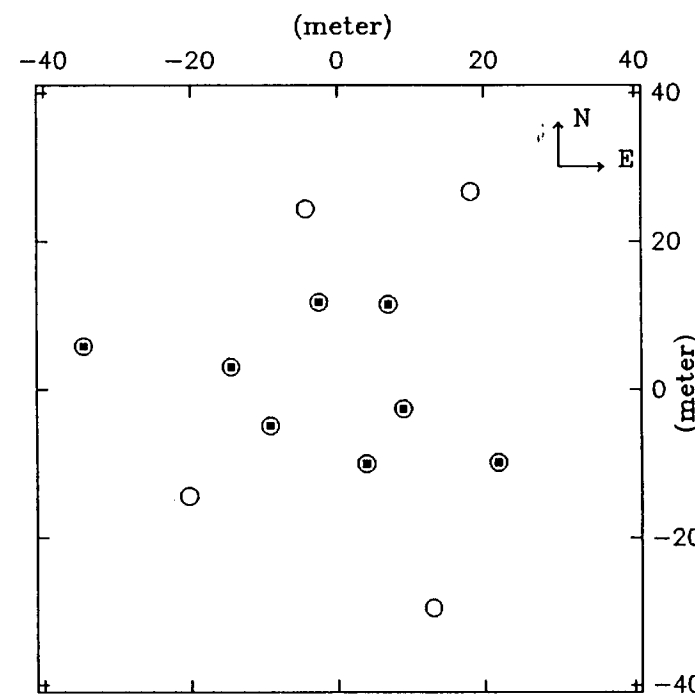


Fig. 1-16



decn29c

00:00:00.00 - 28:59:

File: csma811dn29.bm
Freq: 0.000000 (GHz)
Crval3: 230.0000 GHz
Max: 1.00000
Min: -0.127745
Units: JY/BEAM

Axes: 128 x 128 x 1
-1.50 x 1.50 x

Contours: 14

-0.200	-0.100
-0.050	0.050
0.100	0.200
0.300	0.400
0.500	0.600
0.700	0.800
0.900	1.000

$\delta = 45^\circ$

UvTrack: csma812dp45.uv

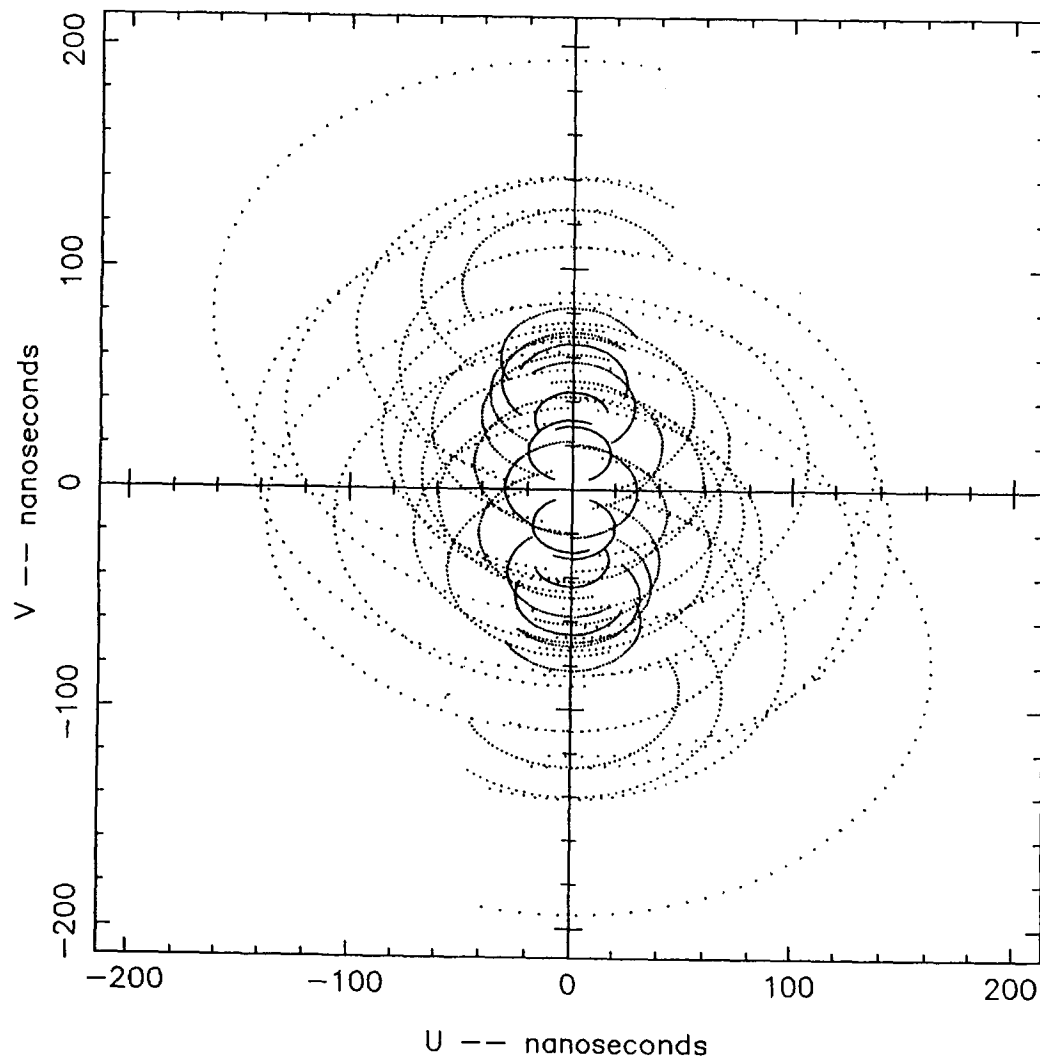
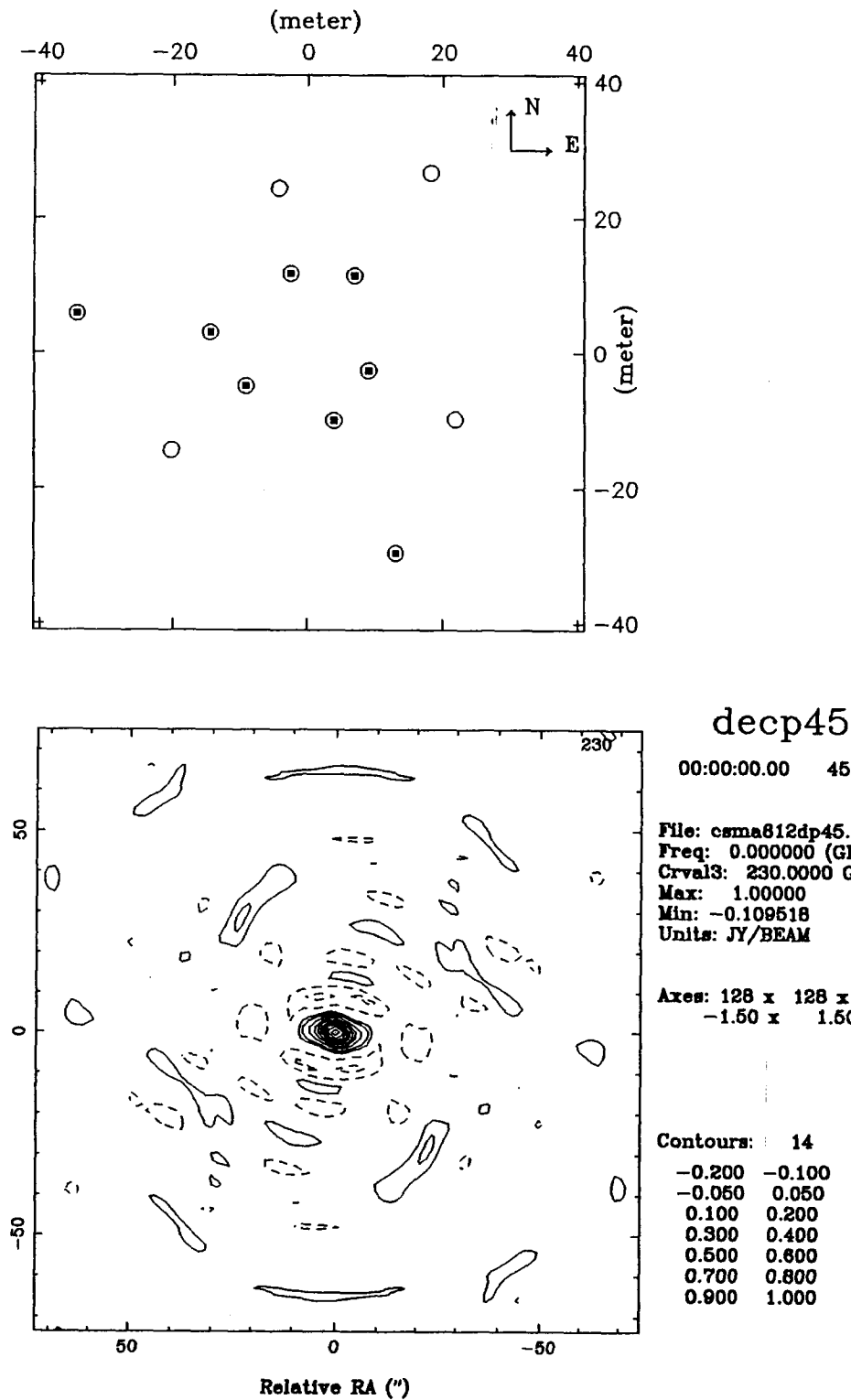


Fig. 1-17



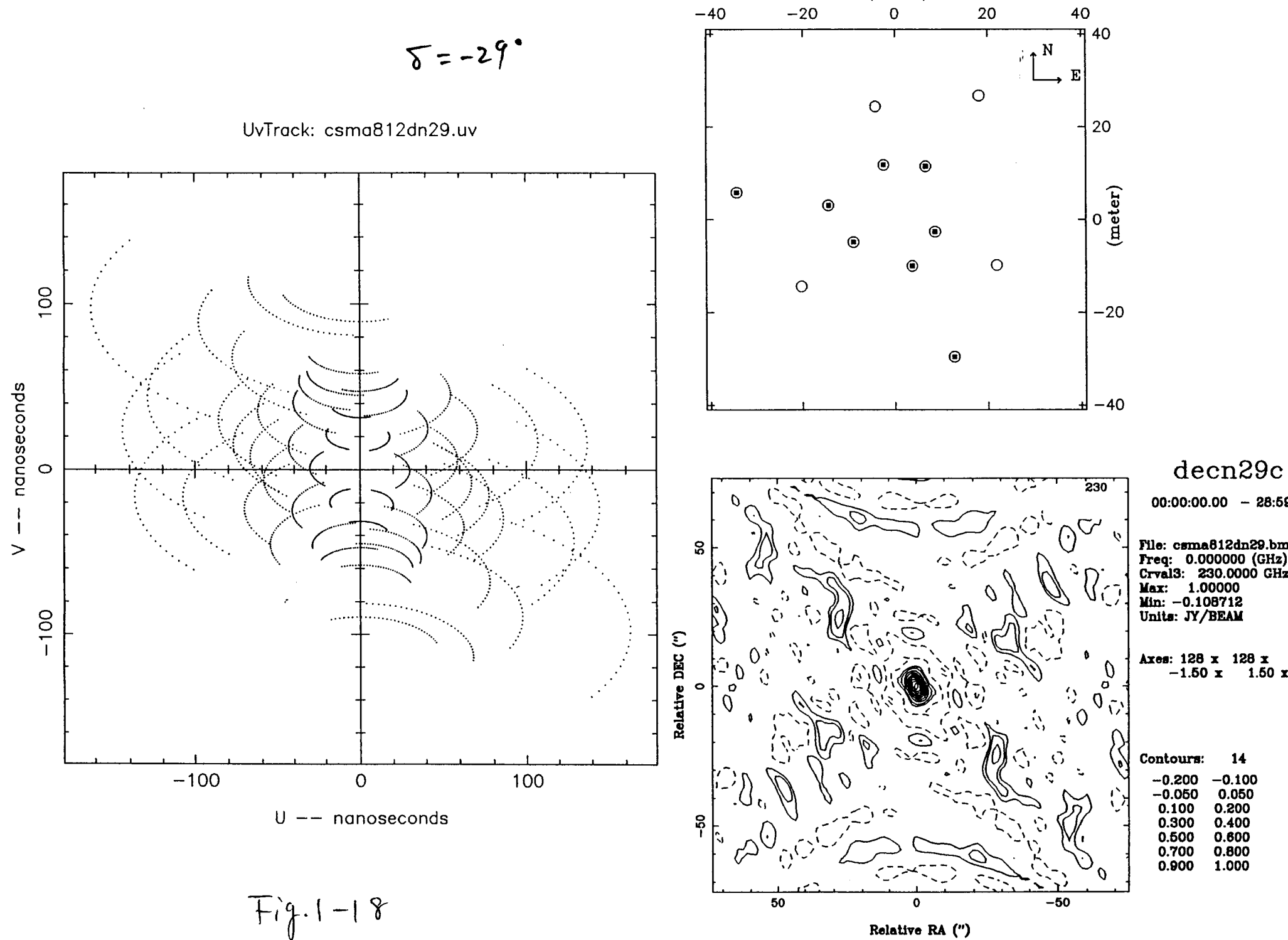


Fig. 1-18

$\delta = 45^\circ$

UvTrack: csma910dp45.uv

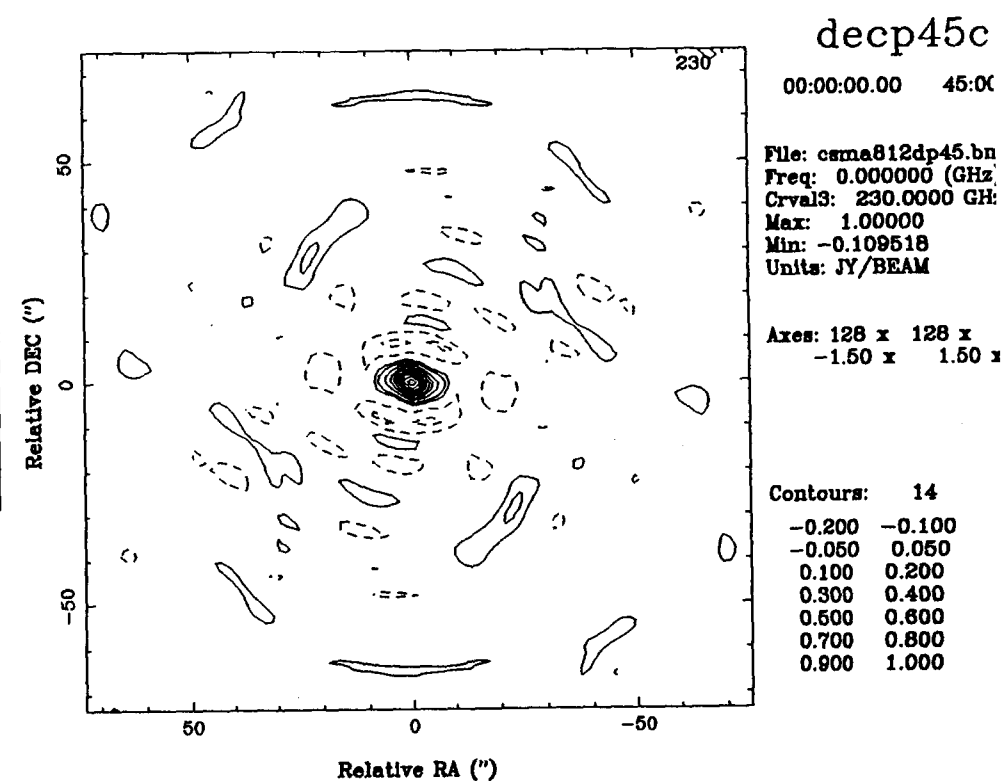
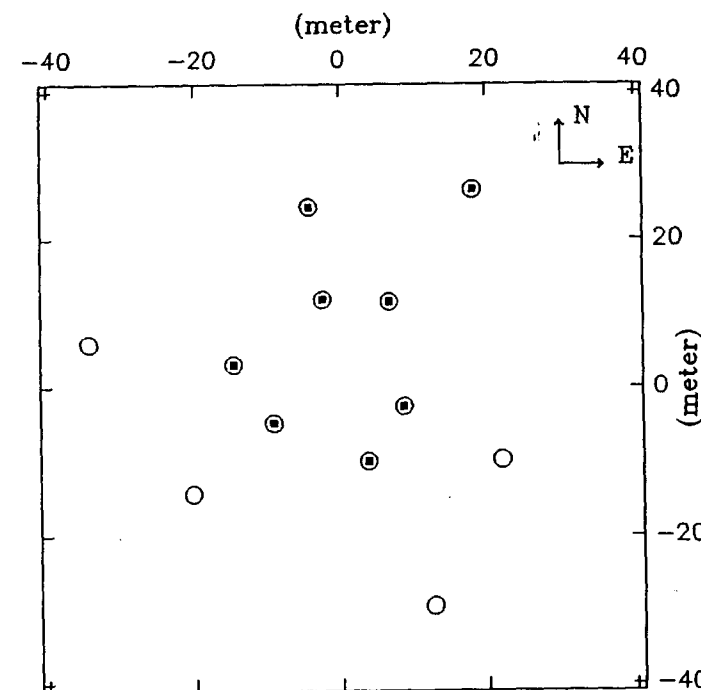
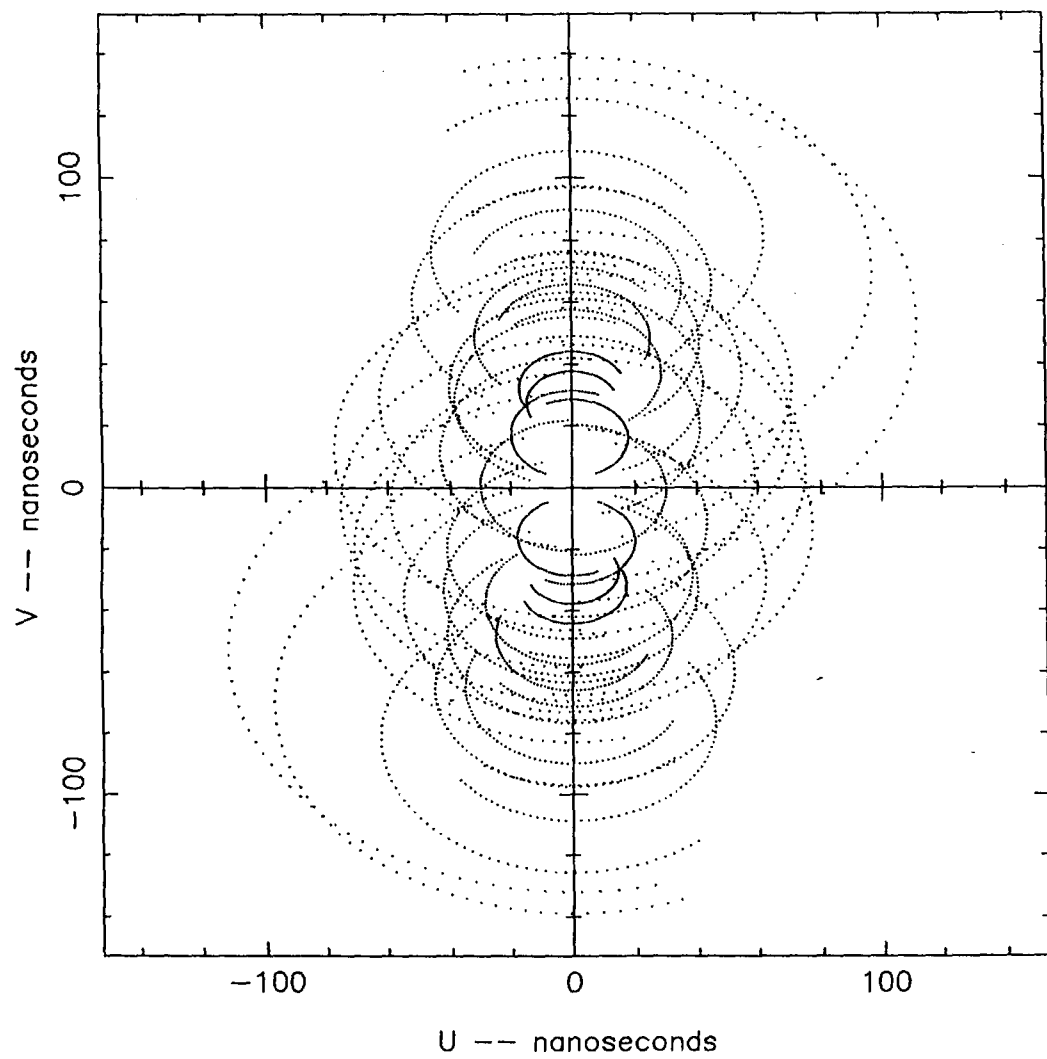


Fig. 1-19

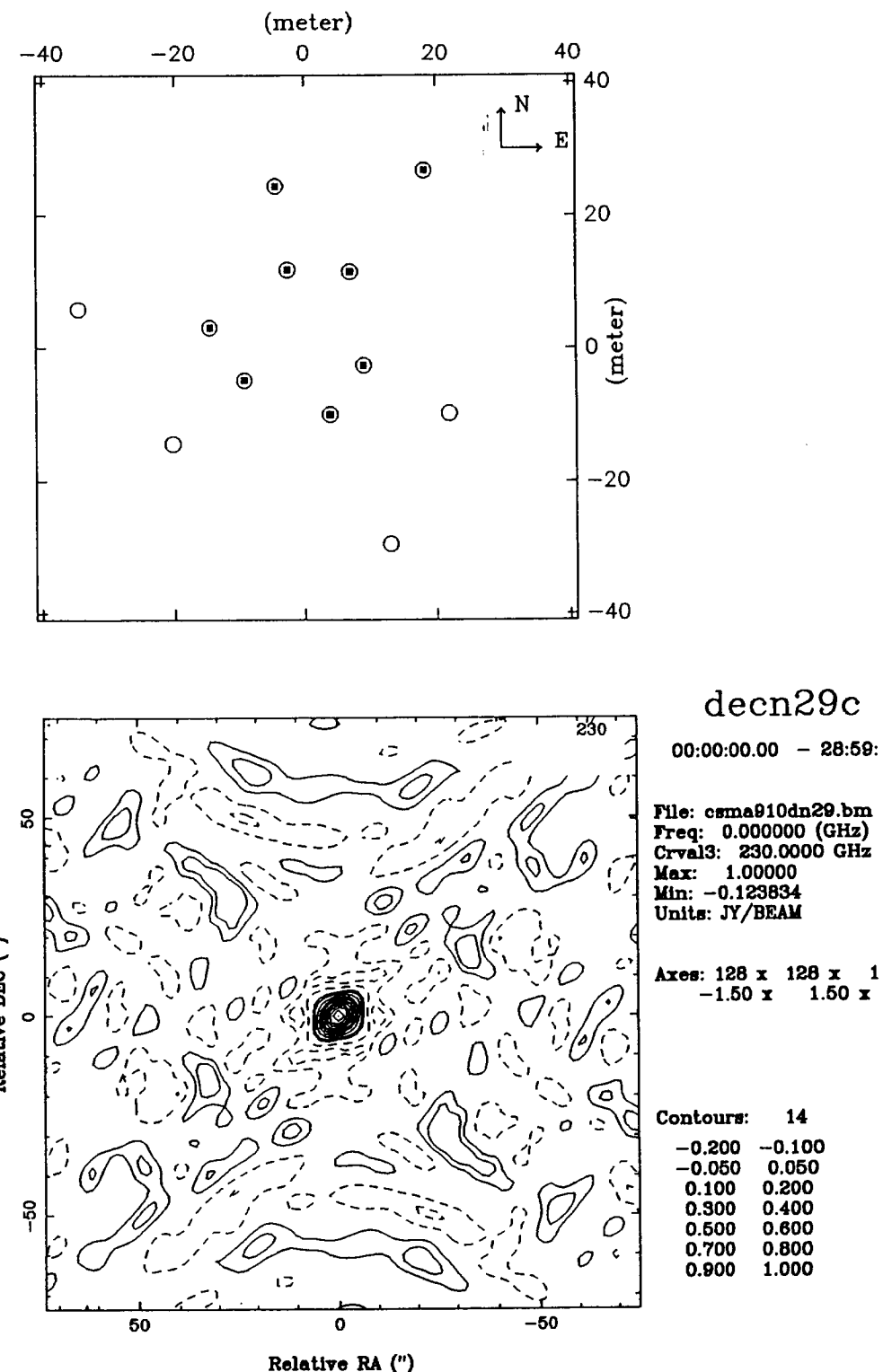
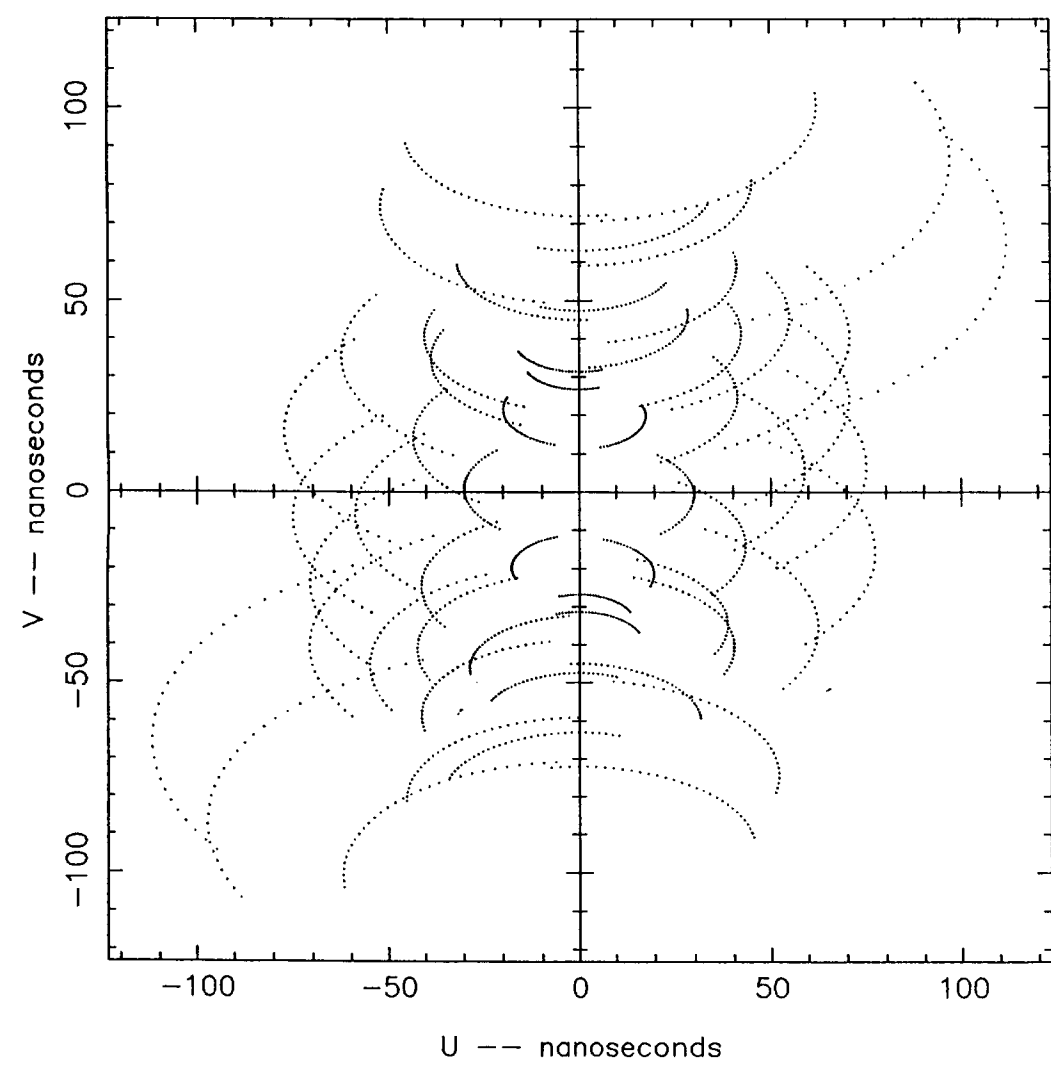


Fig. 1-20

$$\zeta = 45^\circ$$

UvTrack: csma911dp45.uv

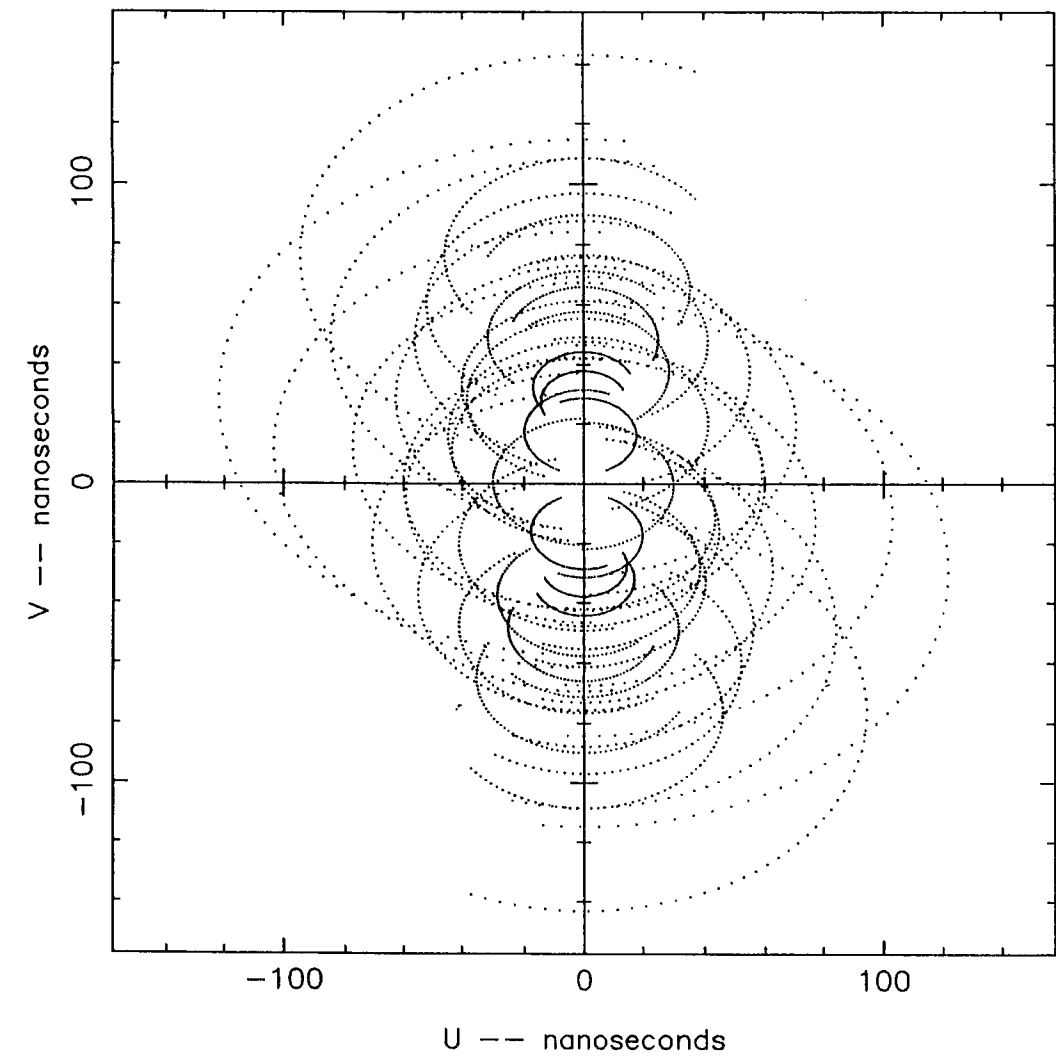
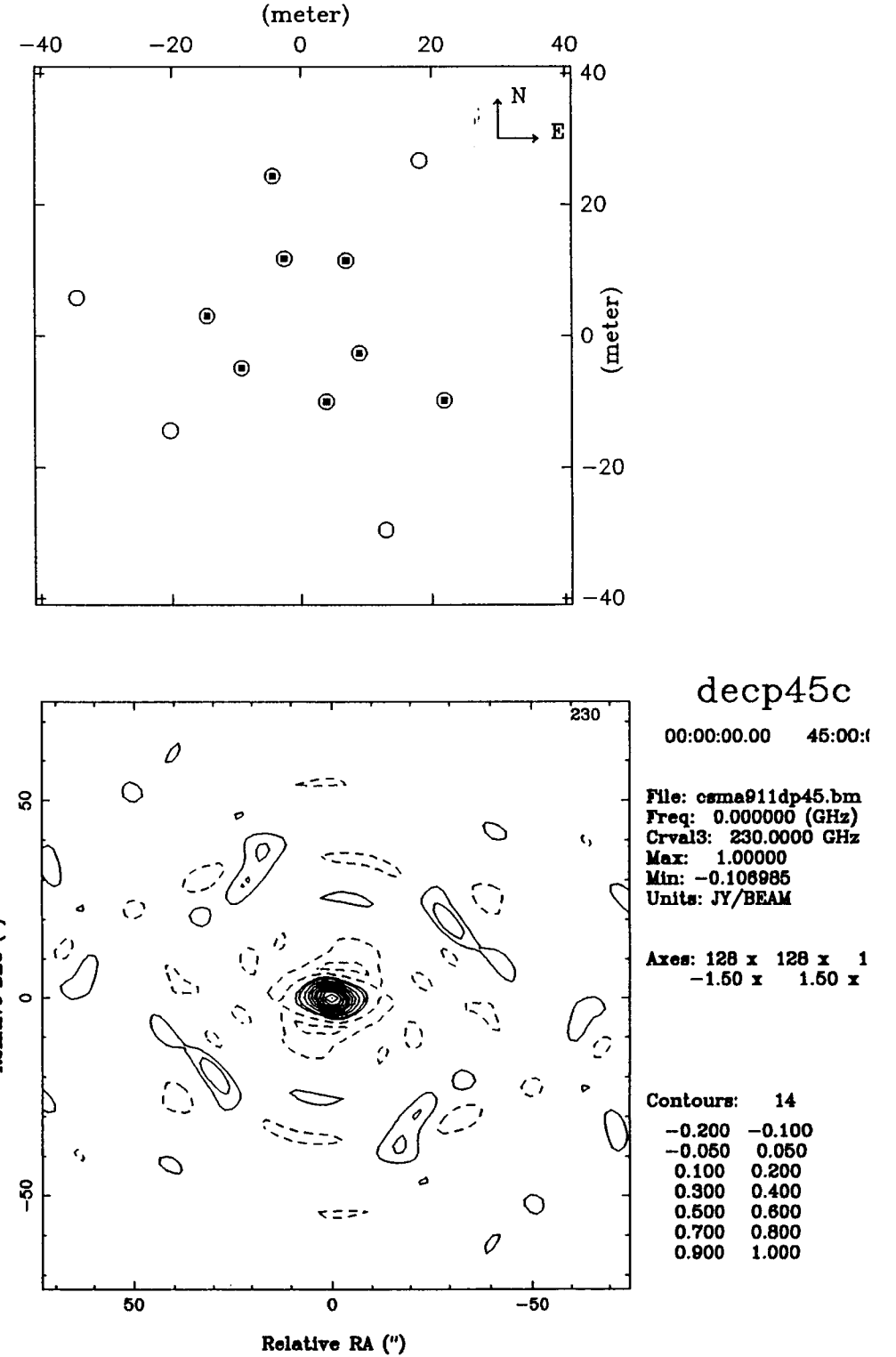


Fig. 1-21



$$\delta = -29^\circ$$

UvTrack: csma911dn29.uv

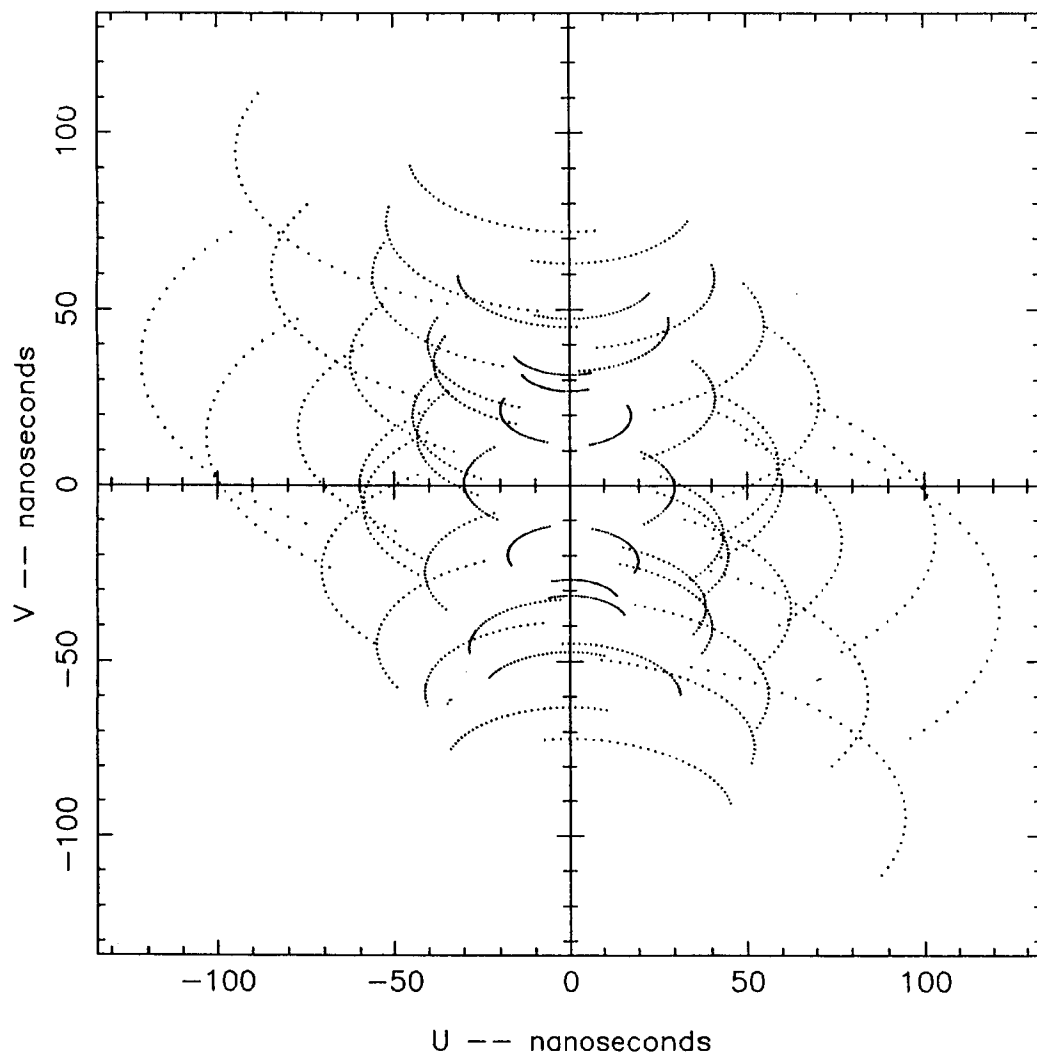
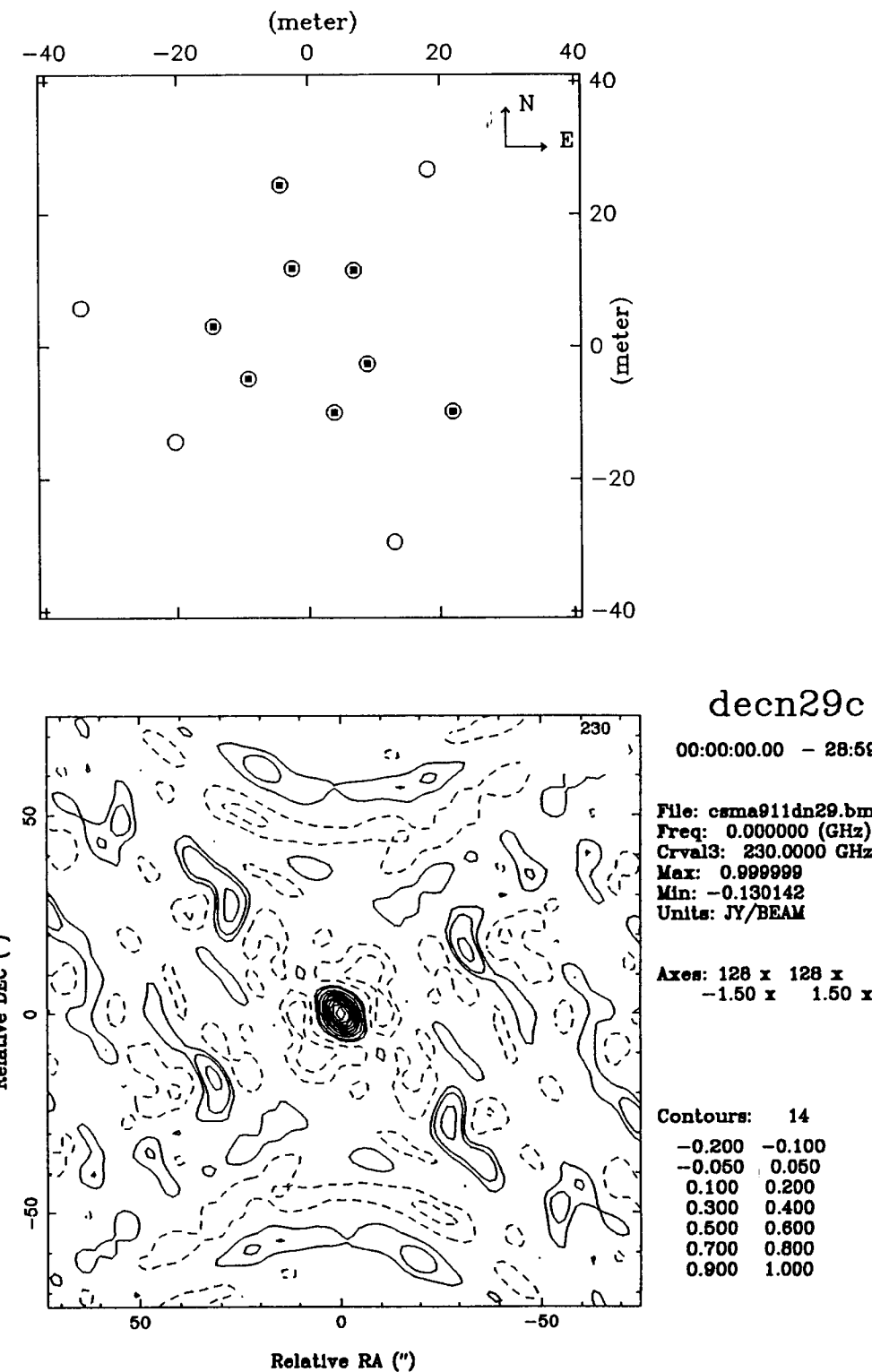
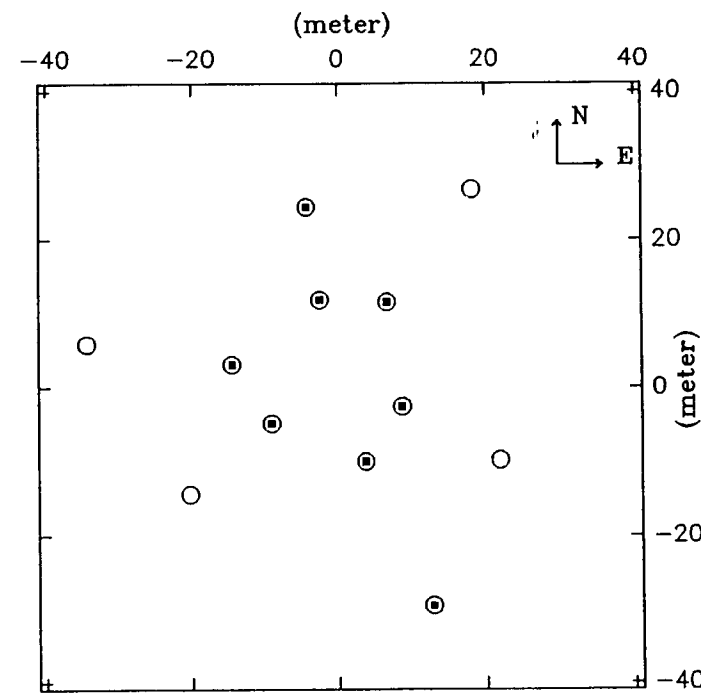
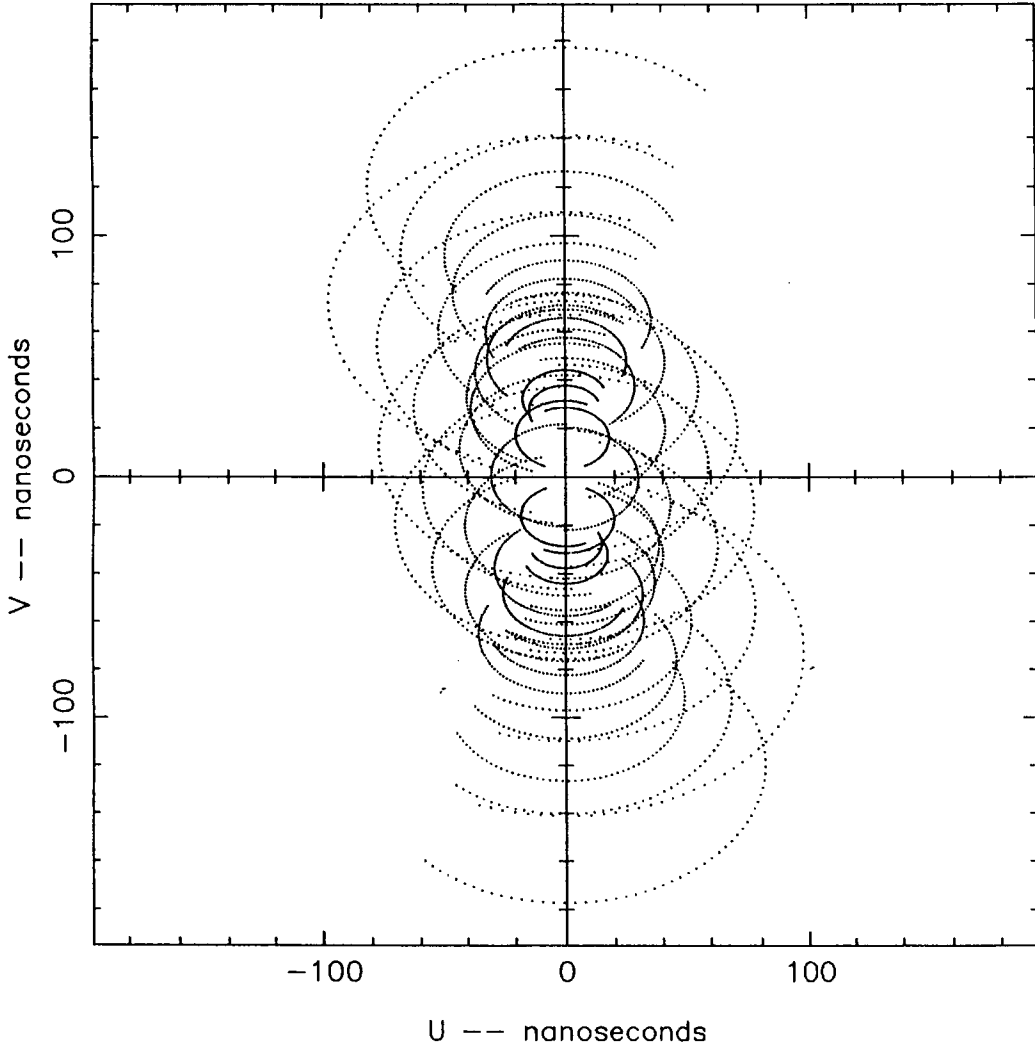


Fig. 1-22



$$\delta = 45^\circ$$

UvTrack: csma912dp45.uv



decp45c

00:00:00.00 45:00:00

File: csma912dp45.bm
Freq: 0.000000 (GHz)
Crval3: 230.0000 GHz
Max: 1.00000
Min: -0.120863
Units: JY/BEAM

Axes: 128 x 128 x 1
-1.50 x 1.50 x 1

Contours: 14

-0.200	-0.100
-0.050	0.050
0.100	0.200
0.300	0.400
0.500	0.600
0.700	0.800
0.900	1.000

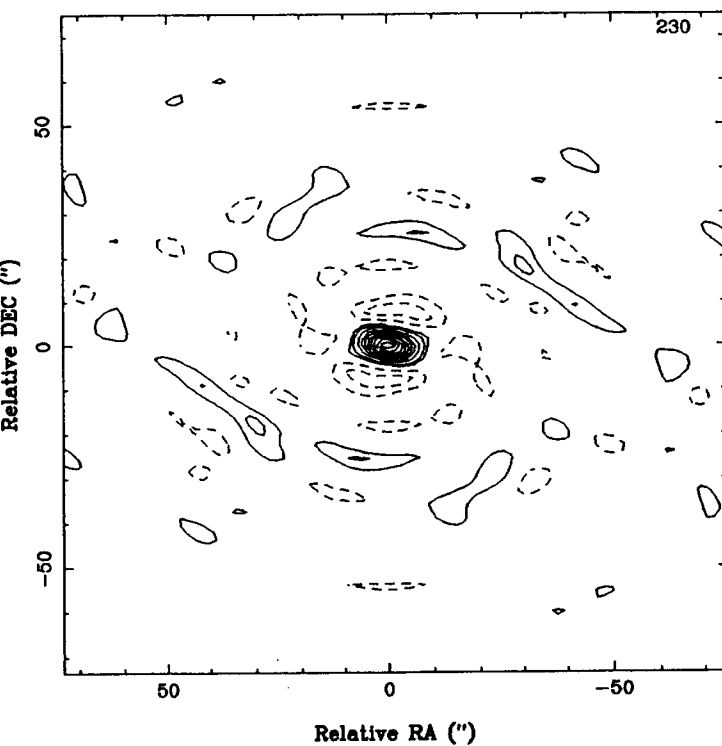
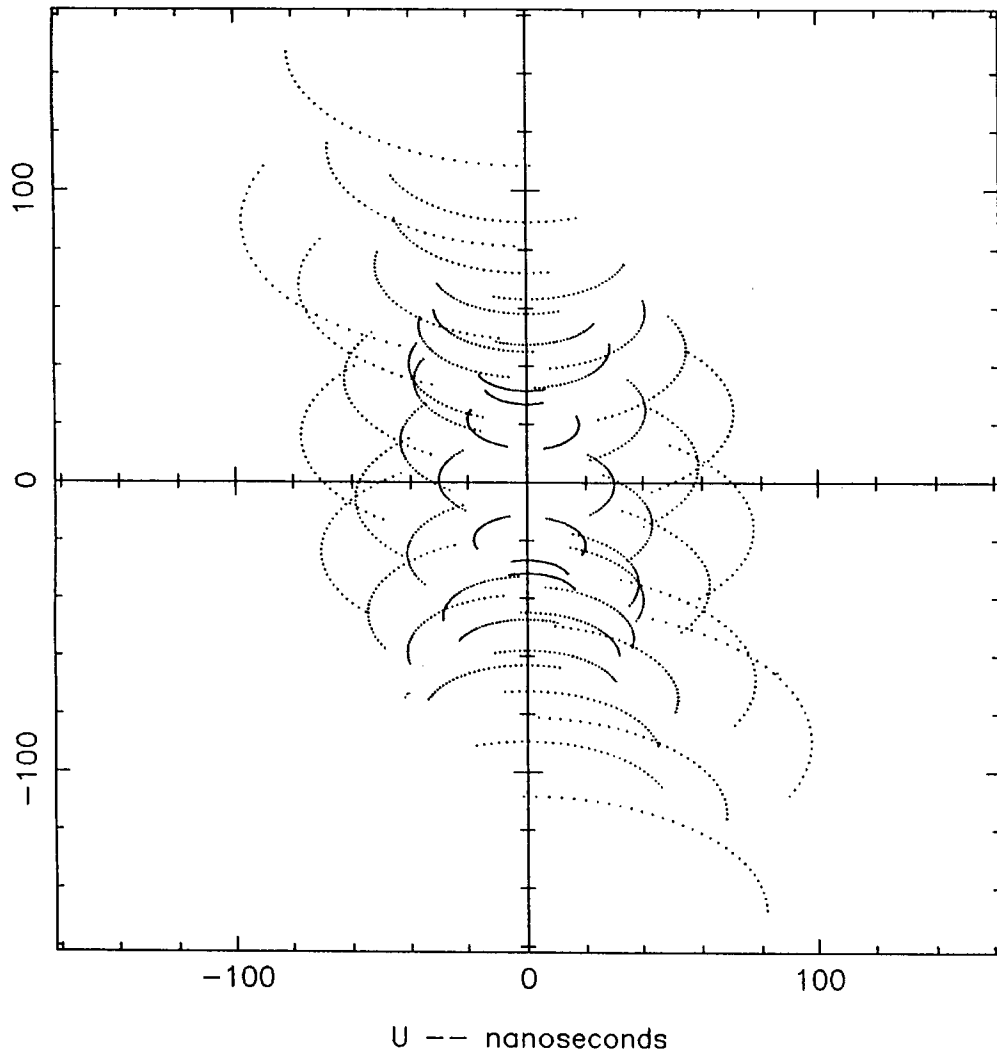


Fig. 1-23

$\delta = -29^\circ$

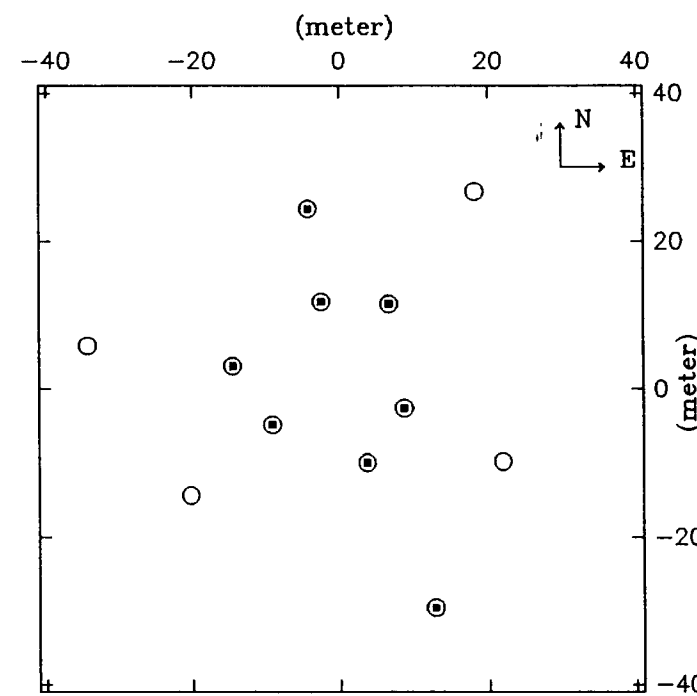
UvTrack: csma912dn29.uv

V --- nanoseconds



U -- nanoseconds

Fig 1-24



decn29c

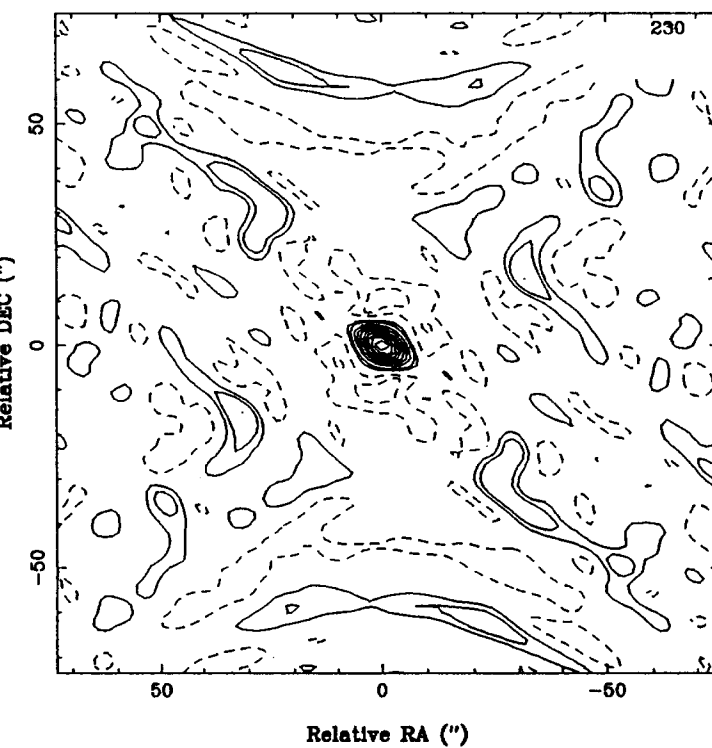
00:00:00.00 - 28:59:

File: csma912dn29.bm
Freq: 0.000000 (GHz)
Crval3: 230.0000 GHz
Max: 1.00000
Min: -0.121400
Units: JY/BEAM

Axes: 128 x 128 x 1
-1.50 x 1.50 x

Contours: 14

-0.200	-0.100
-0.050	0.050
0.100	0.200
0.300	0.400
0.500	0.600
0.700	0.800
0.900	1.000



Relative RA (")

$\delta = +45^\circ$

UvTrack: csma1011dp45.uv

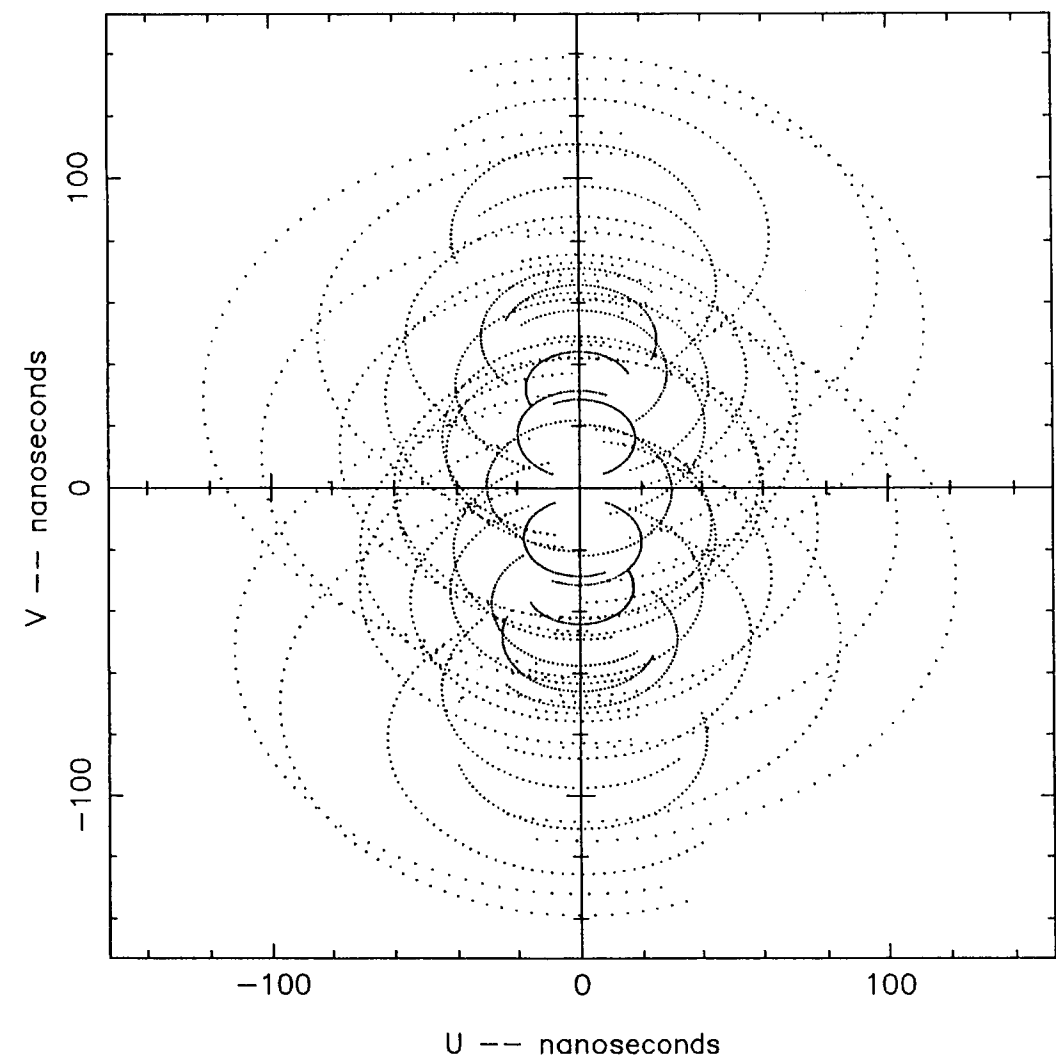
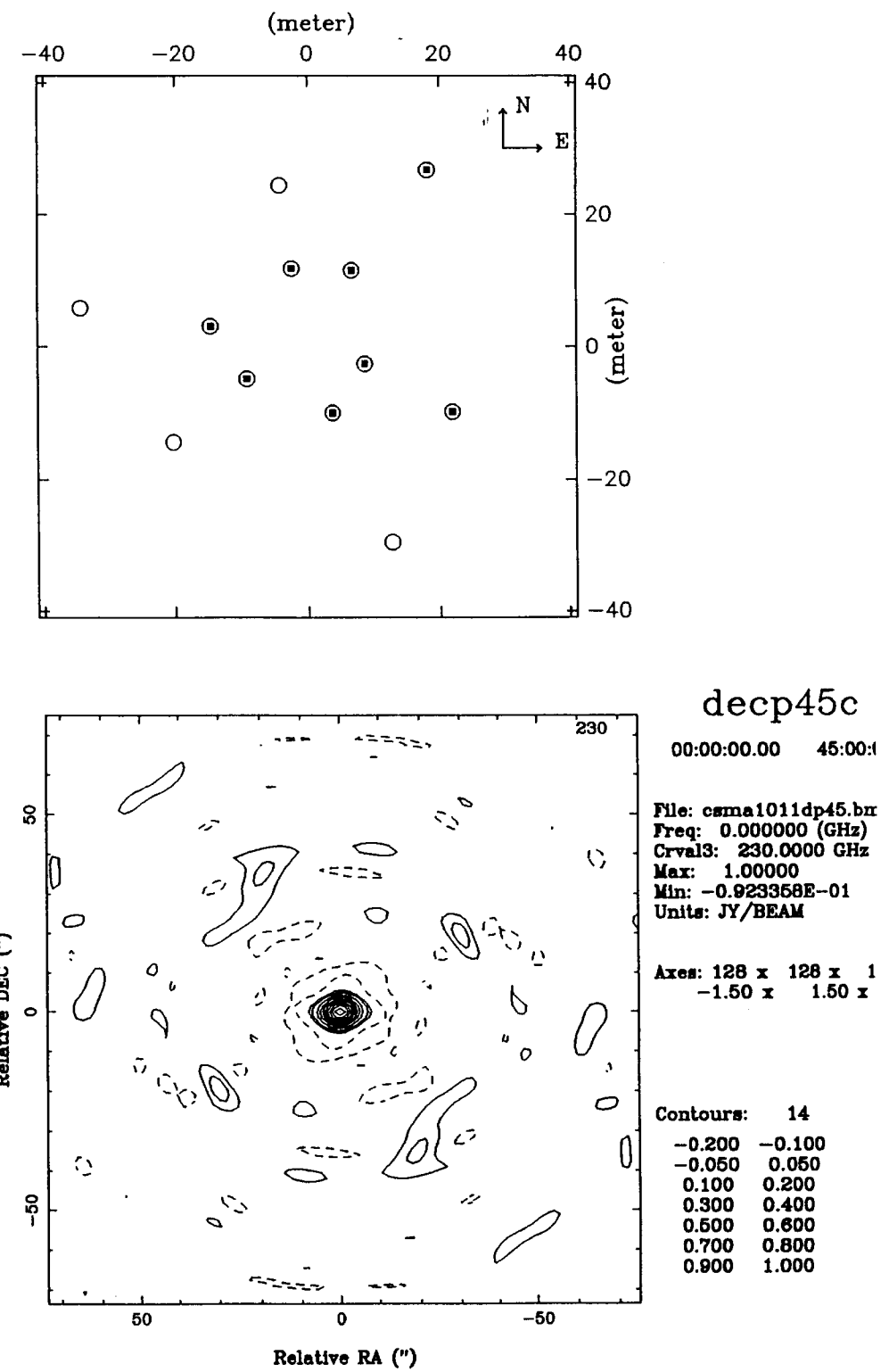


Fig. 1-25



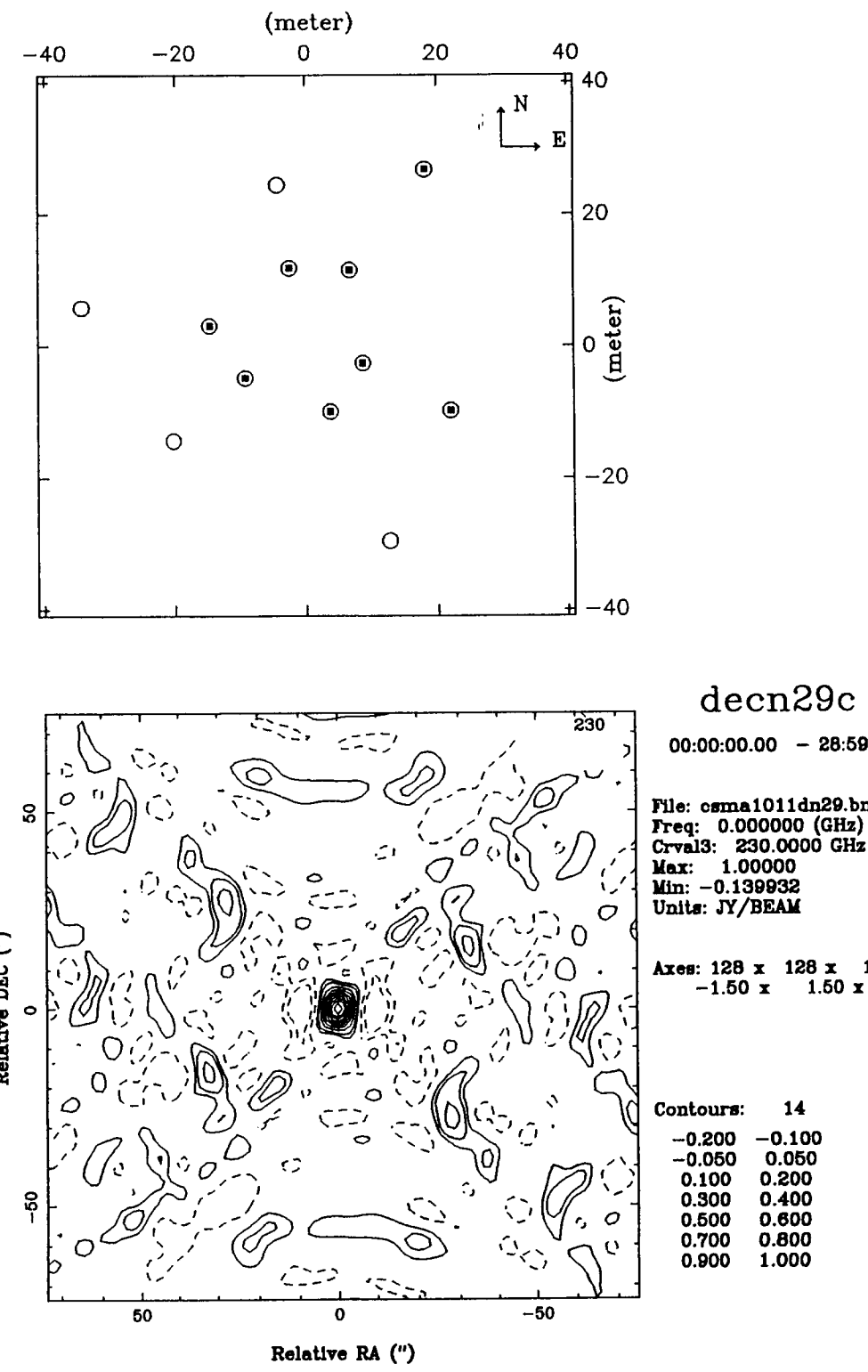
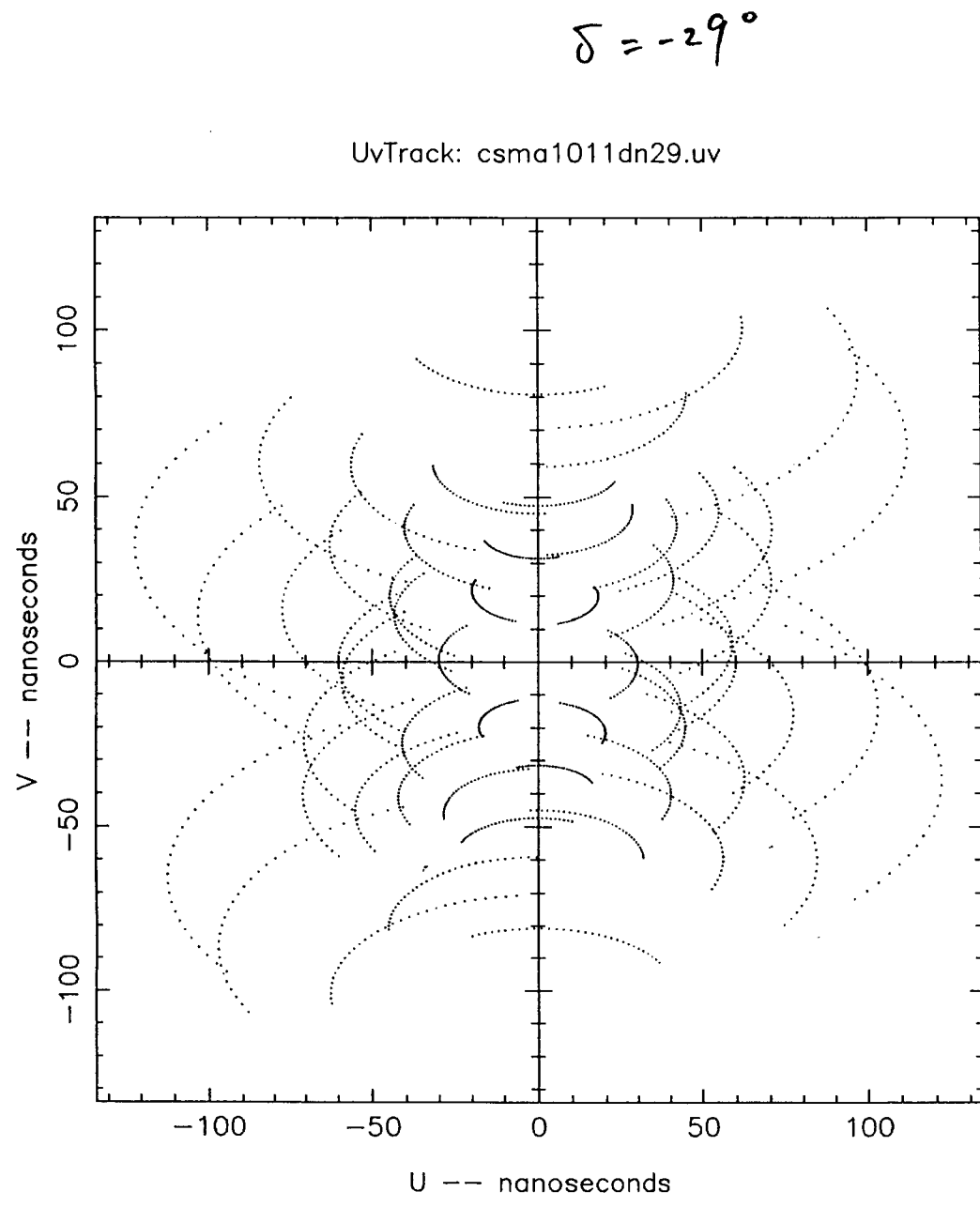


Fig.1-26

$\delta = 45^\circ$

UvTrack: csma1012dp45.uv

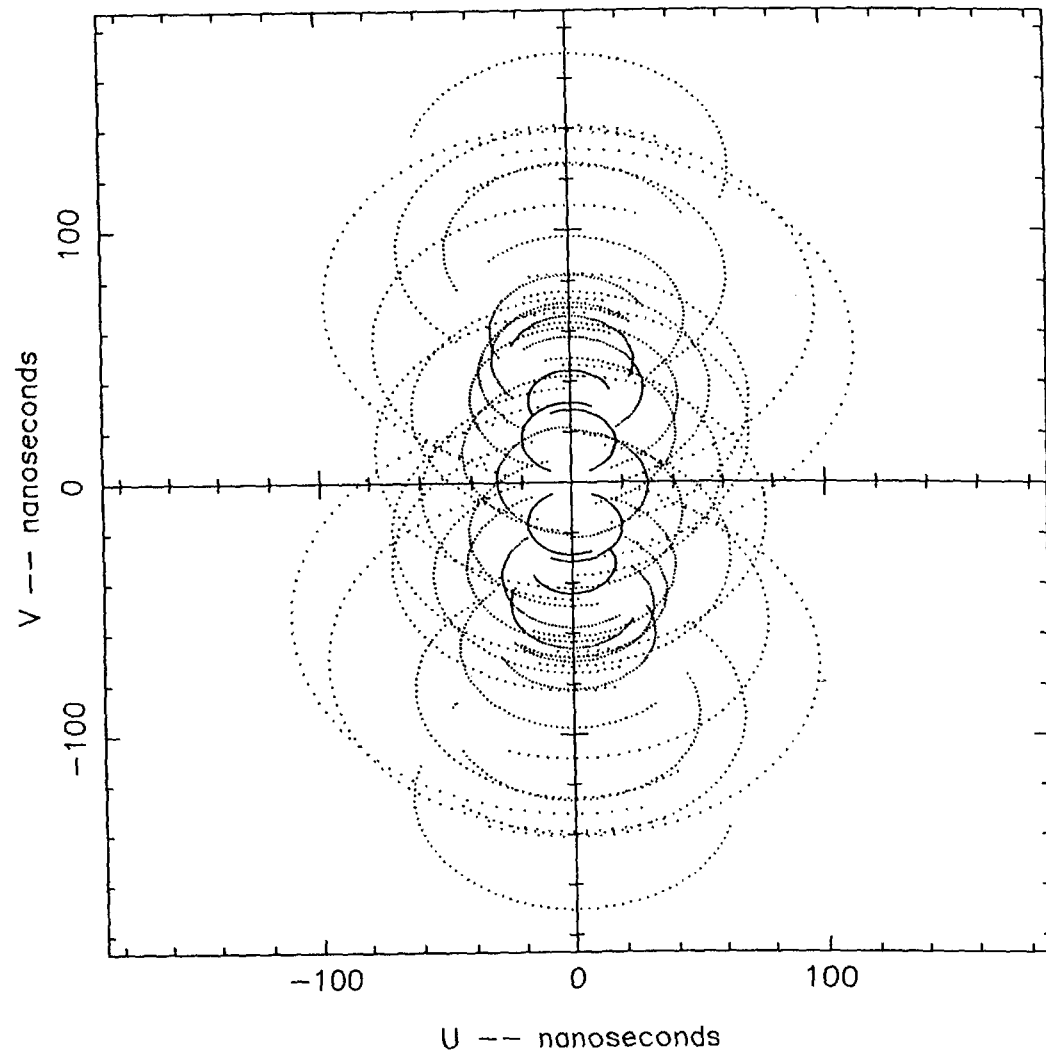
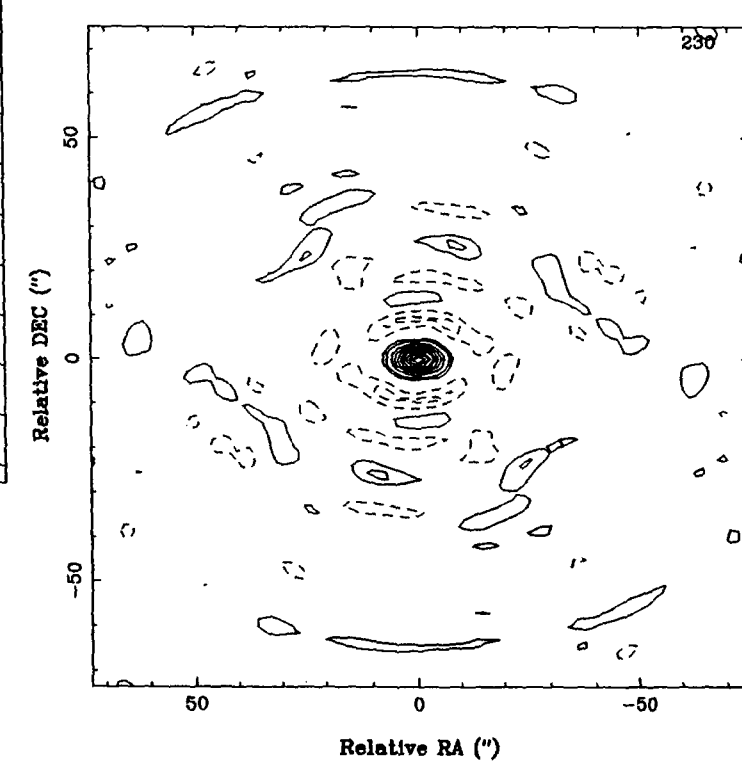
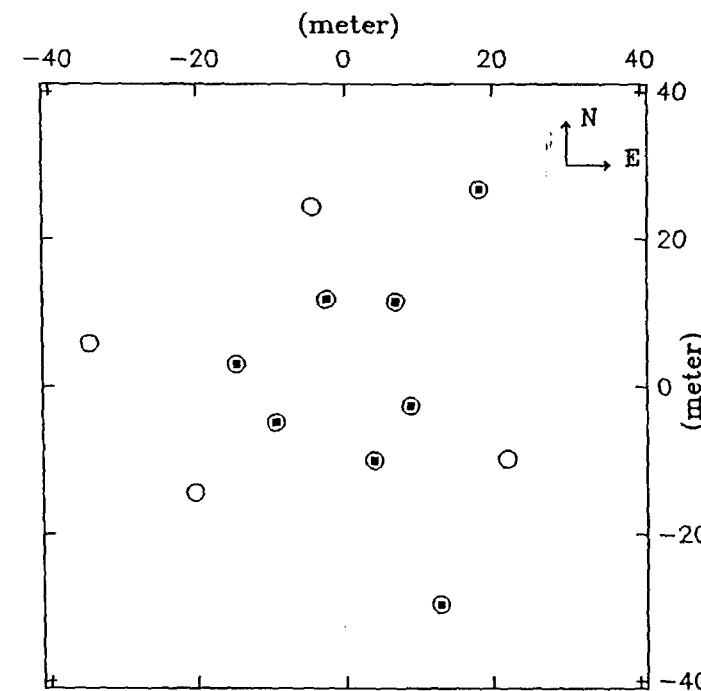


Fig 1-27



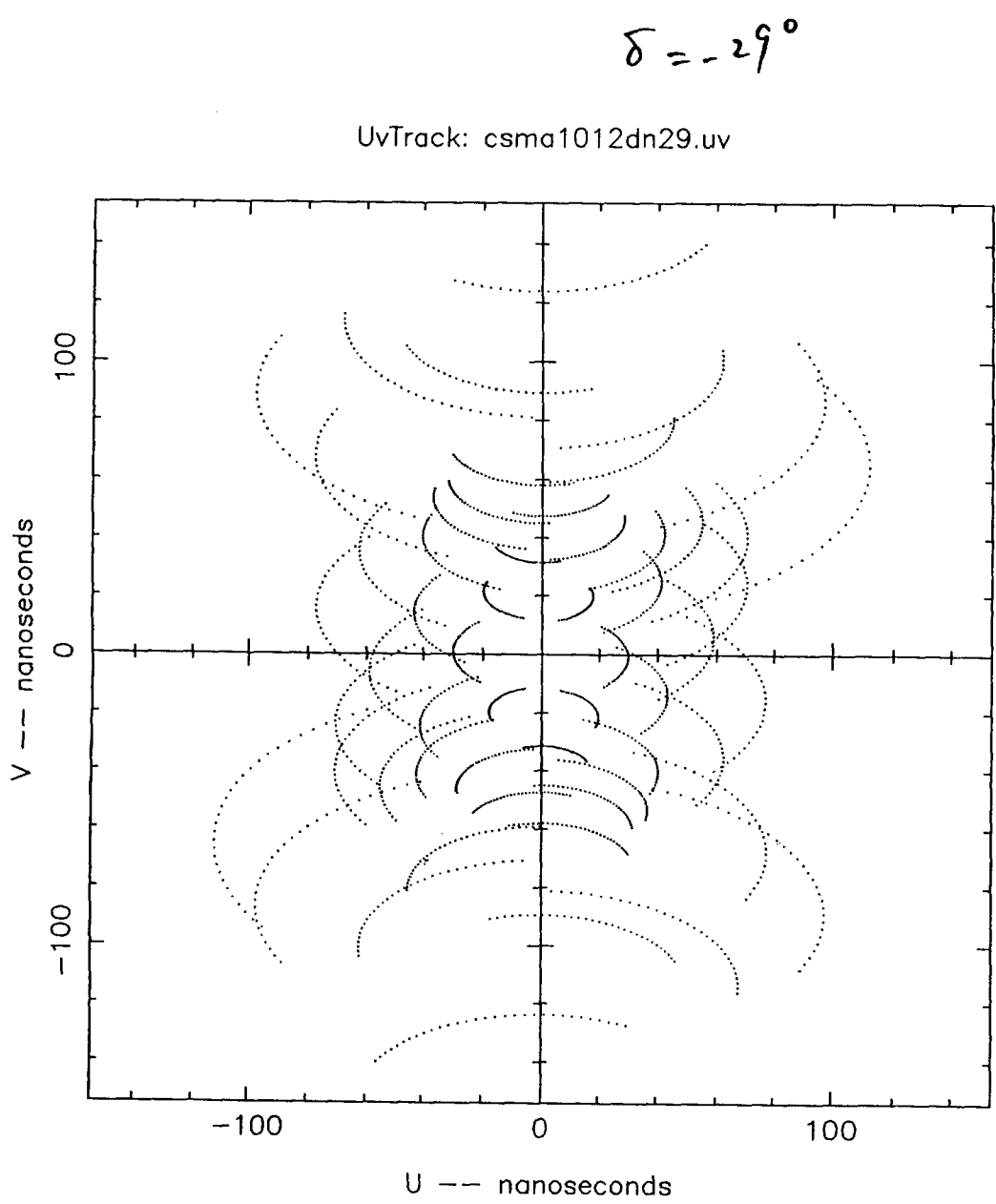
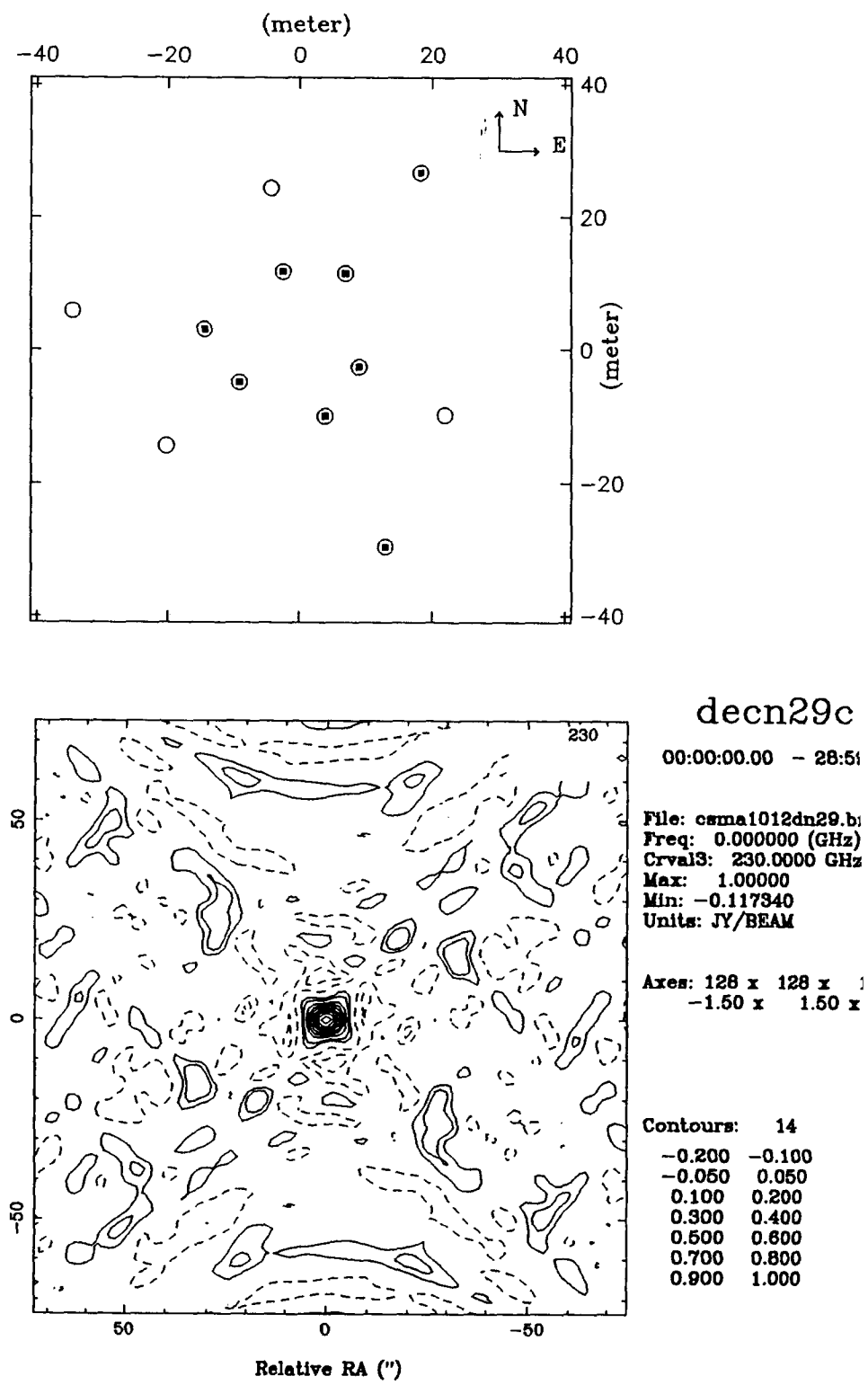


Fig. 1-28



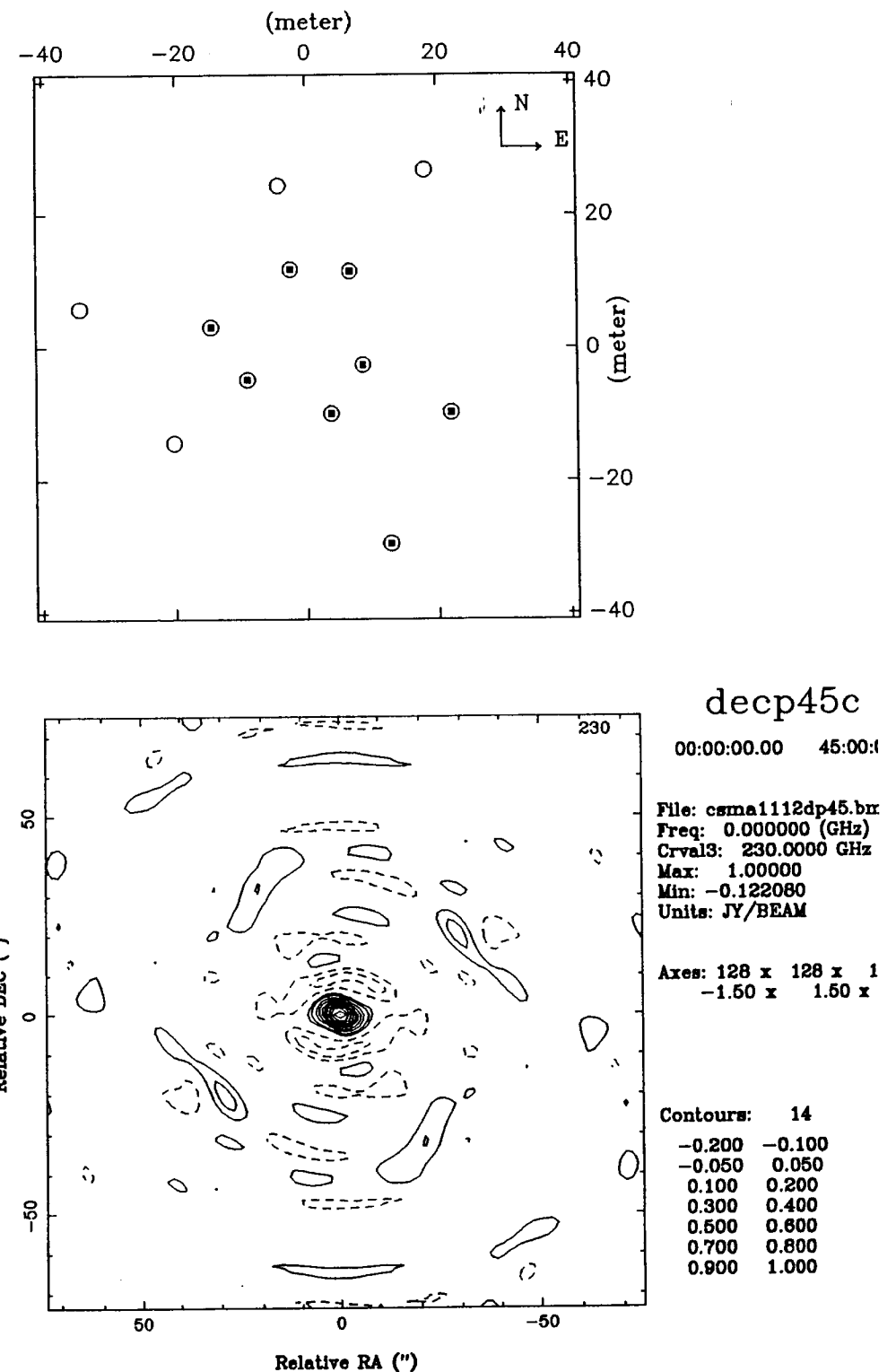
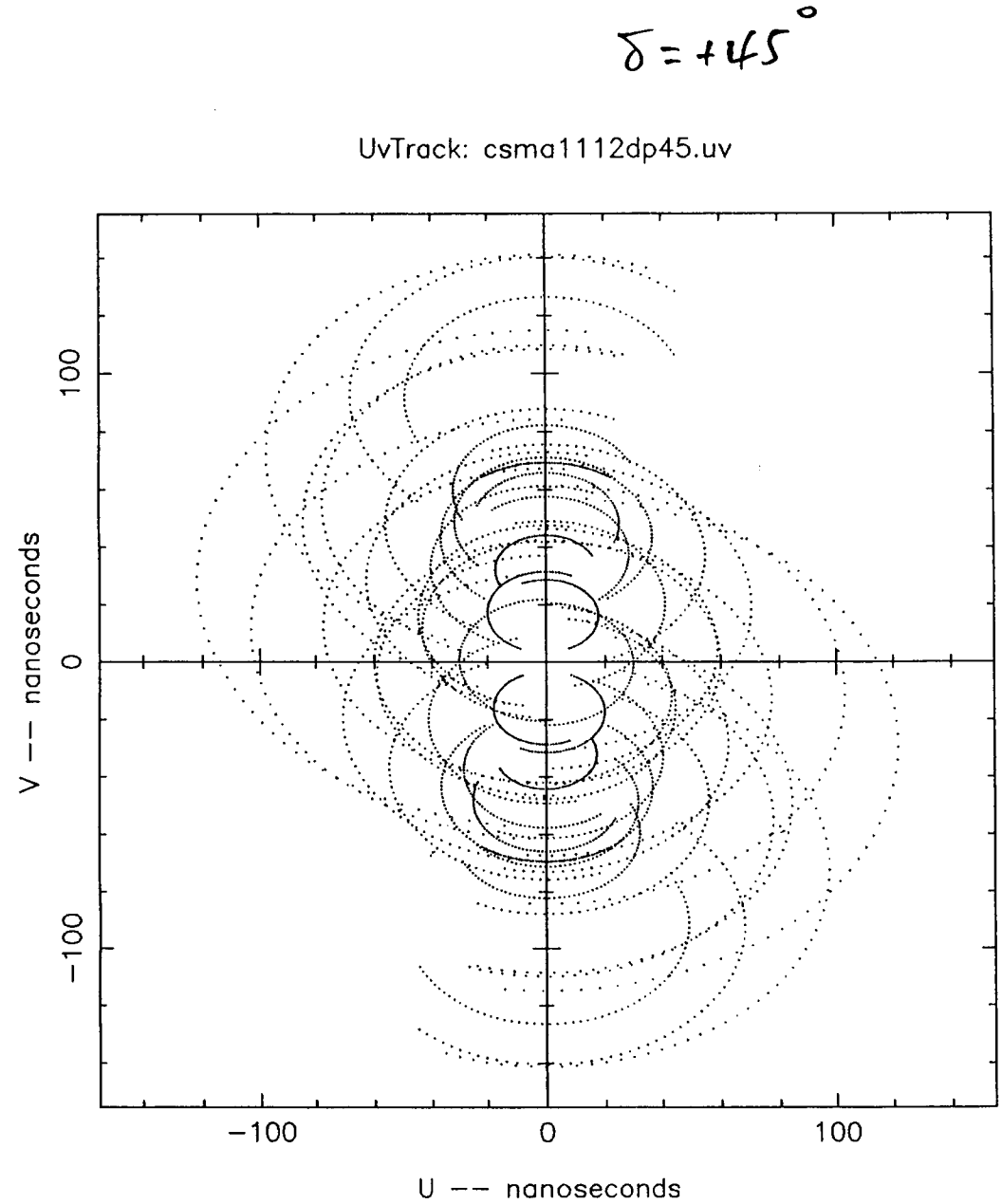
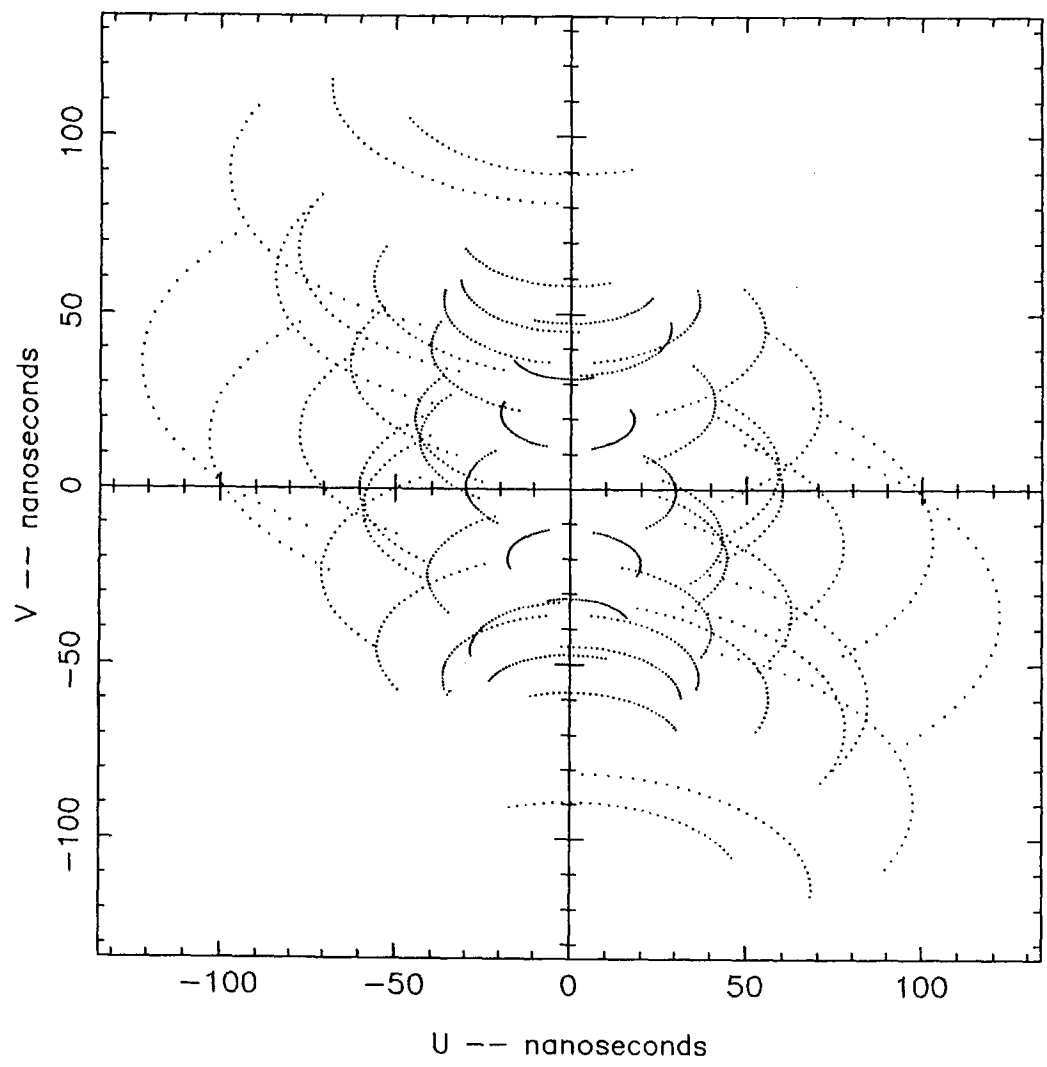


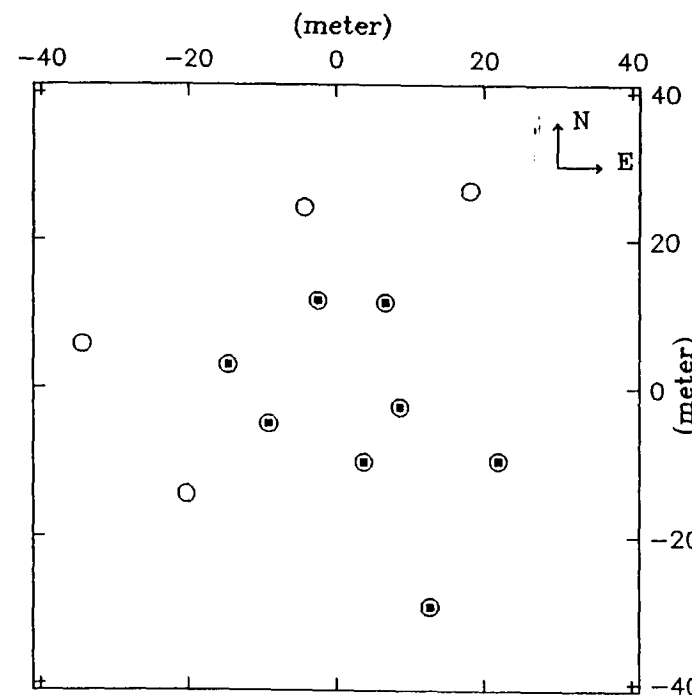
Fig. 1-29

UvTrack: csma11112dn29.uv



$$\delta = -29^\circ$$

Fig 1-30



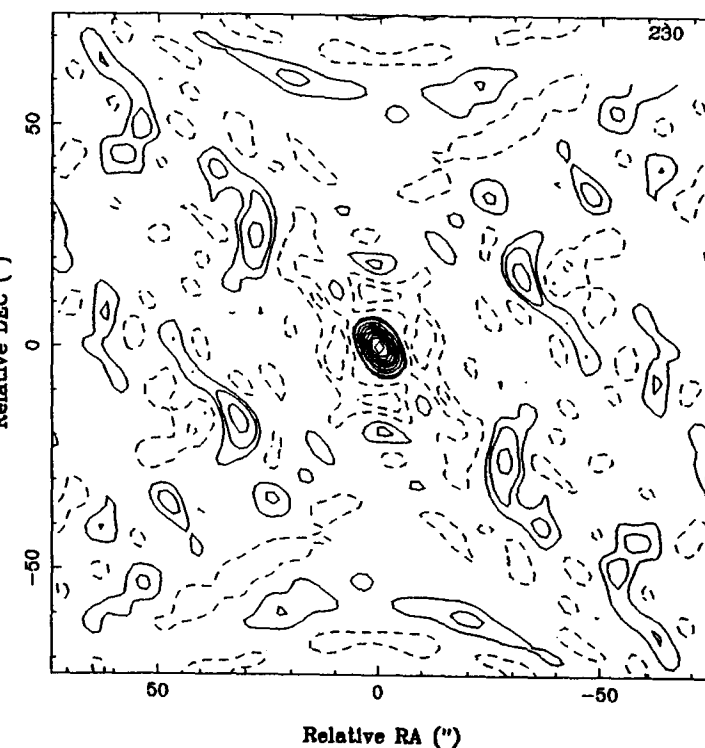
decn29c

00:00:00.00 - 28:59:

File: csma1112dn29.bnr
Freq: 0.000000 (GHz)
Crval3: 230.0000 GHz
Max: 0.999999
Min: -0.132963
Units: JY/BEAM

Axes: 128 x 128 x 1
-1.50 x 1.50 x

Contours: 14
-0.200 -0.100
-0.050 0.050
0.100 0.200
0.300 0.400
0.500 0.600
0.700 0.800
0.900 1.000



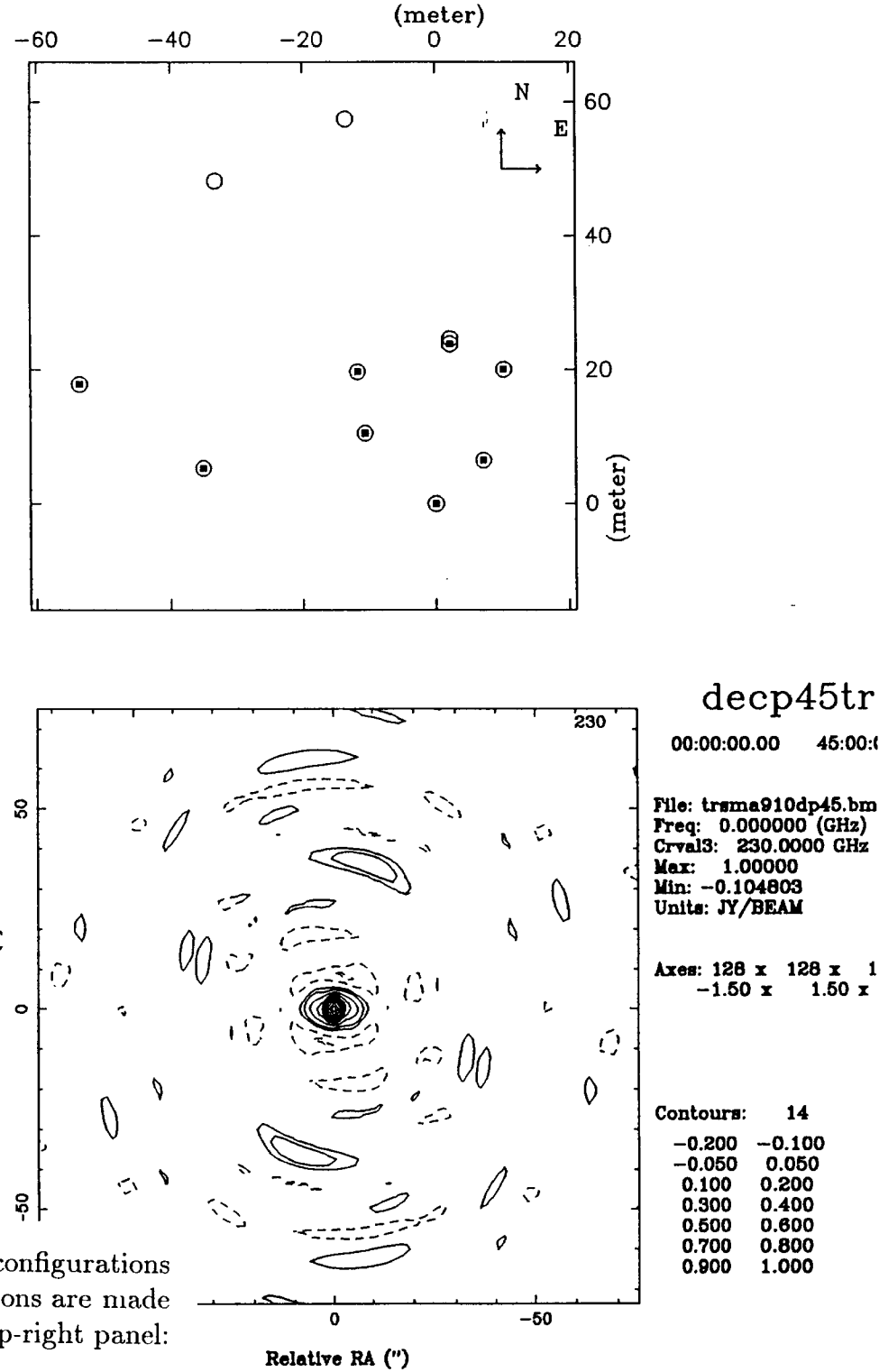
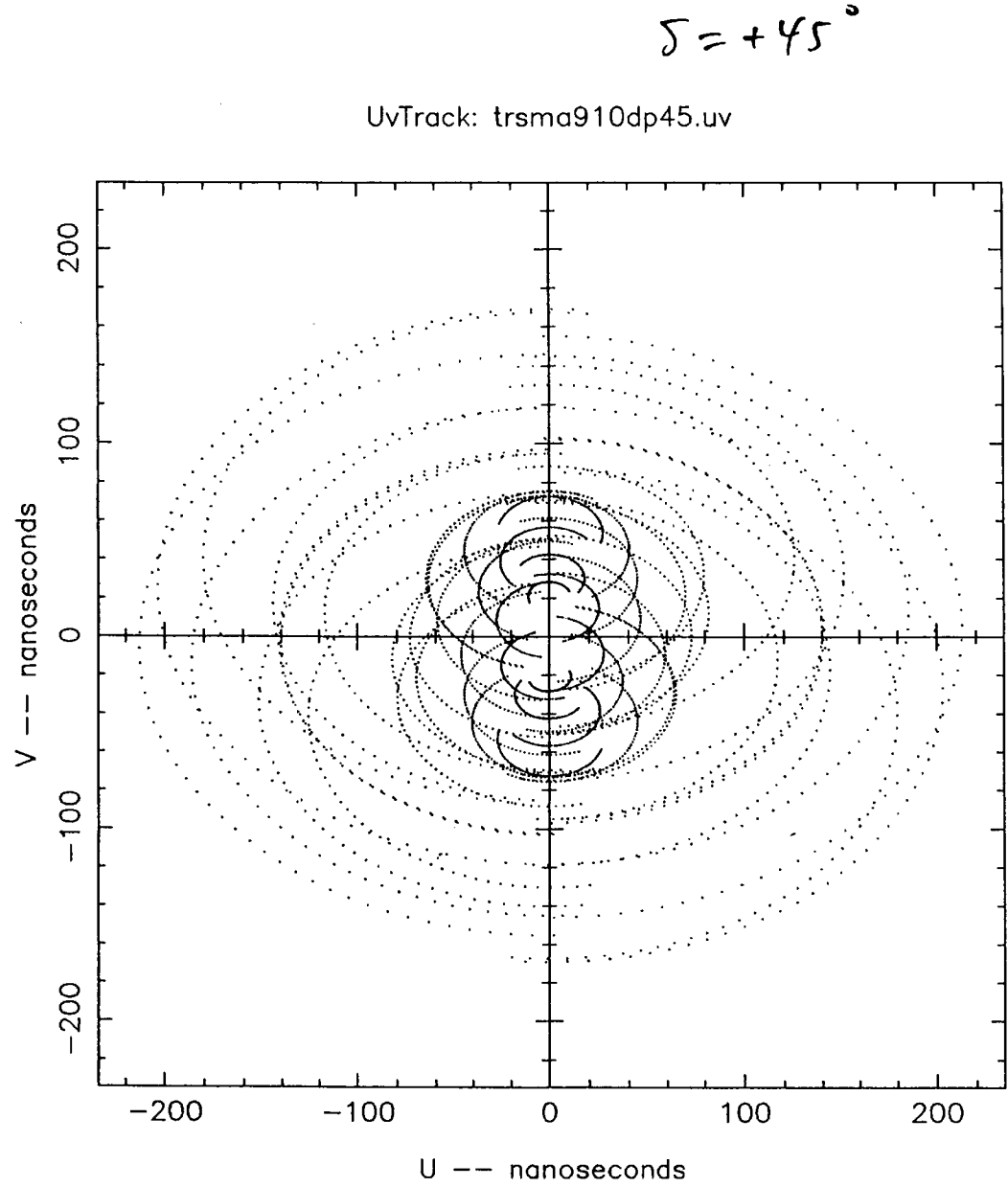


Fig. 2: A total of 6 tangential configurations, where 2 adjacent triangular configurations shared 2 common pads. Simulations of synthesis beams of these configurations are made for the two declinations of $\delta = 45^\circ$ and $\delta = -29^\circ$. Left panel: uv-tracks; top-right panel: layout of configurations; bottom-right panel: contours of synthesis beam.

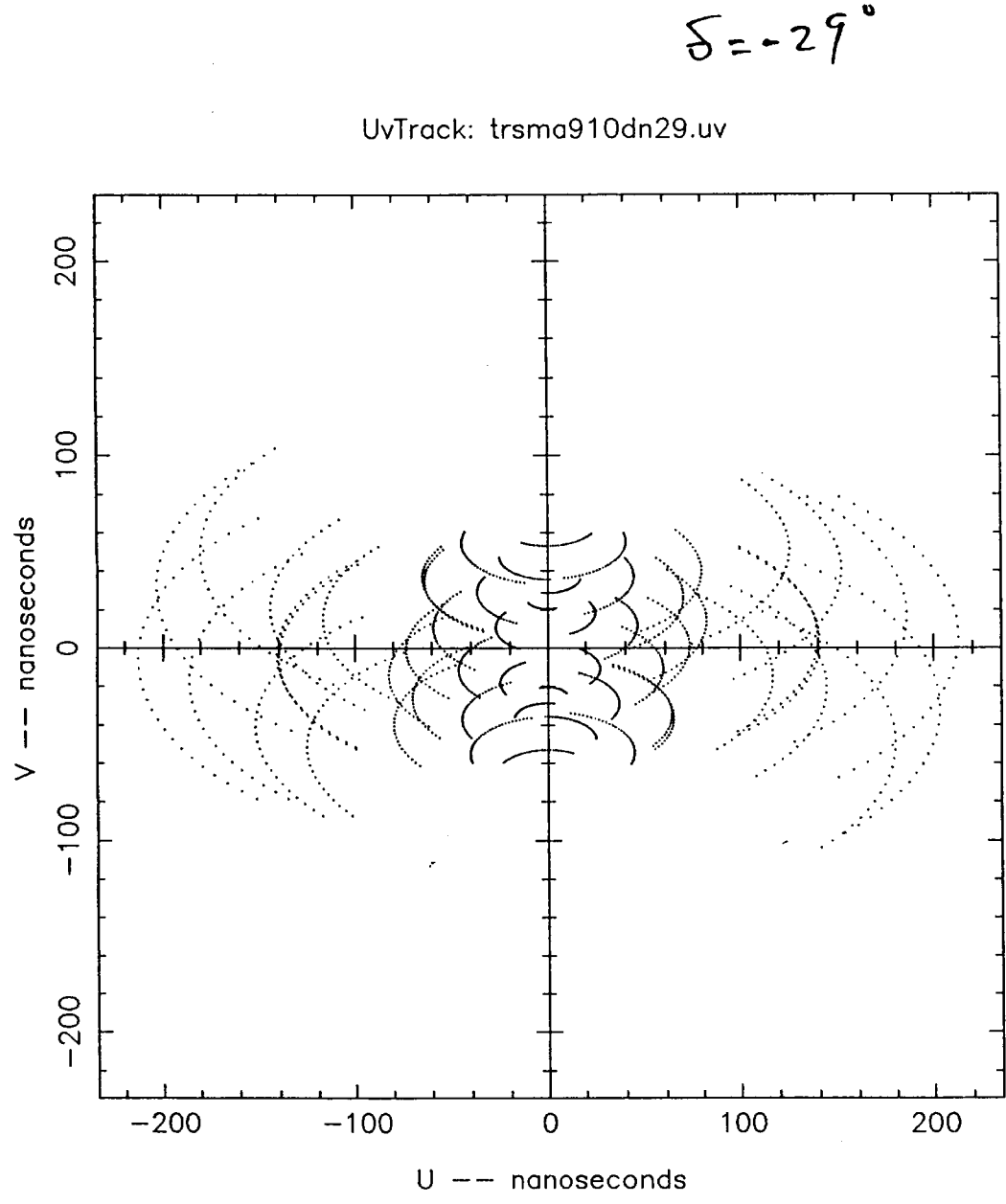
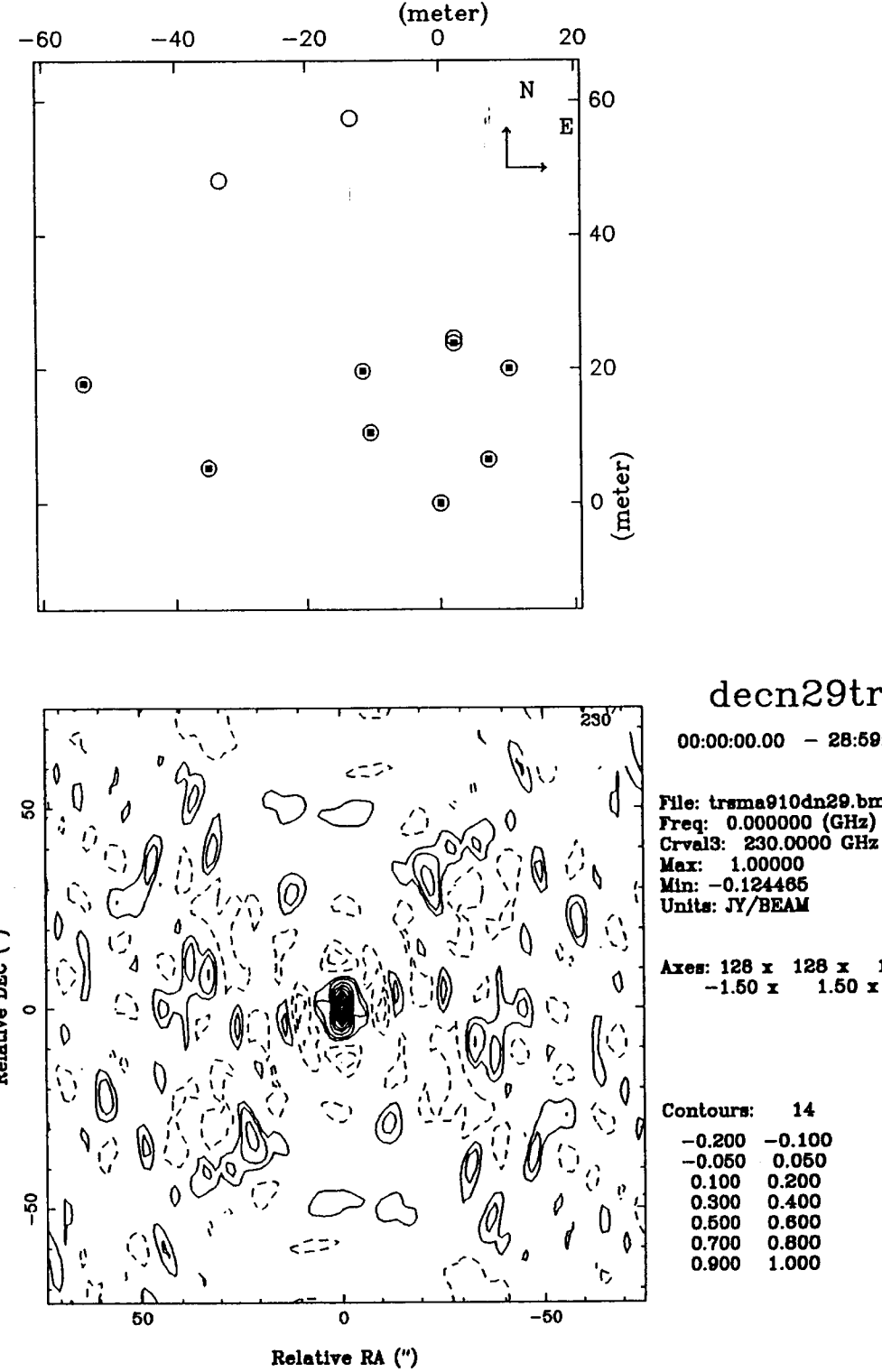


Fig. 2 - L



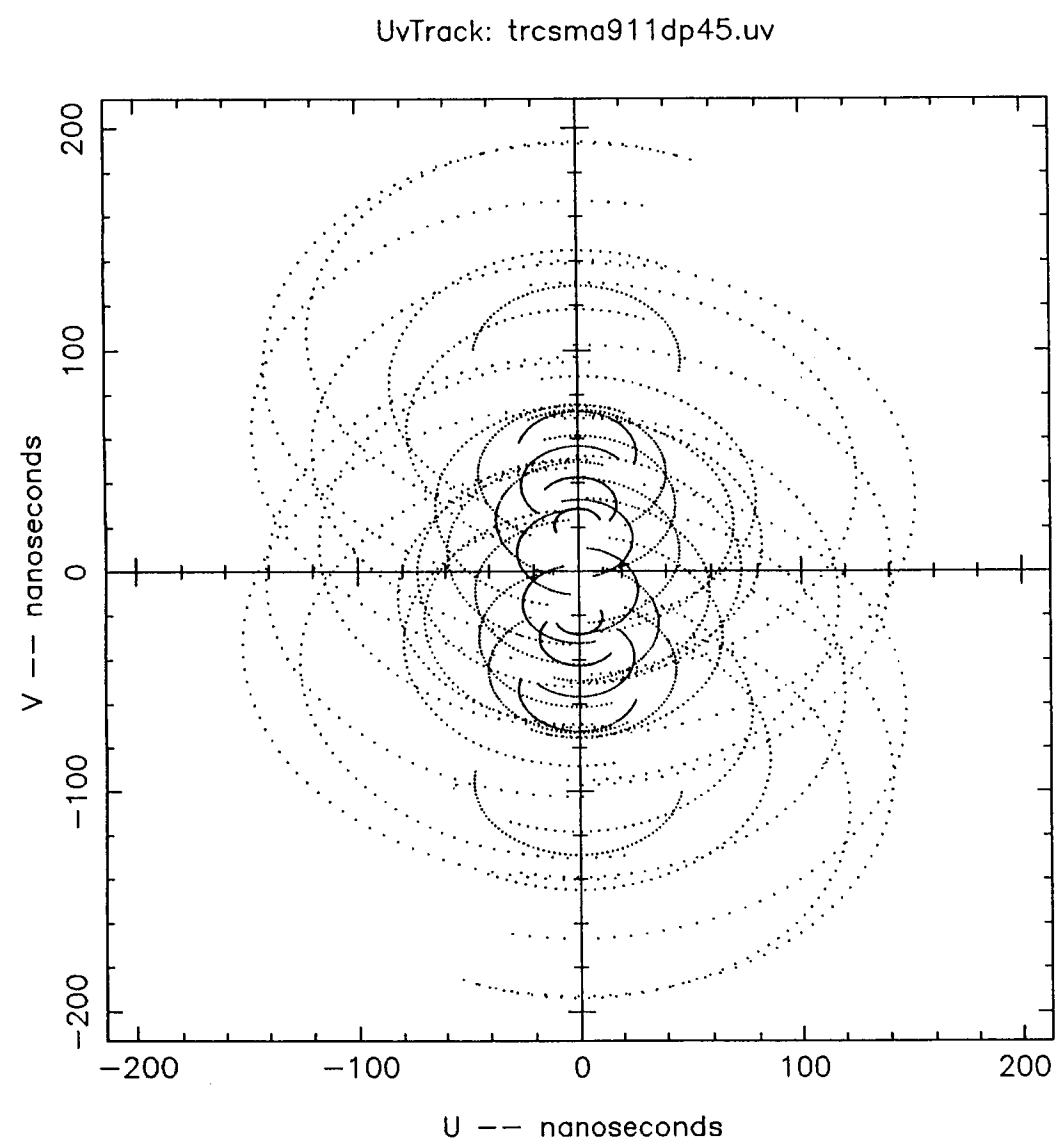
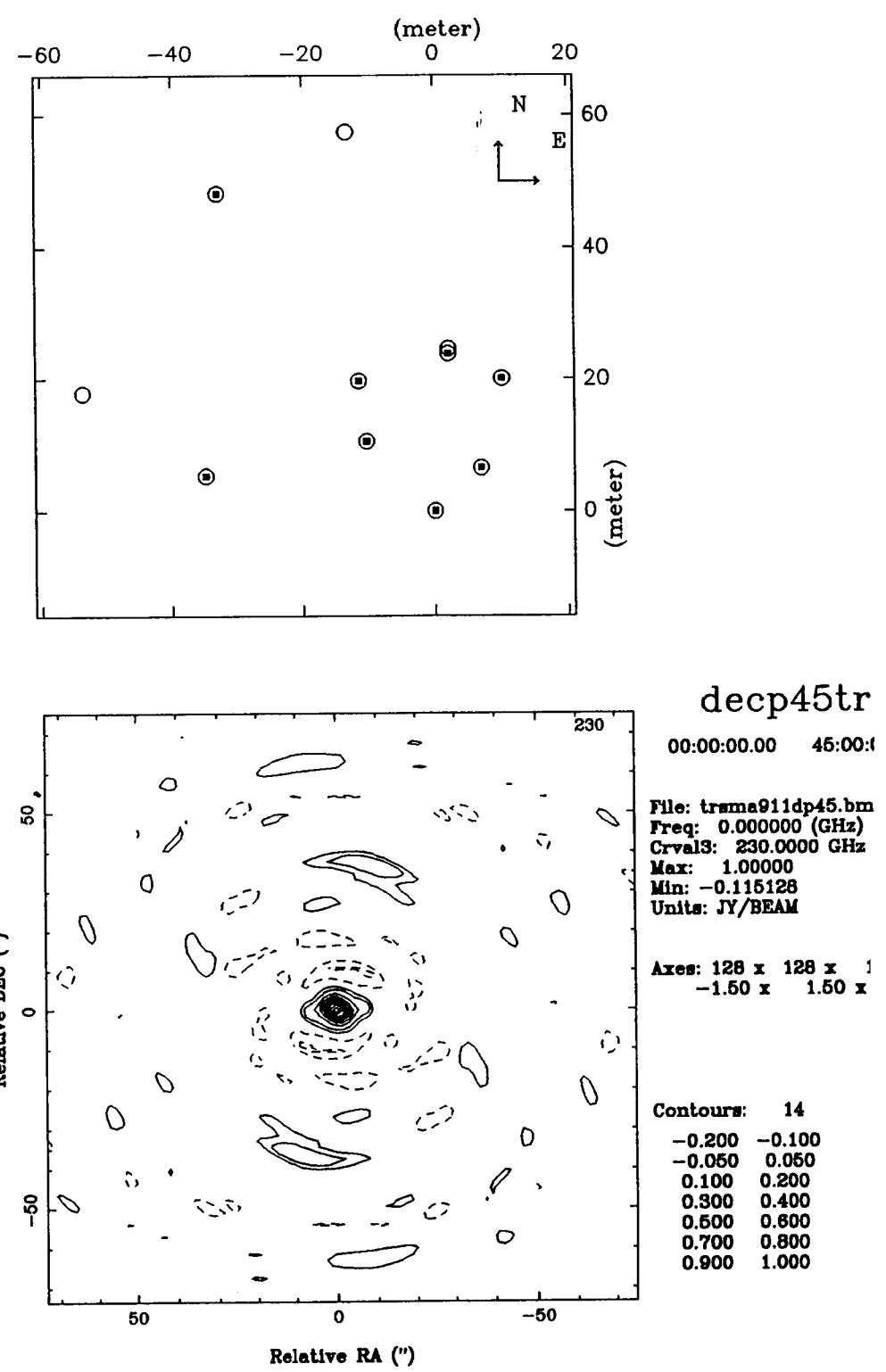


Fig 2-3



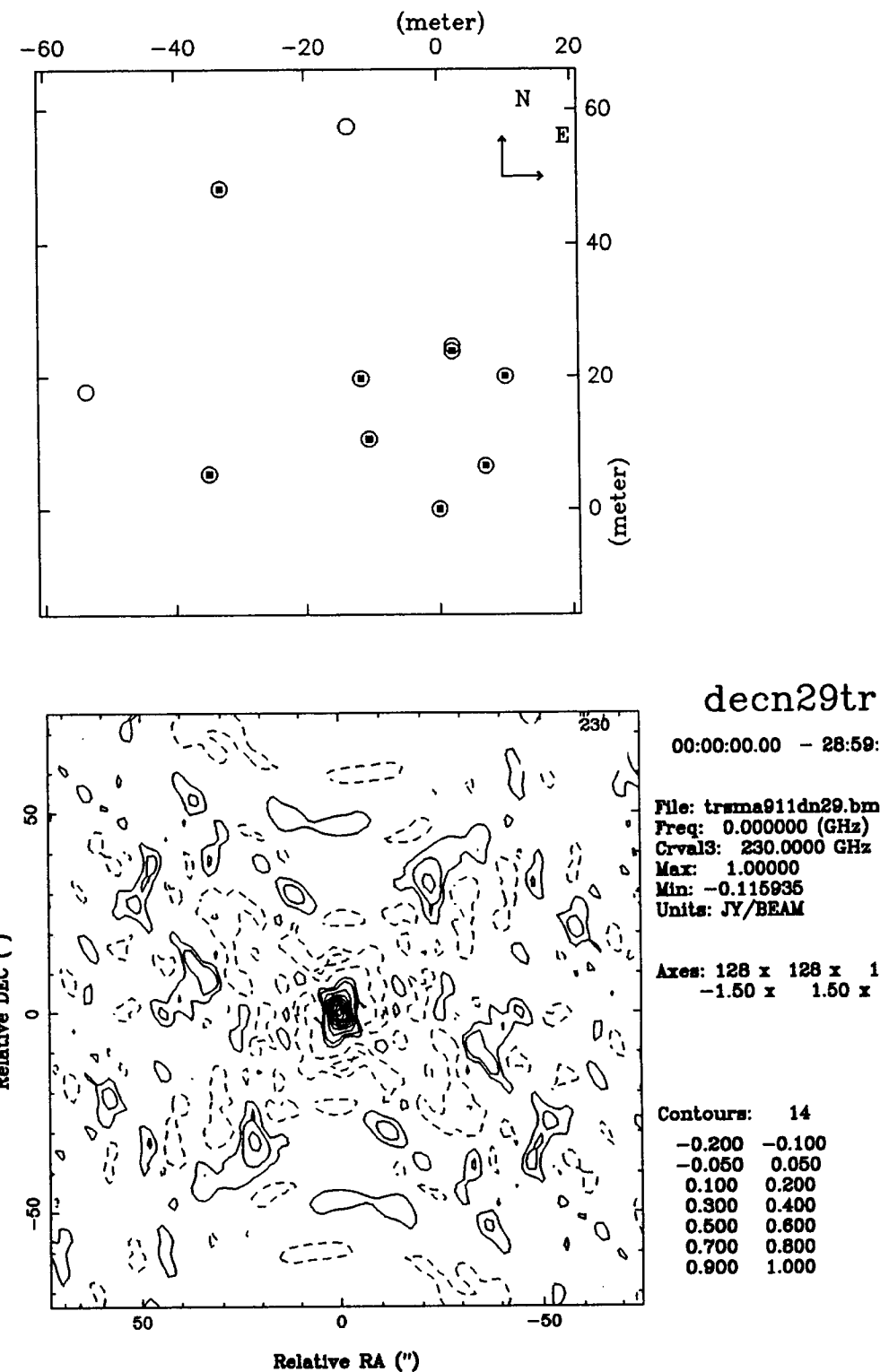
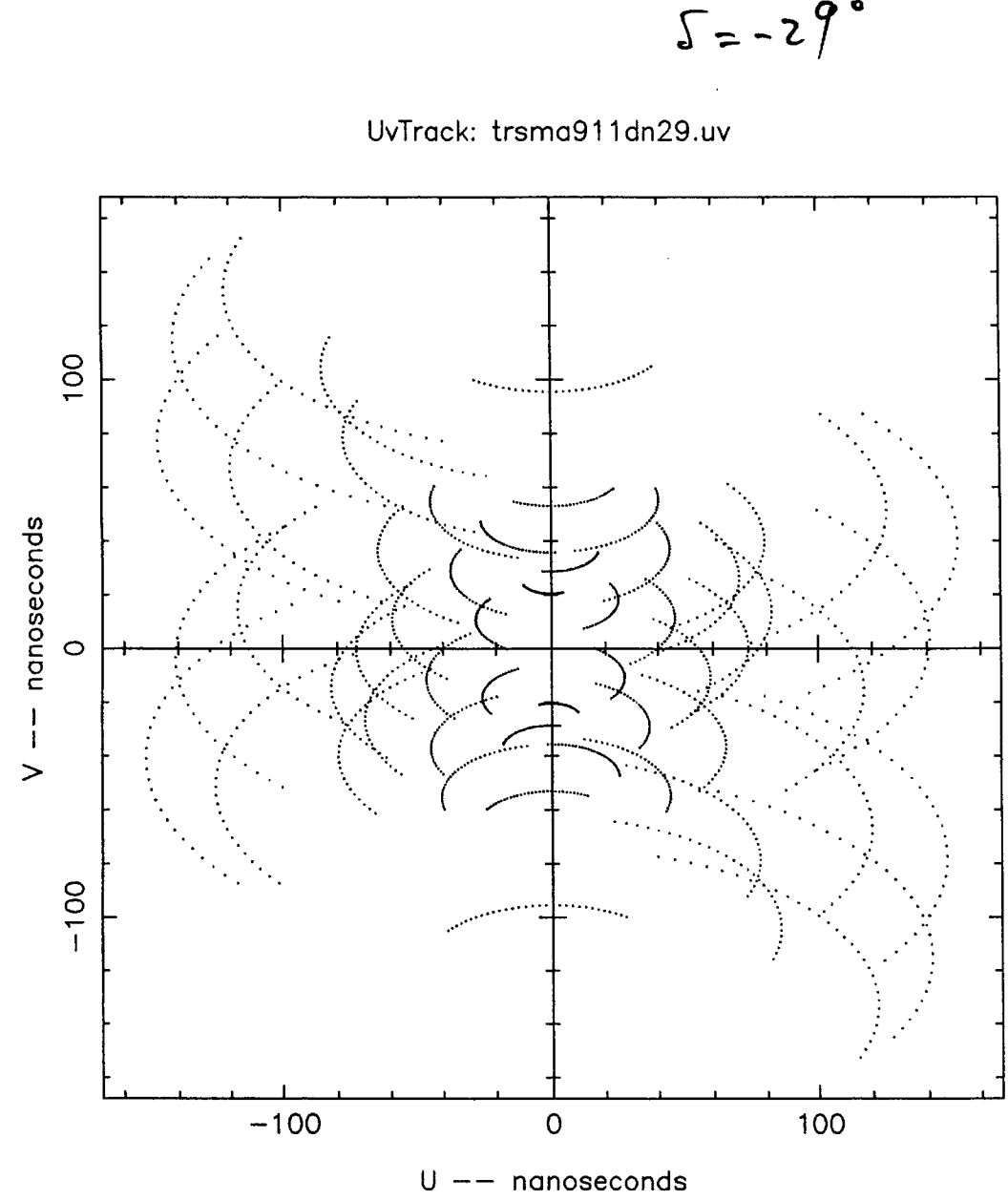


Fig 2-4

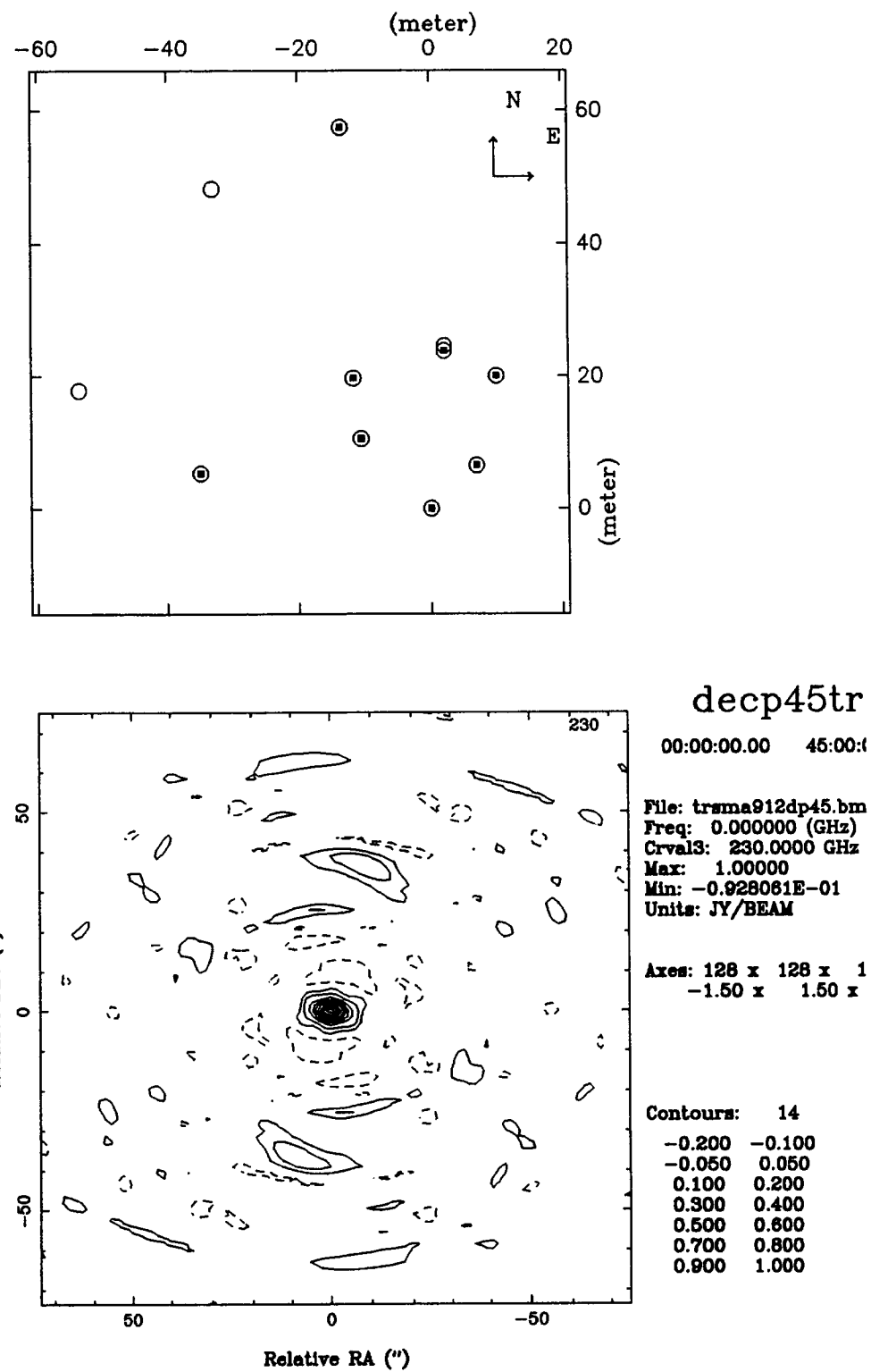
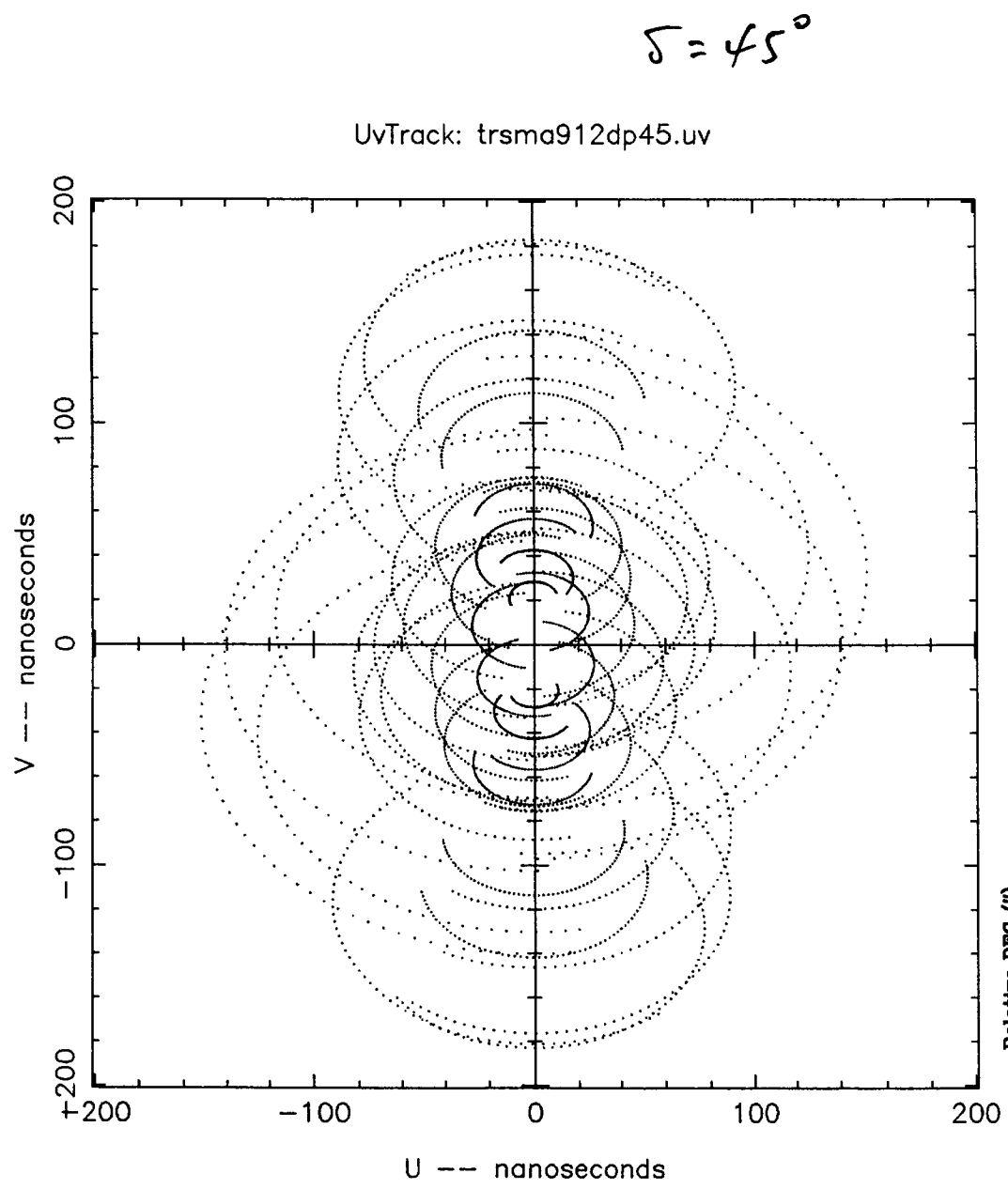
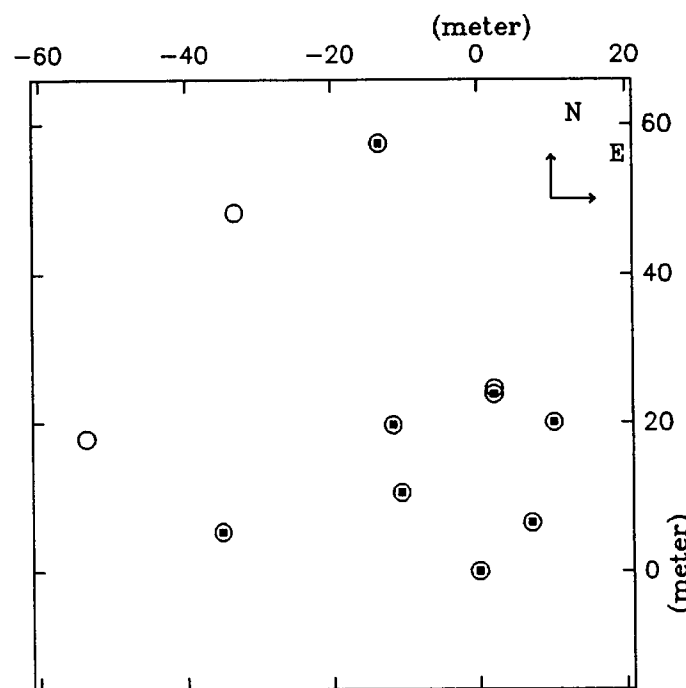
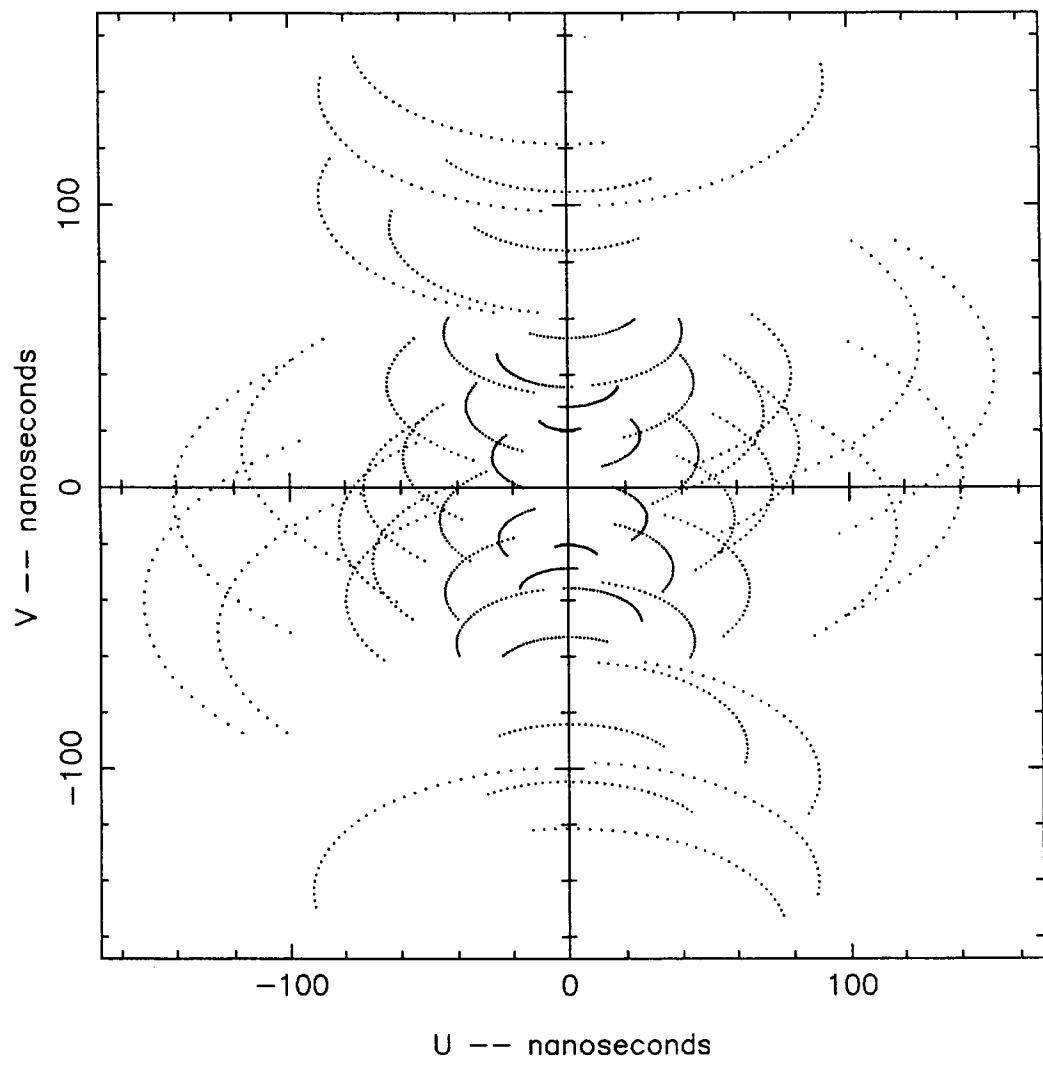


Fig. 2-5

UvTrack: trsma912dn29.uv

$$\delta = -29^\circ$$



decn29tr

00:00:00.00 - 28:59:

File: trsma912dn29.bm
Freq: 0.000000 (GHz)
Crval3: 230.0000 GHz
Max: 1.00000
Min: -0.118921
Units: JY/BEAM

Axes: 128 x 128 x 1
-1.50 x 1.50 x

Contours: 14
-0.200 -0.100
-0.050 0.050
0.100 0.200
0.300 0.400
0.500 0.600
0.700 0.800
0.900 1.000

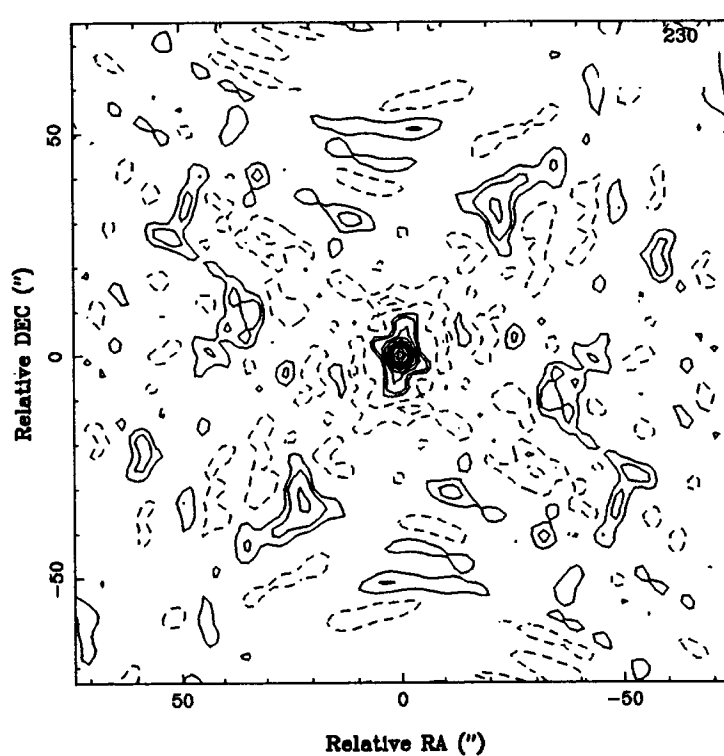


Fig 2-6

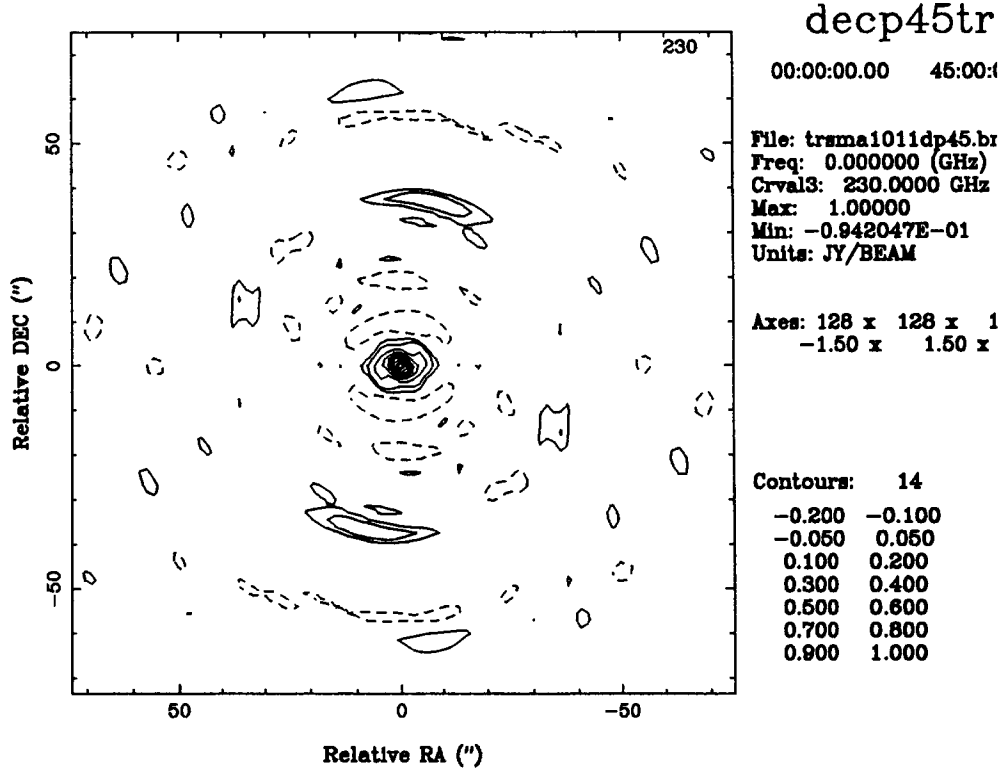
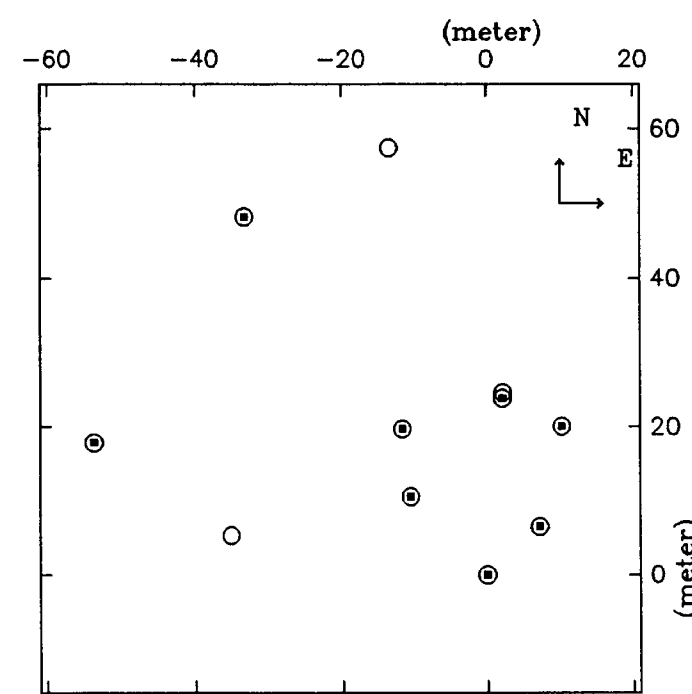
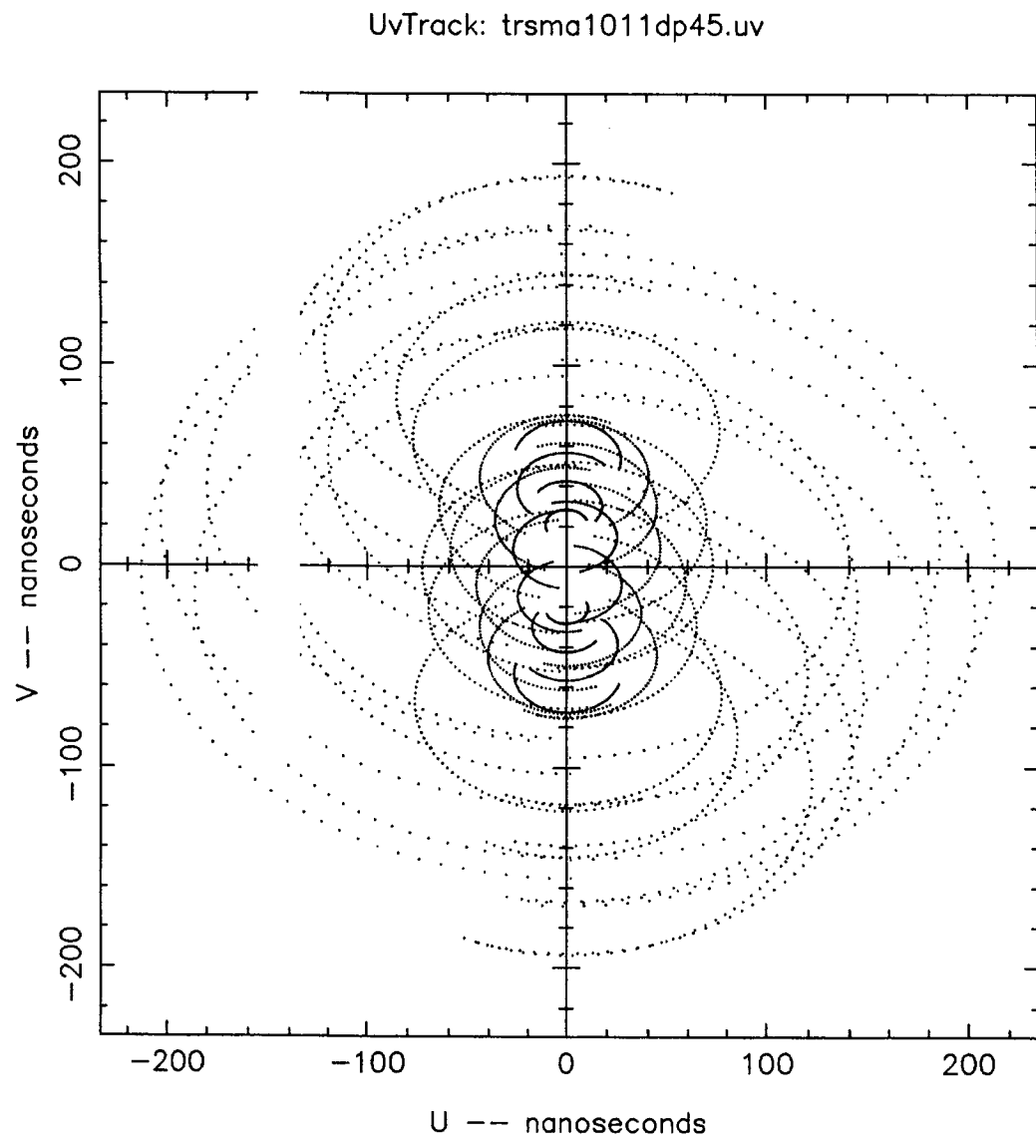


Fig. 2-7

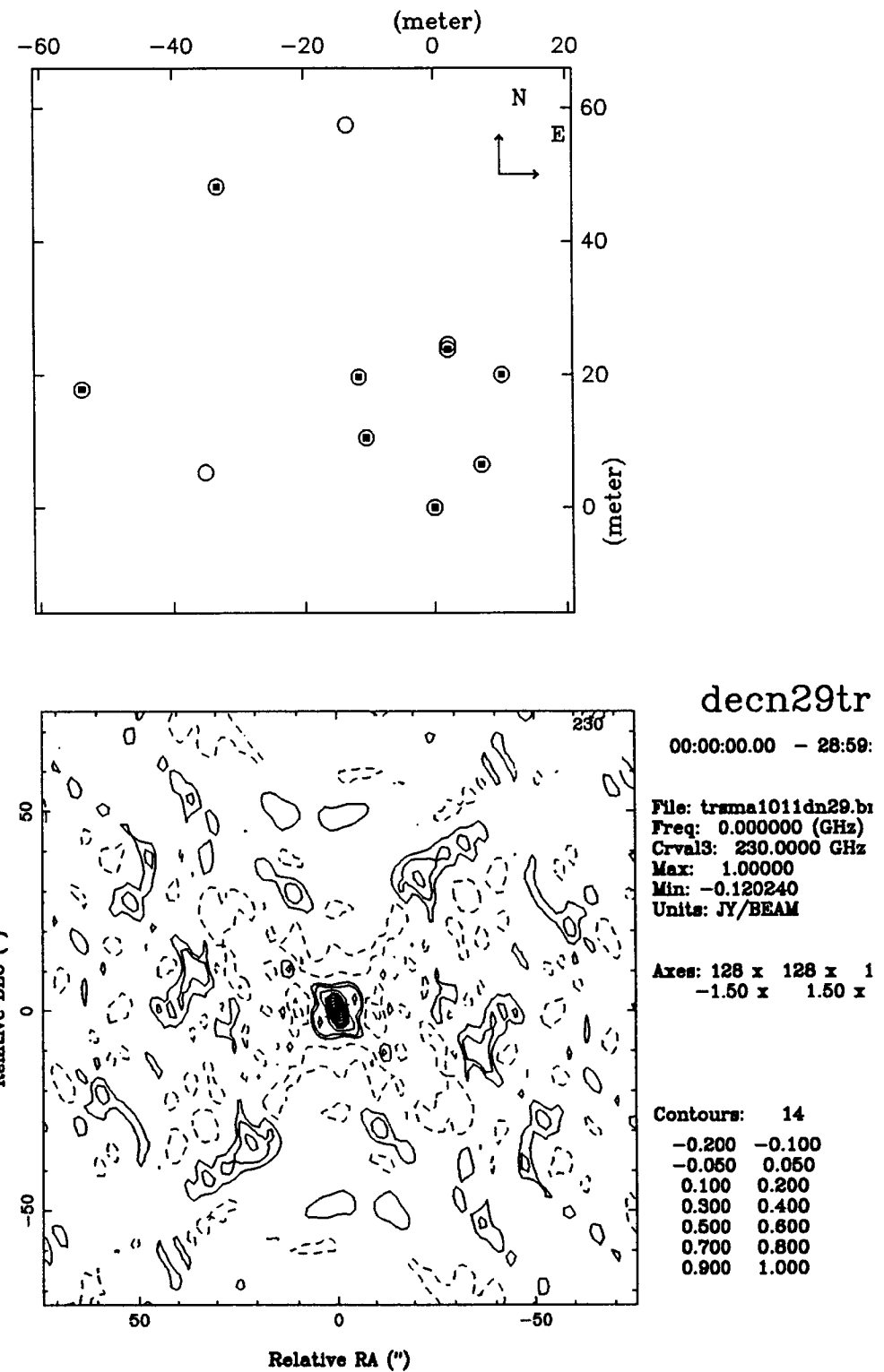
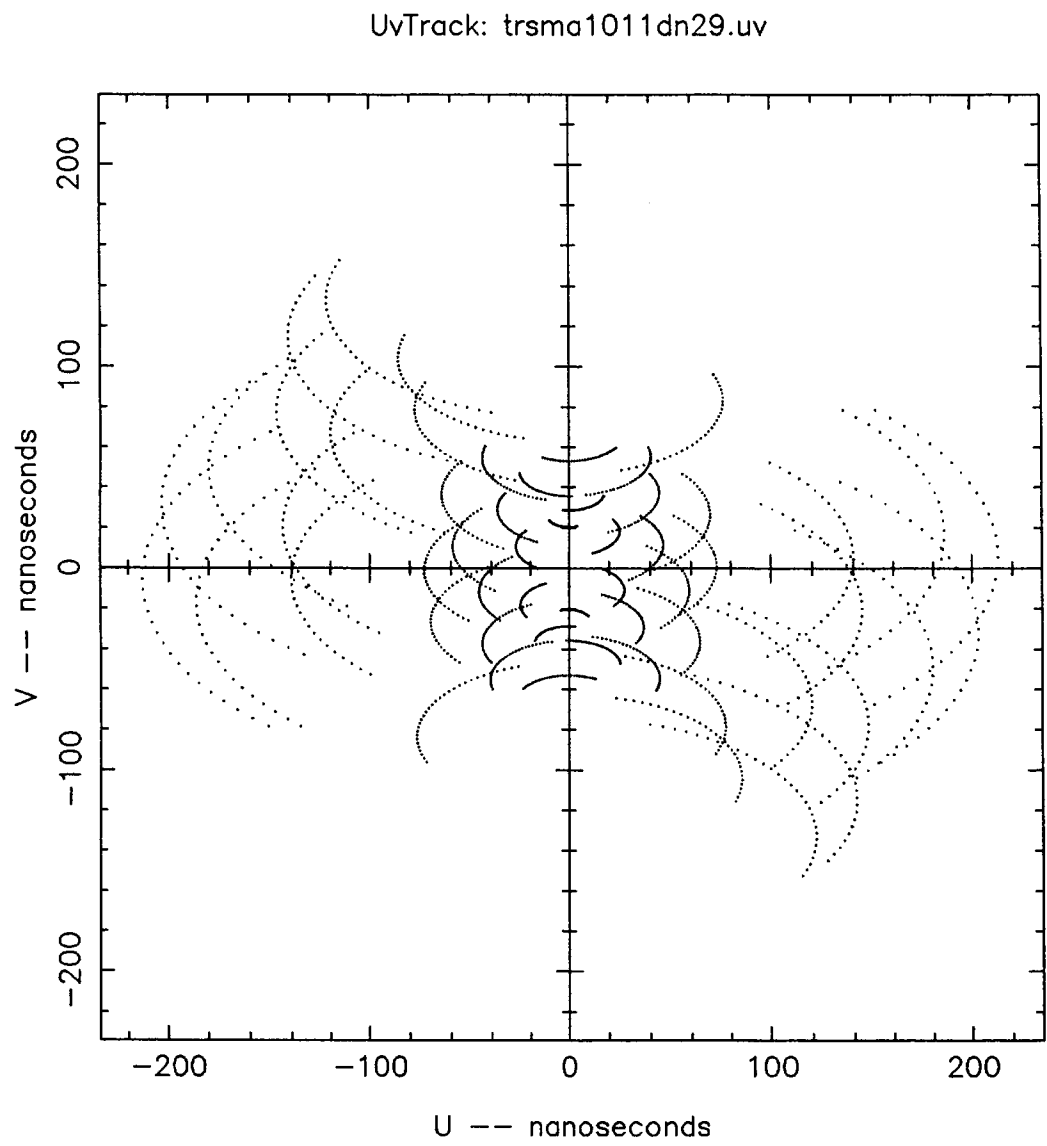


Fig. 2-8

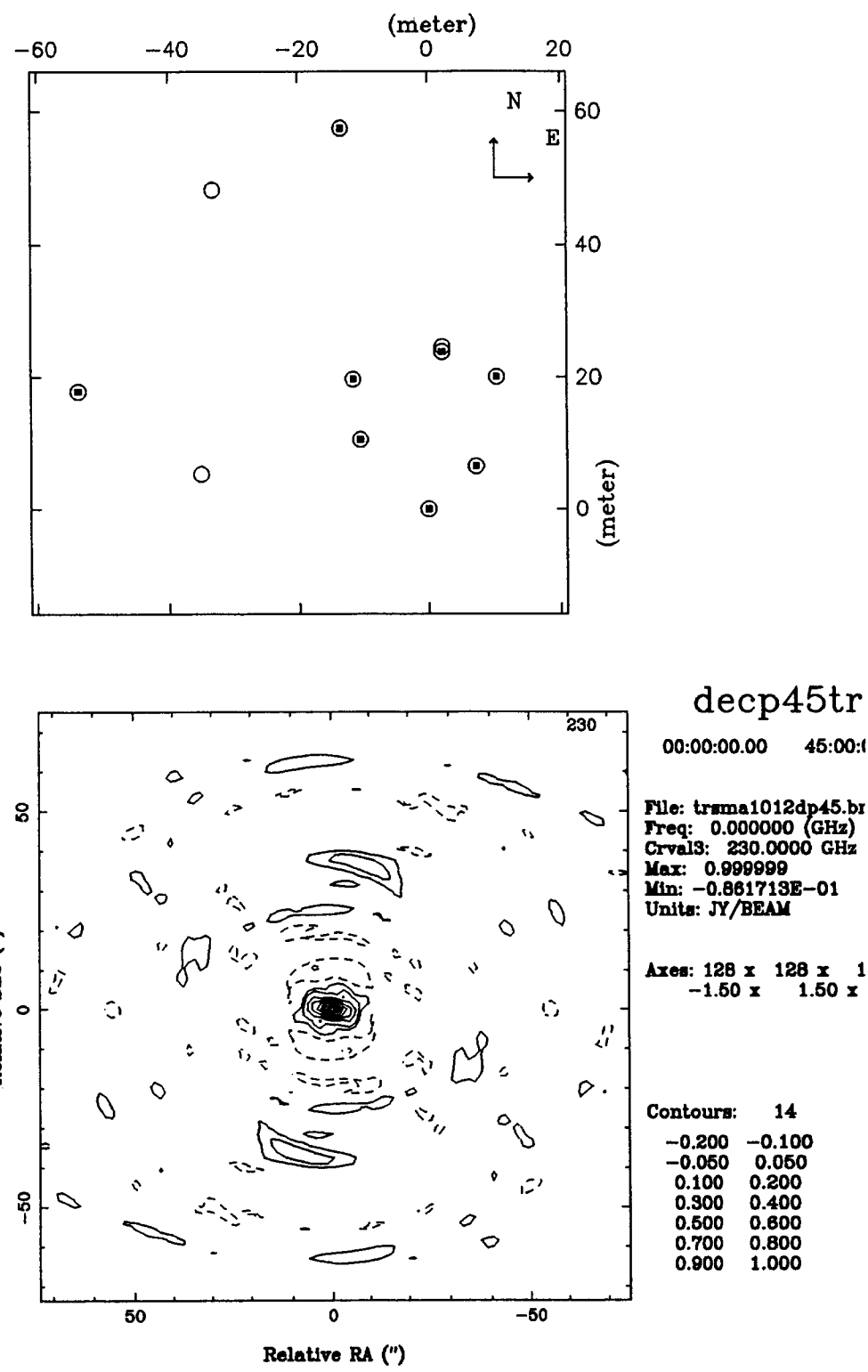
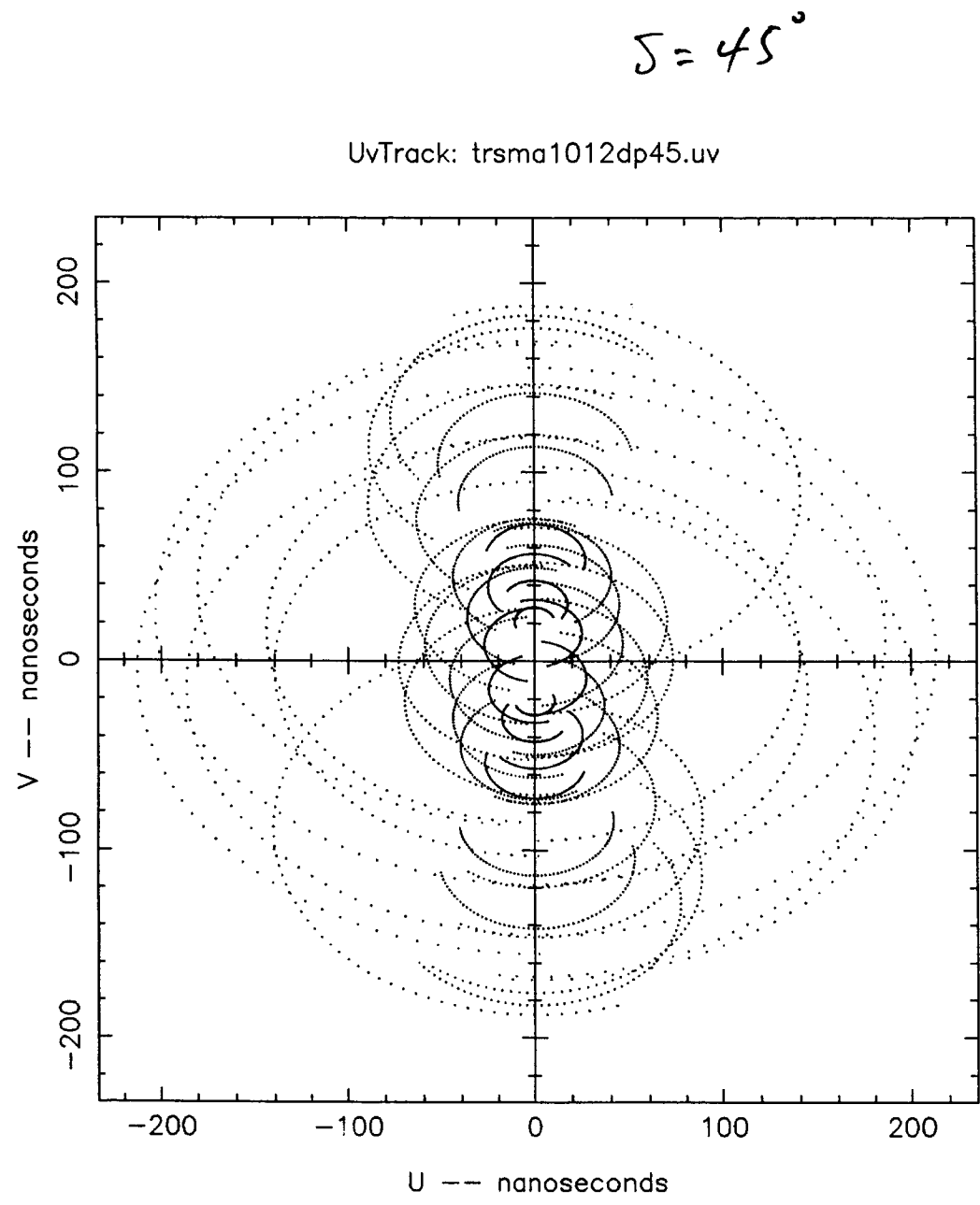


Fig. 2-9

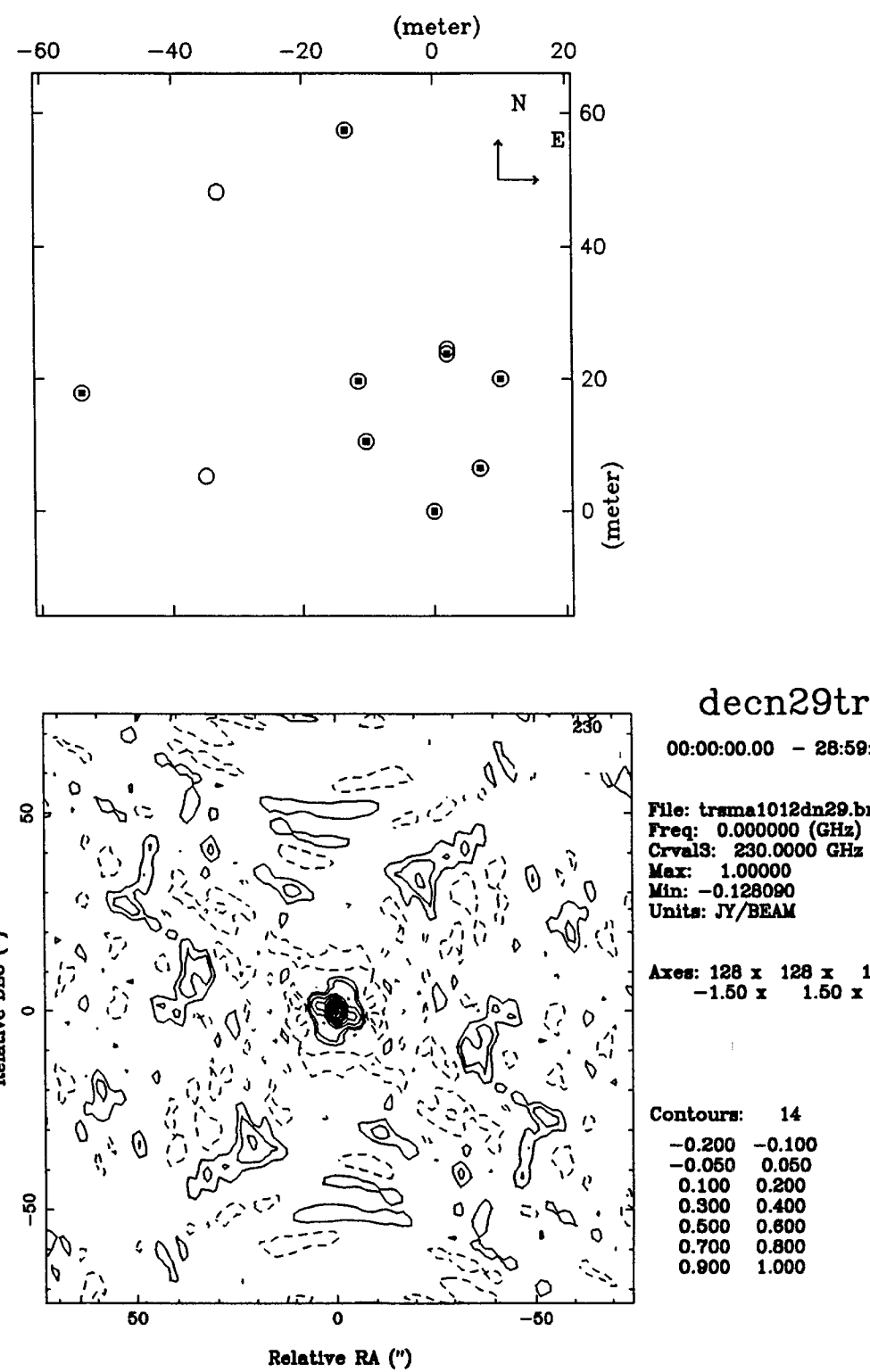
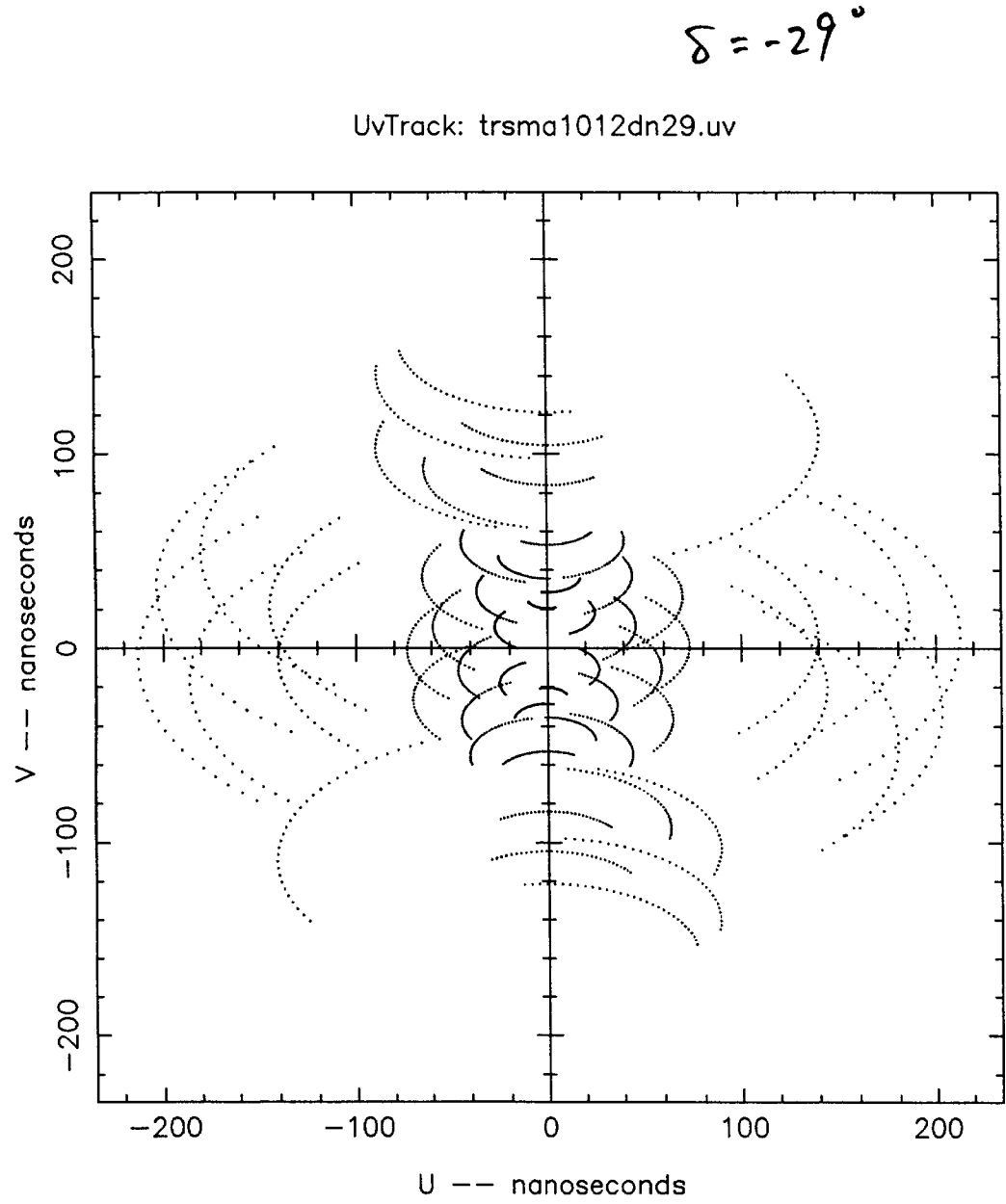


Fig. 2-10

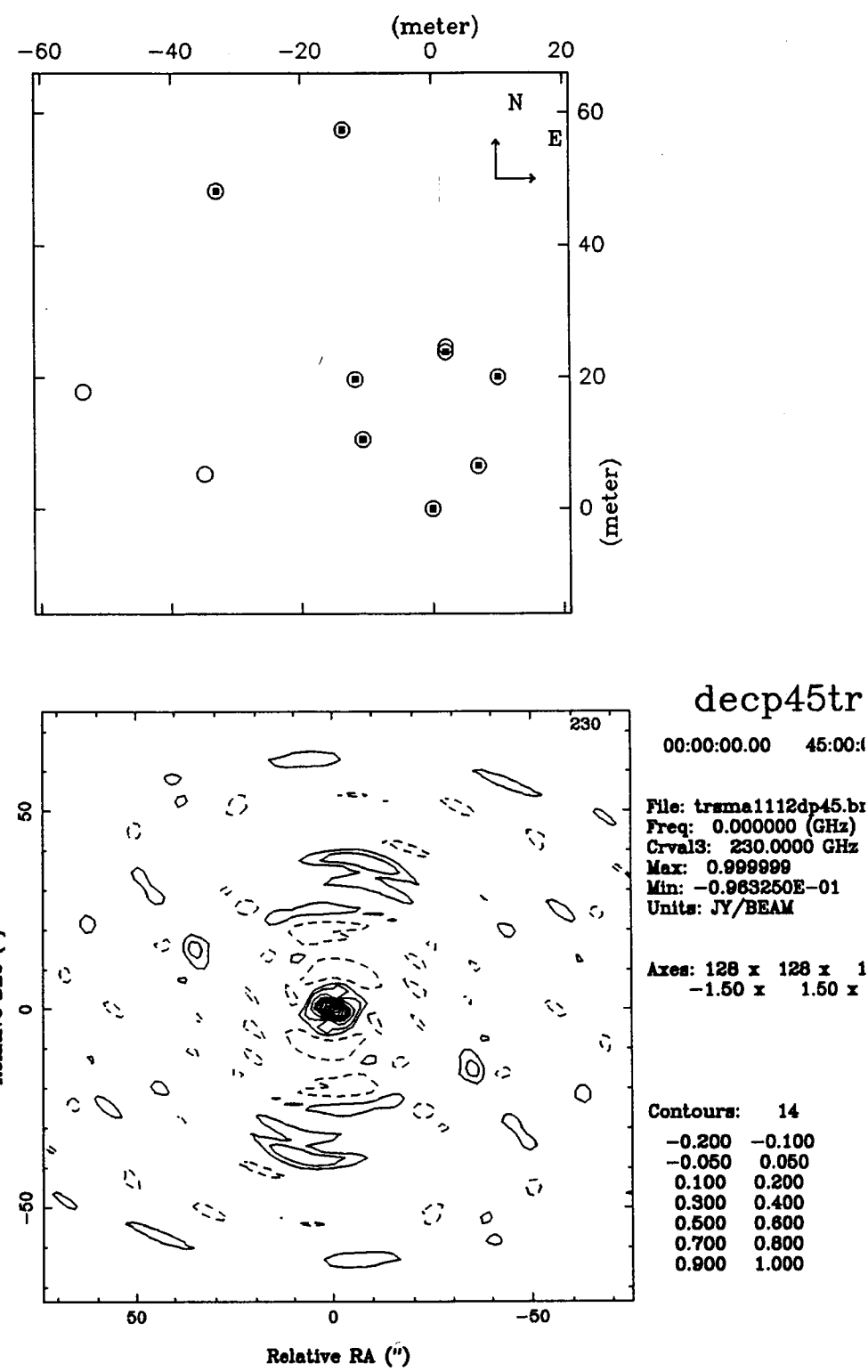
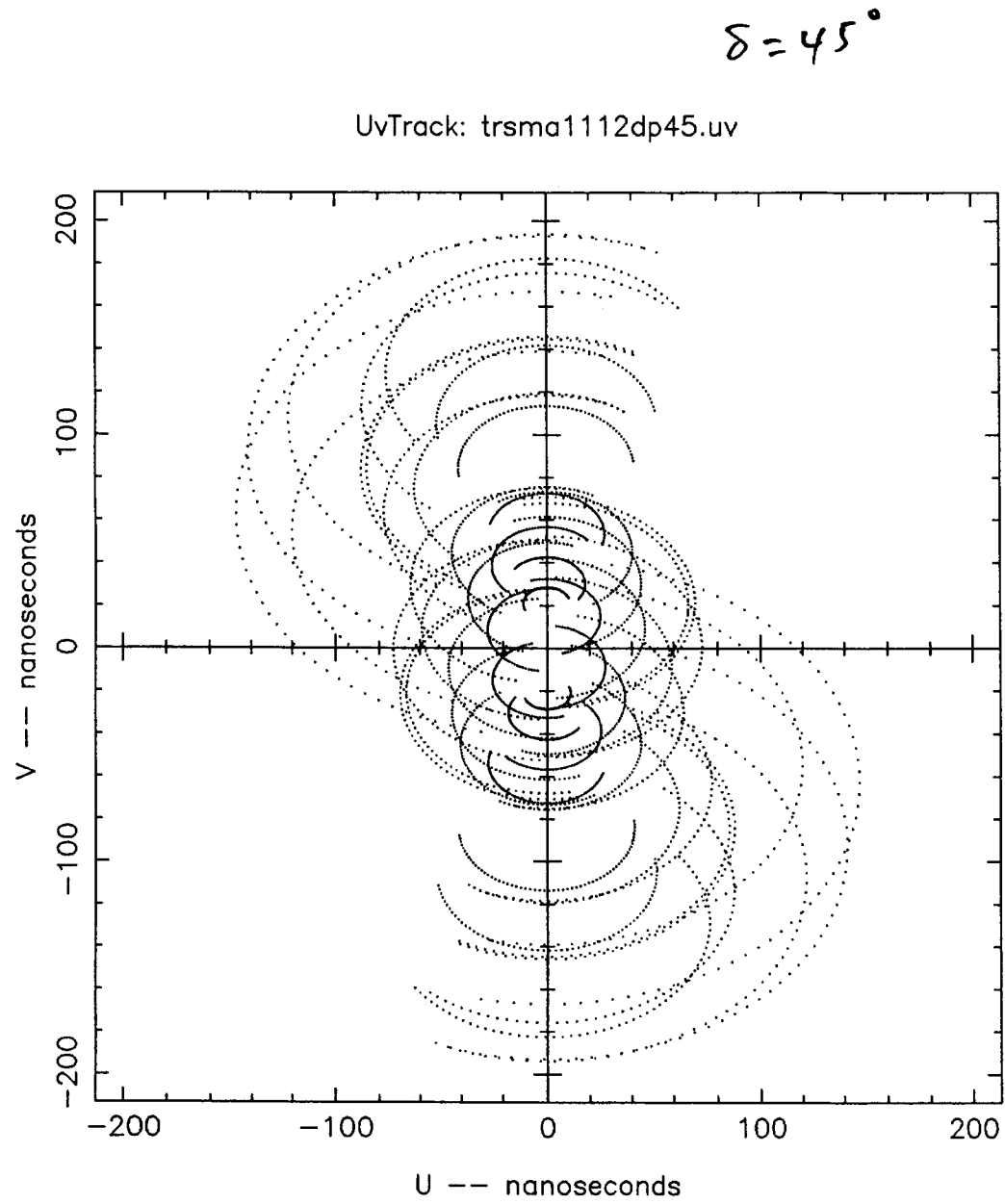


Fig 2-11

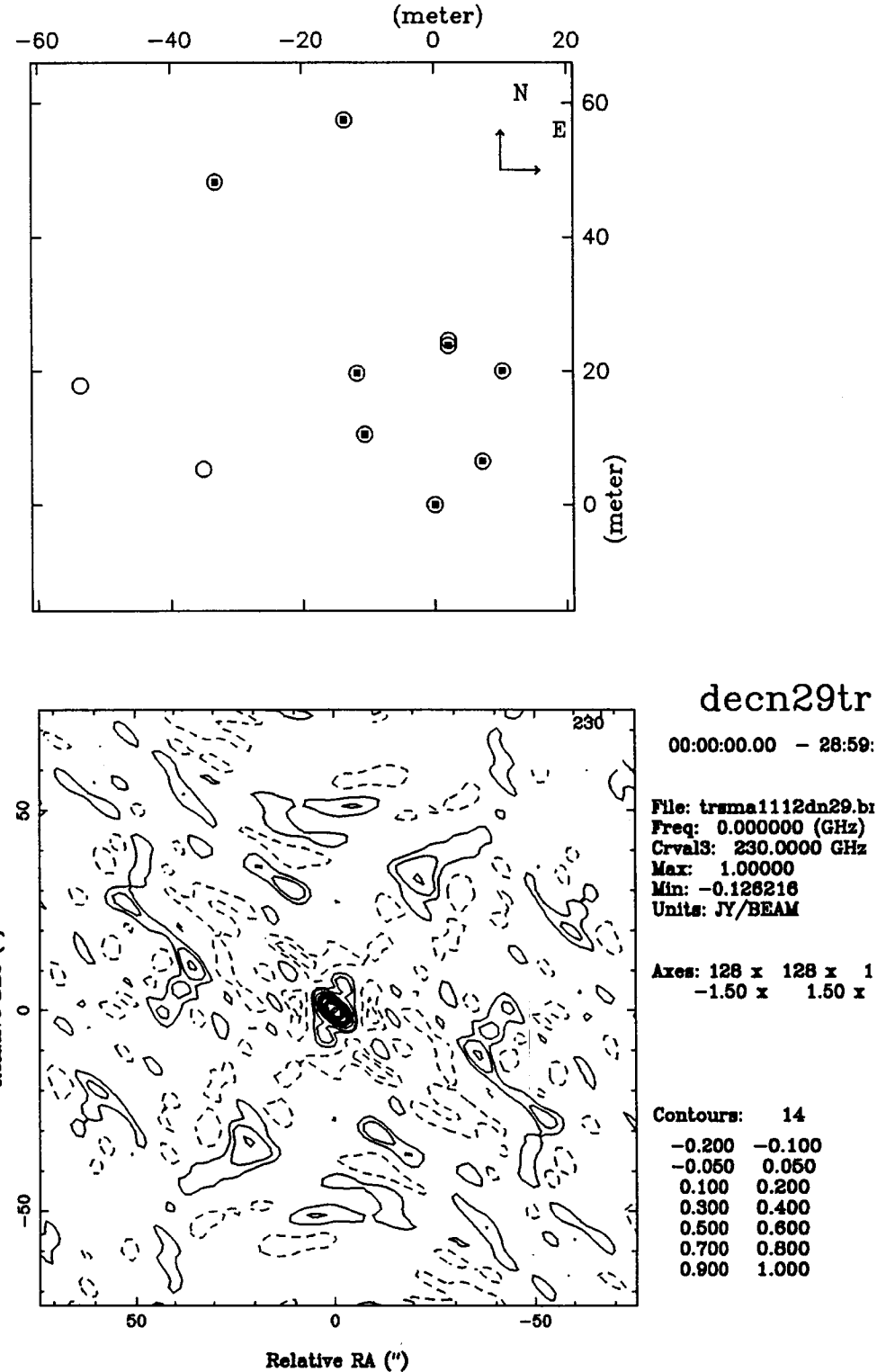
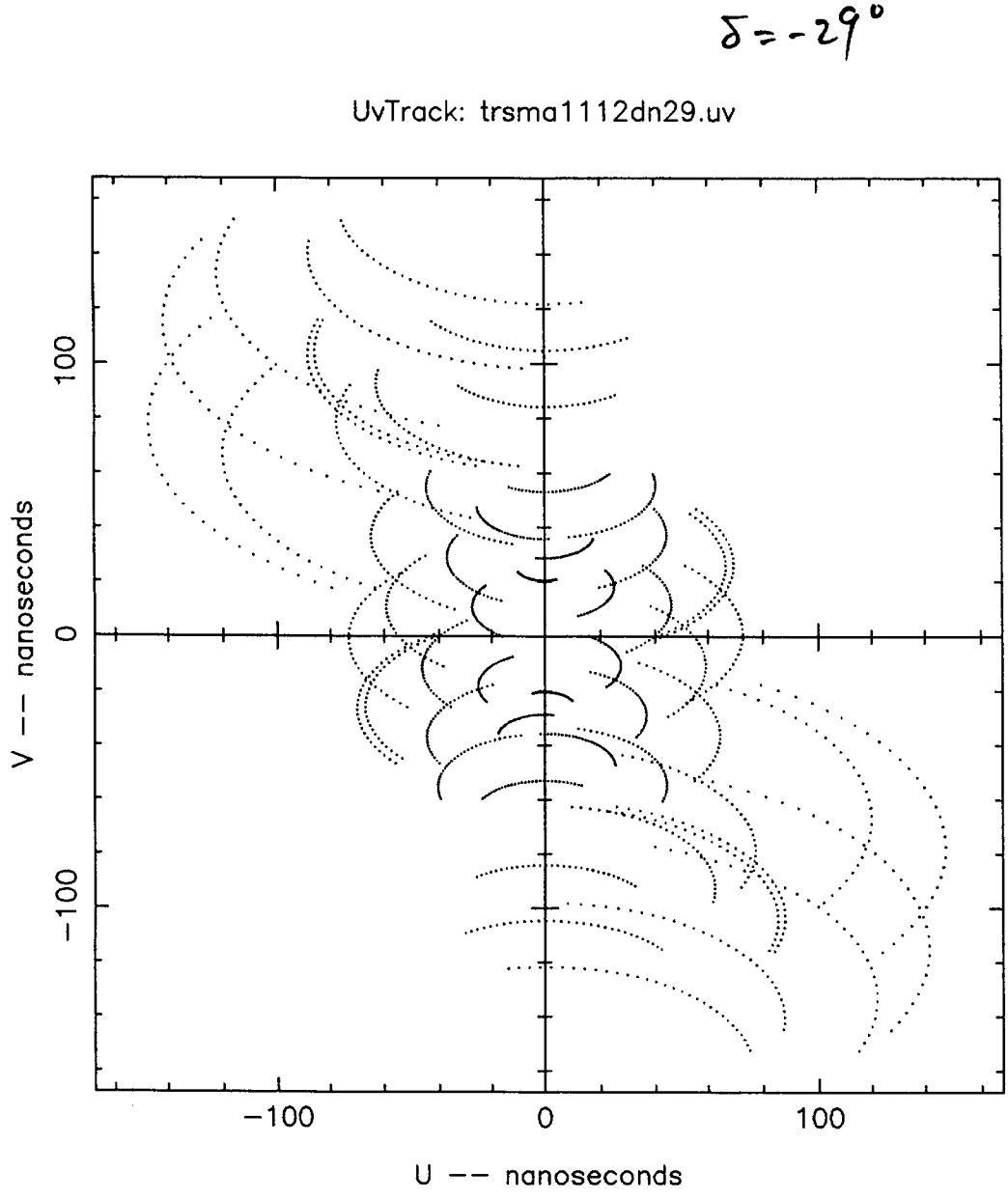


Fig. 2-12

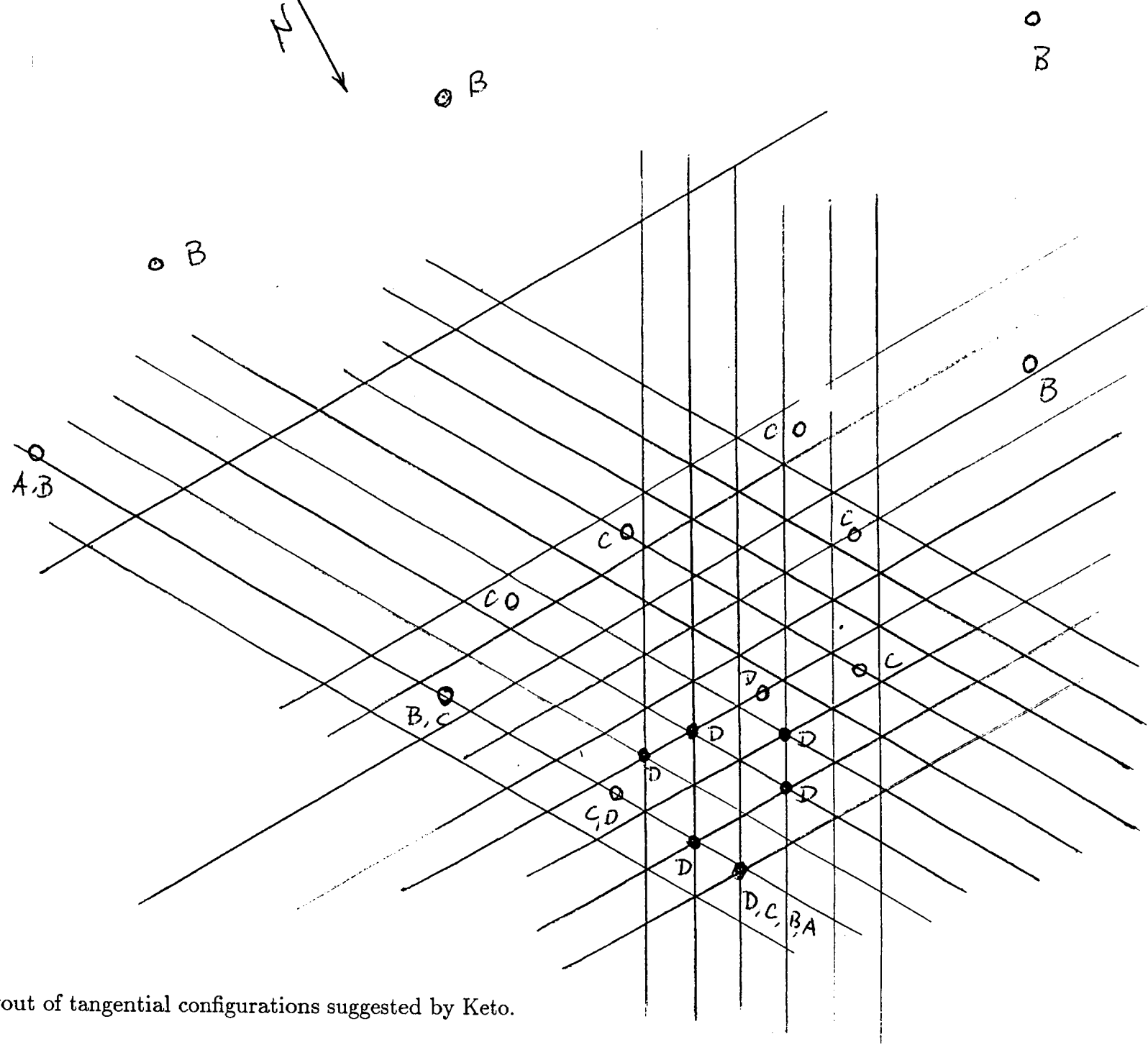
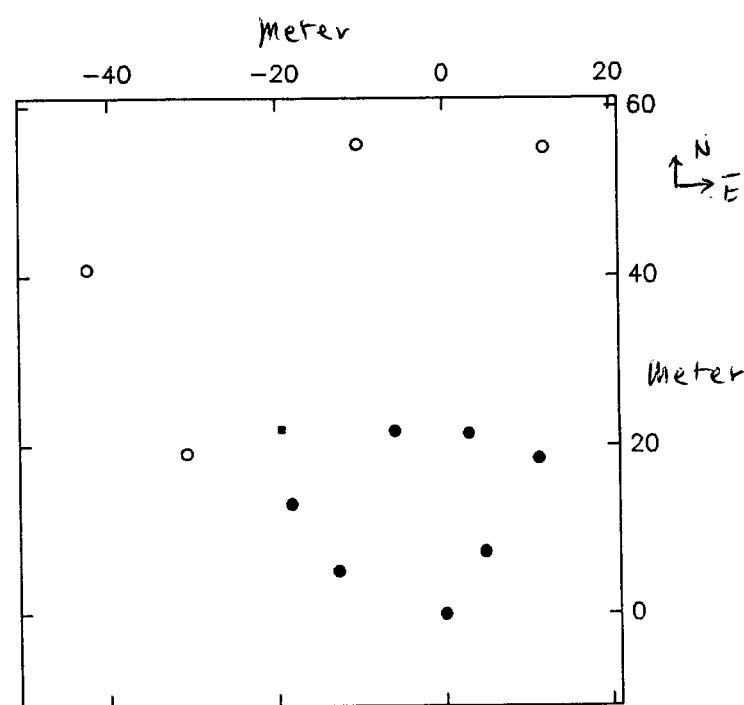
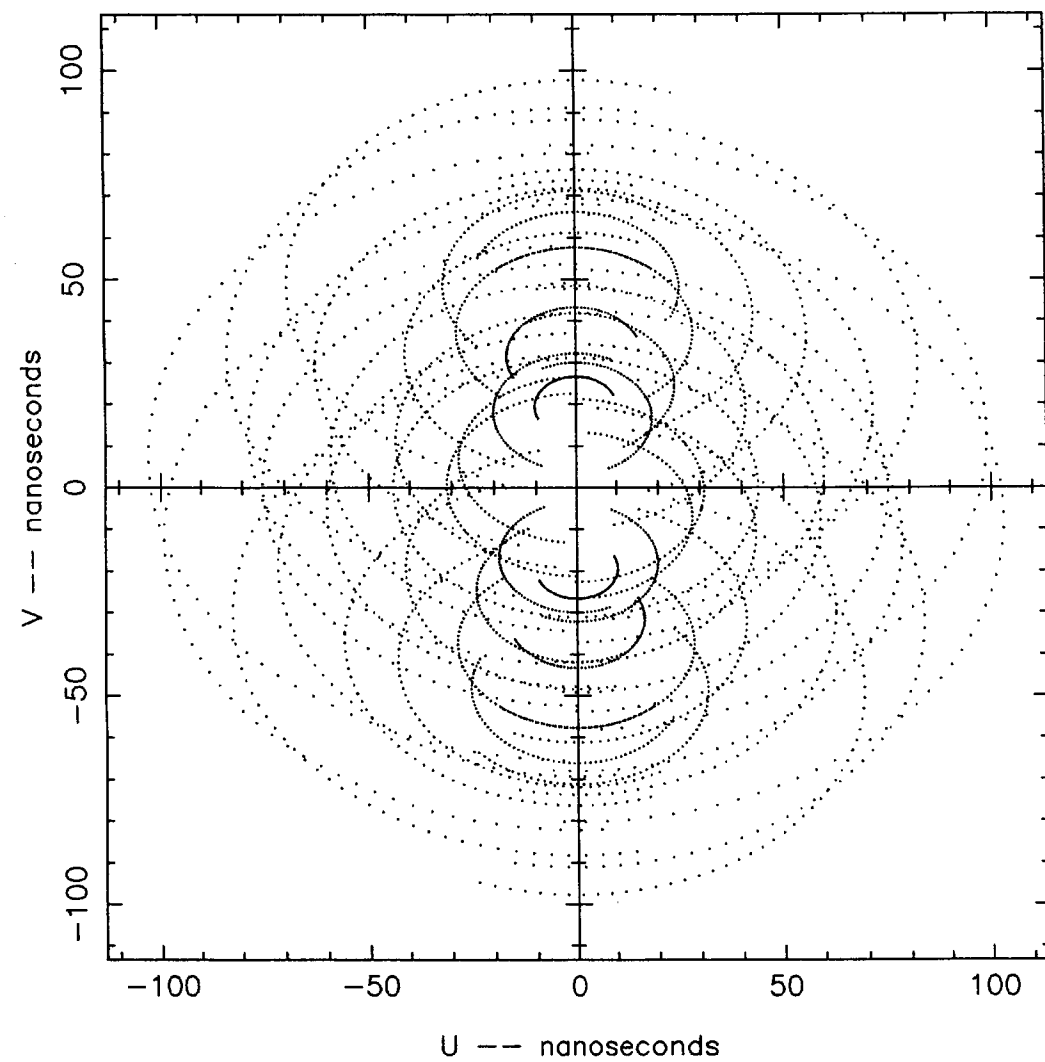


Fig. 3: A layout of tangential configurations suggested by Keto.

$\delta = 45^\circ$

UvTrack: optd8dp45.uv



decp45ot

00:00:00.00 45:00:1

File: optd8dp45.bm
Freq: 0.00000 (GHz)
Crval3: 230.0000 GHz
Max: 1.00000
Min: -0.121813
Units: JY/BEAM

Axes: 128 x 128 x 1
-1.50 x 1.50 x 1

Contours: 14

-0.200	-0.100
-0.050	0.050
0.100	0.200
0.300	0.400
0.500	0.600
0.700	0.800
0.900	1.000

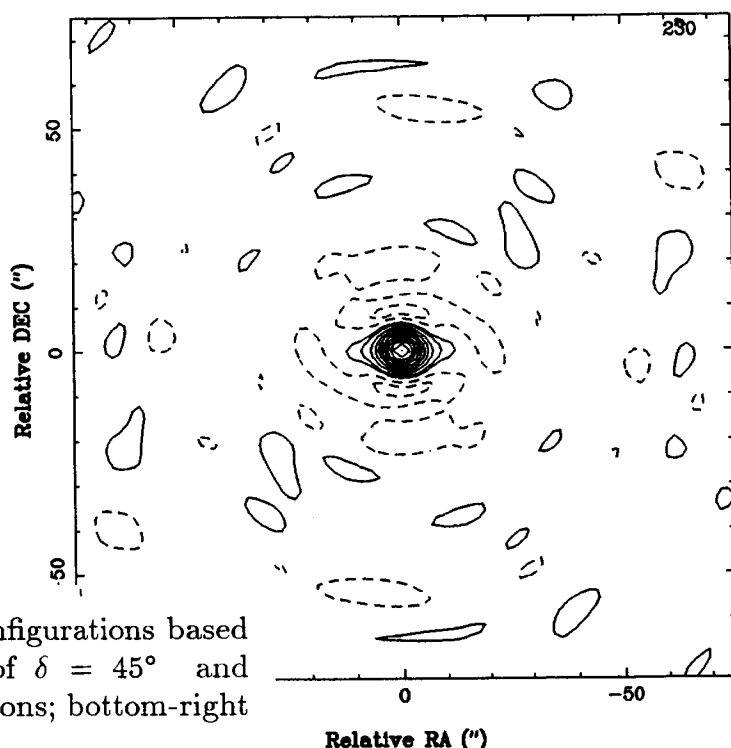


Fig. 4: Simulations of synthesis beams obtained from the D and C configurations based on Keto's design. Calculations are made for the two declinations of $\delta = 45^\circ$ and $\delta = -29^\circ$. Left panel: uv-tracks; top-right panel: layout of configurations; bottom-right panel: contours of synthesis beam.

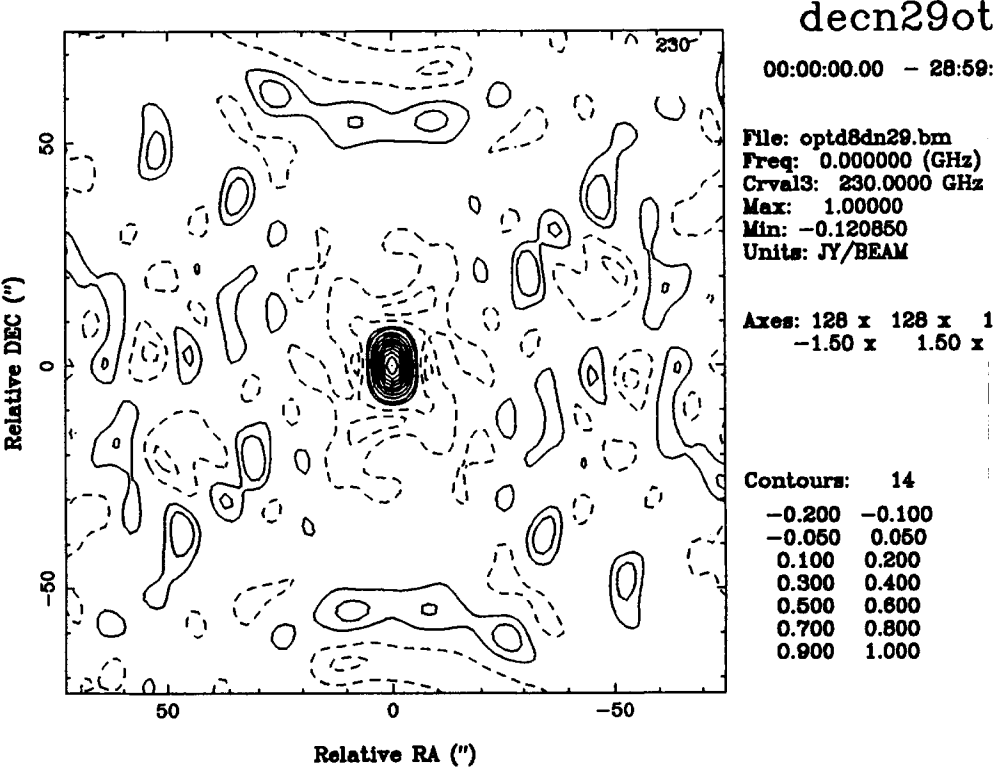
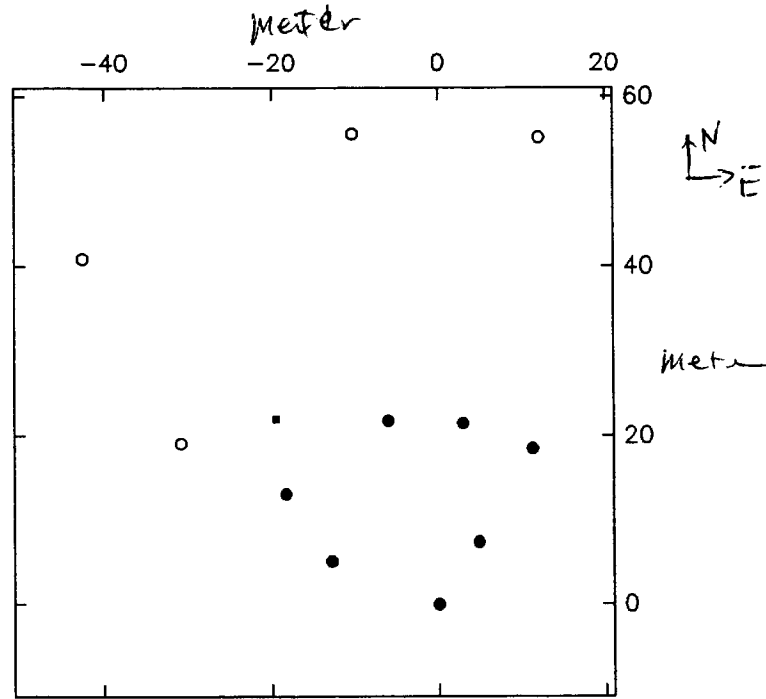
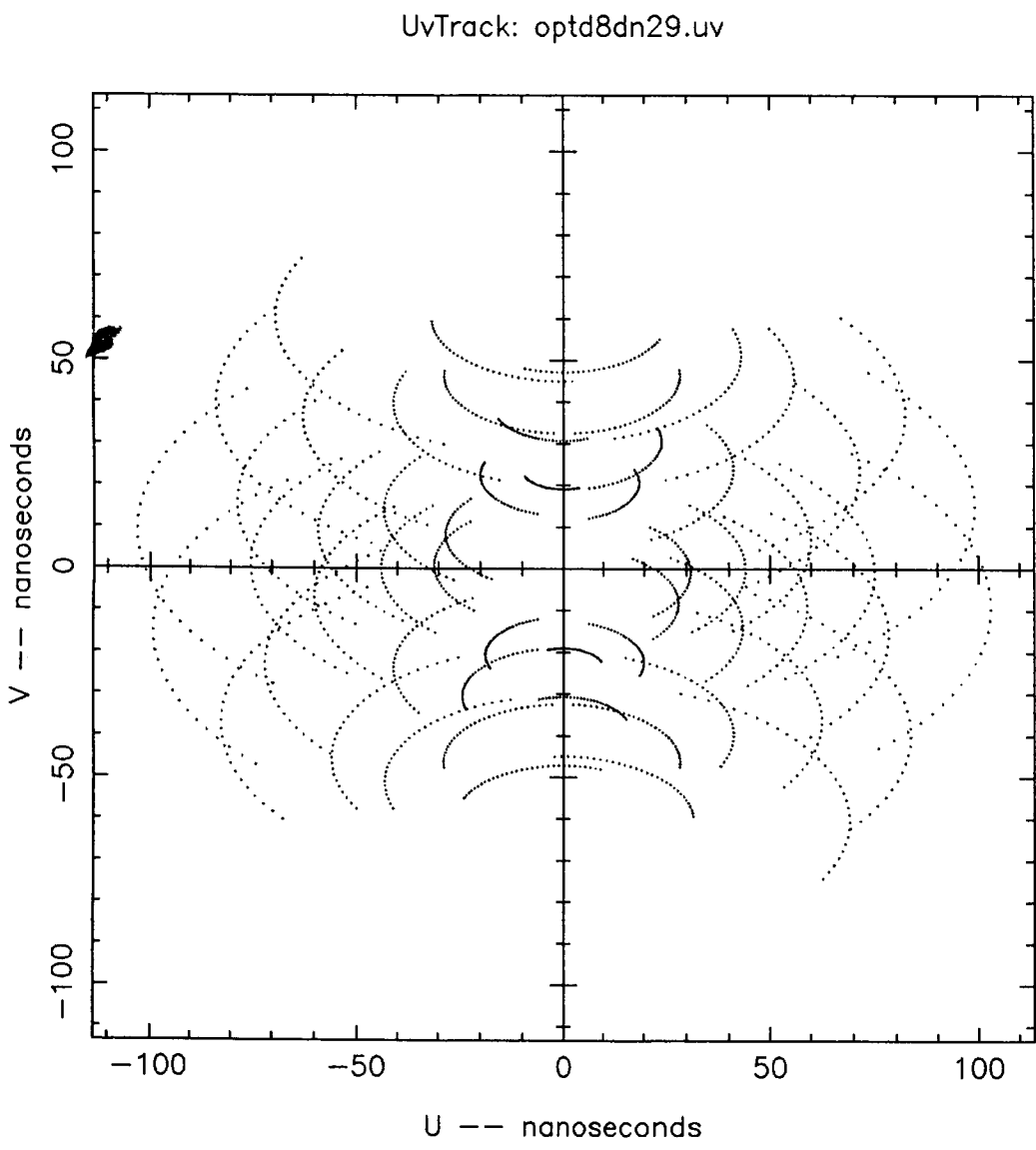


Fig. 4-2

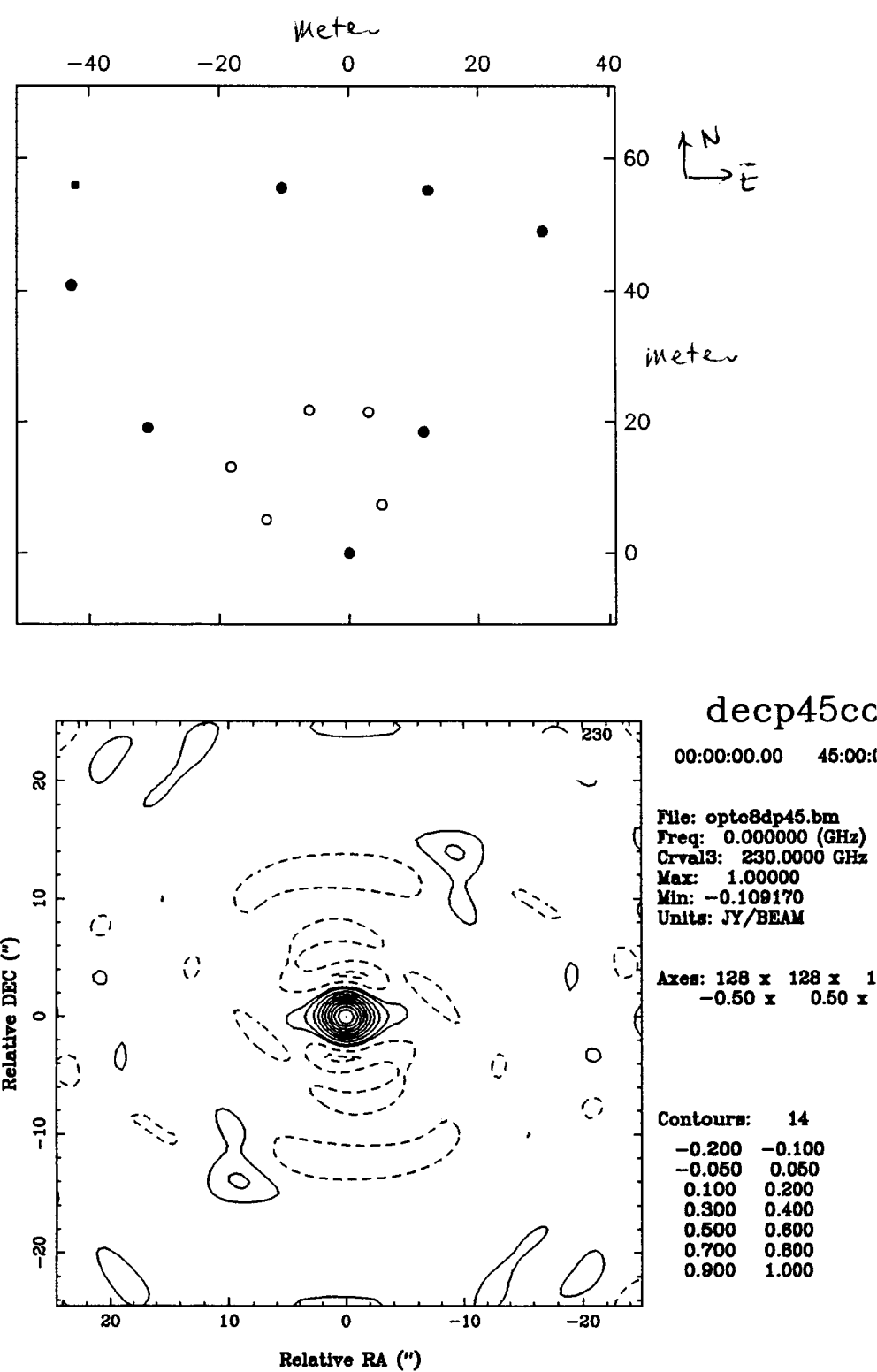
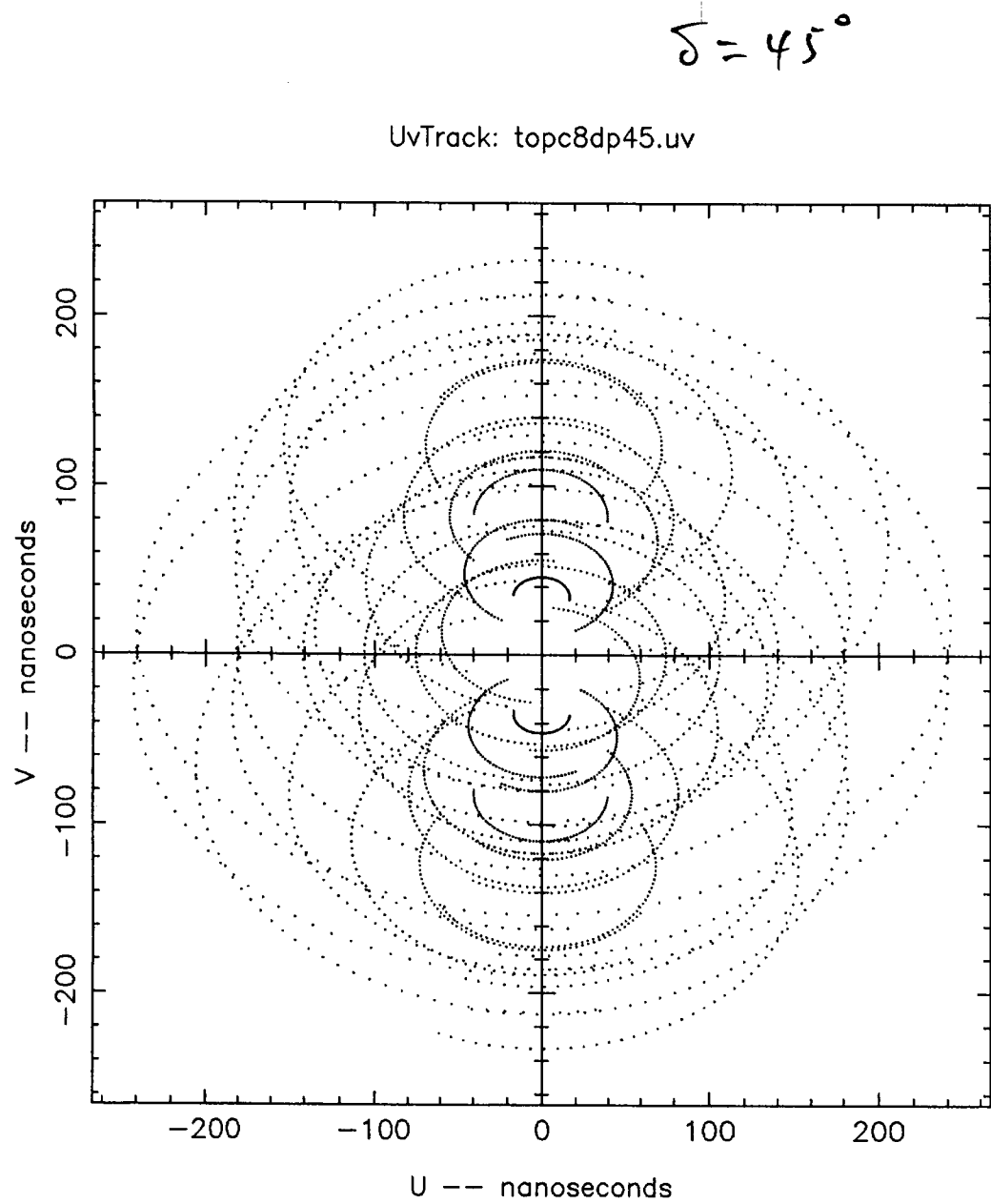
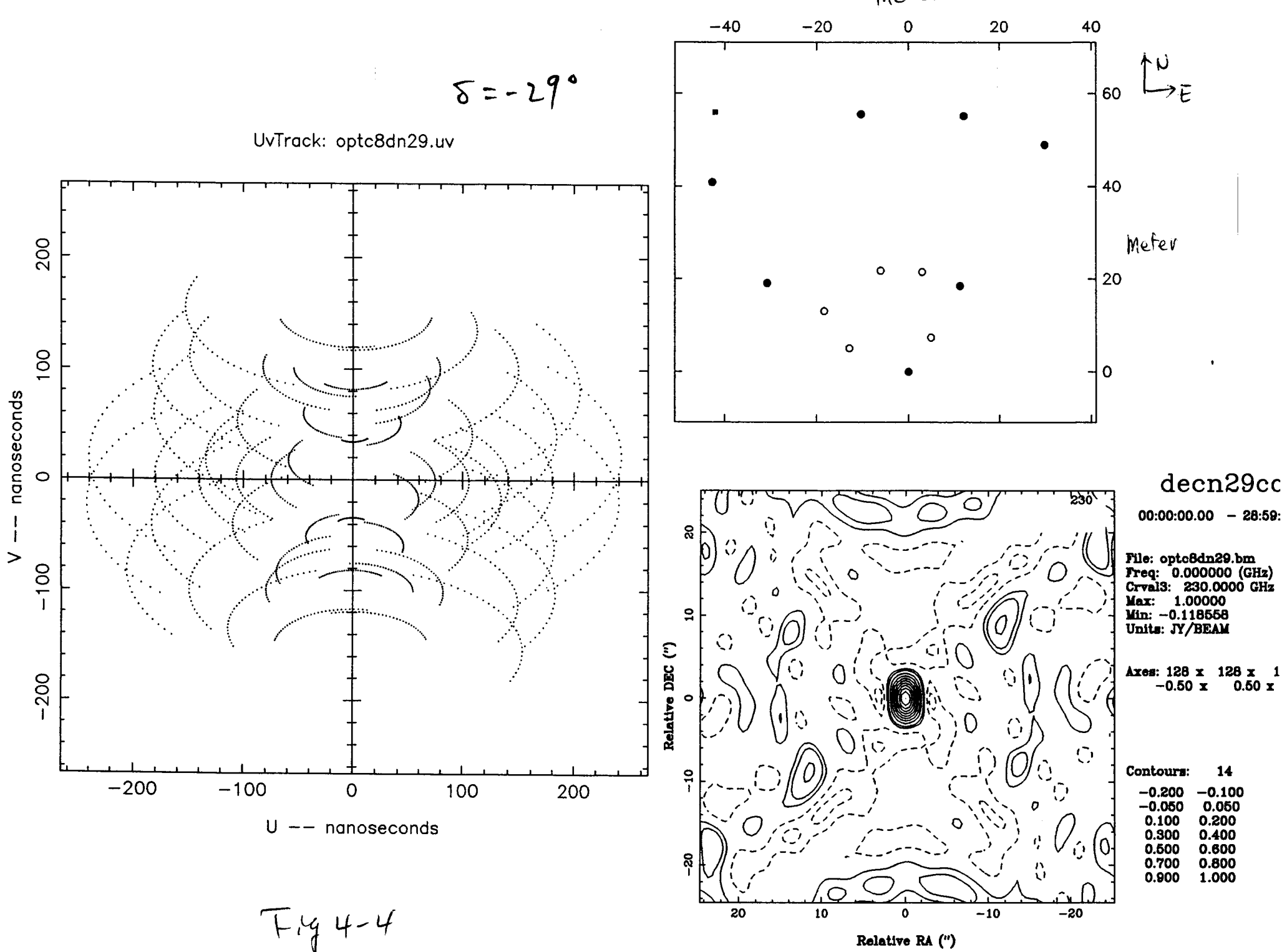


Fig 4-3



↑ N

NESTING OF 2 ADJACENT CONFIGURATIONS

- 2 ANTENNAS SHARED BETWEEN ADJACENT RINGS $\Rightarrow 6$
 $\Rightarrow 18$ TOTAL ($6+4+4+4$) TO FILL OUT 4 CONFIGS
- 2 EXTRA ANTENNAS PER RING, TO ACCOMMODATE SPLIT
 $\Rightarrow 26$ MAX ($8+6+6+6$)

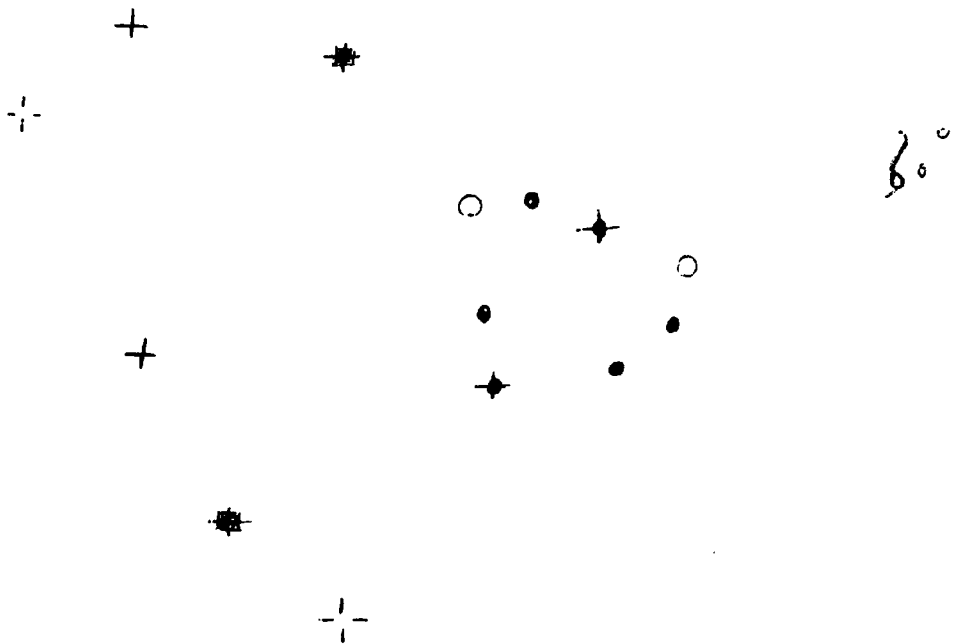


Fig. 5: A layout of tangential configurations suggested by Masson.

- D config basic 6
- D config B option
- + C config basic 6
- + C config B option
- ◆ D,C shared
- ★ C,B shared

$$\delta = 45^\circ$$

UvTrack: tcmc8dp45.uv

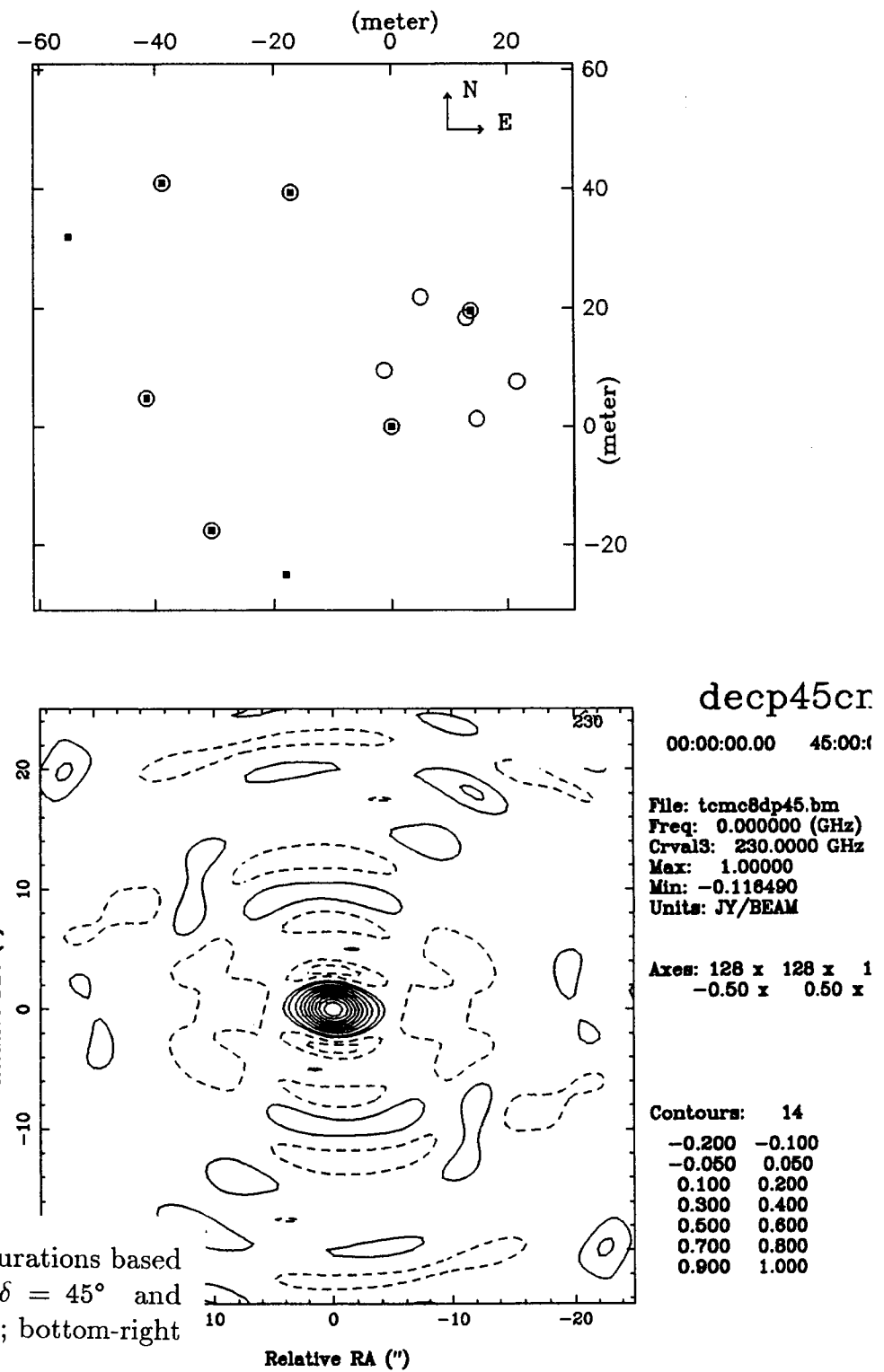
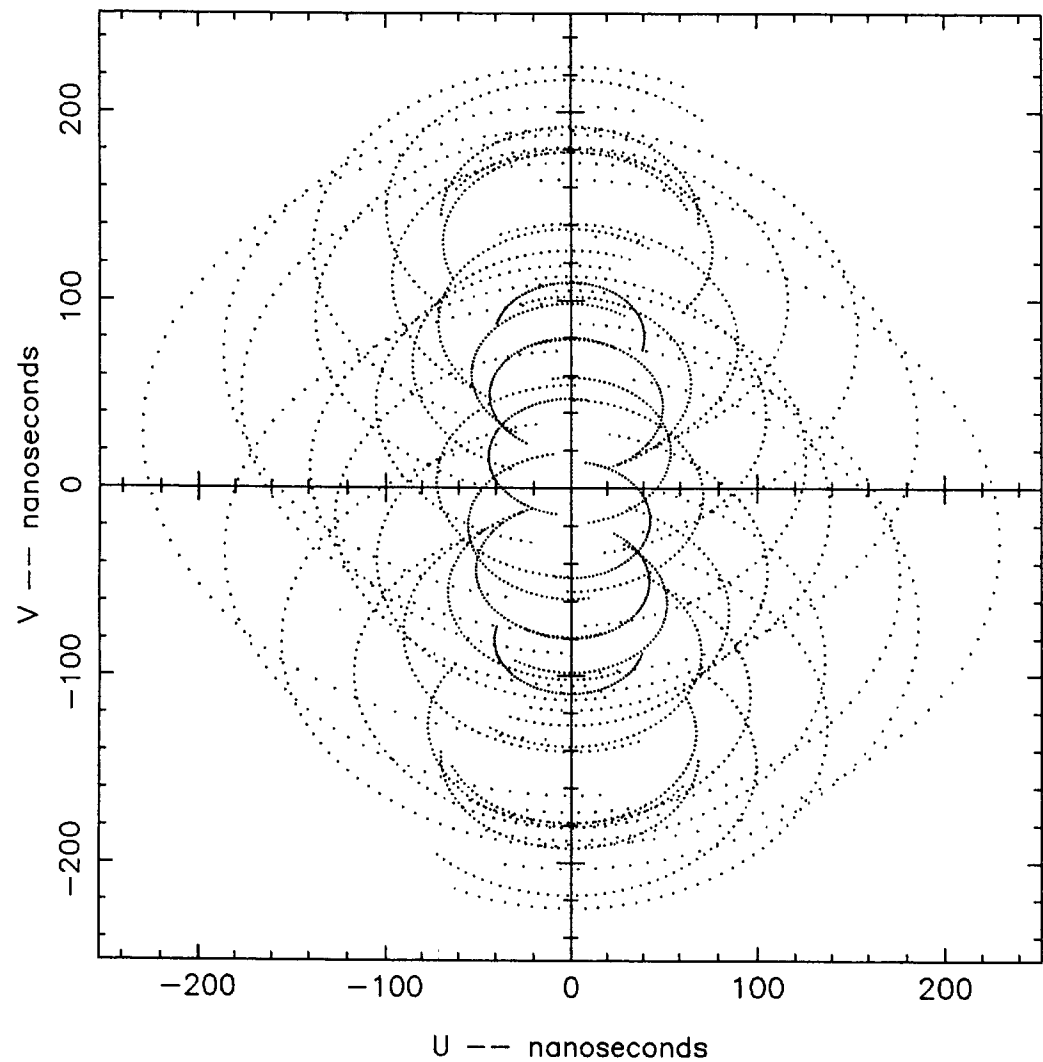


Fig. 6: Simulations of synthesis beams obtained from the D and C configurations based on Masson's design. Calculations are made for the two declinations of $\delta = 45^\circ$ and $\delta = -29^\circ$. Left panel: uv-tracks; top-right panel: layout of configurations; bottom-right panel: contours of synthesis beam.

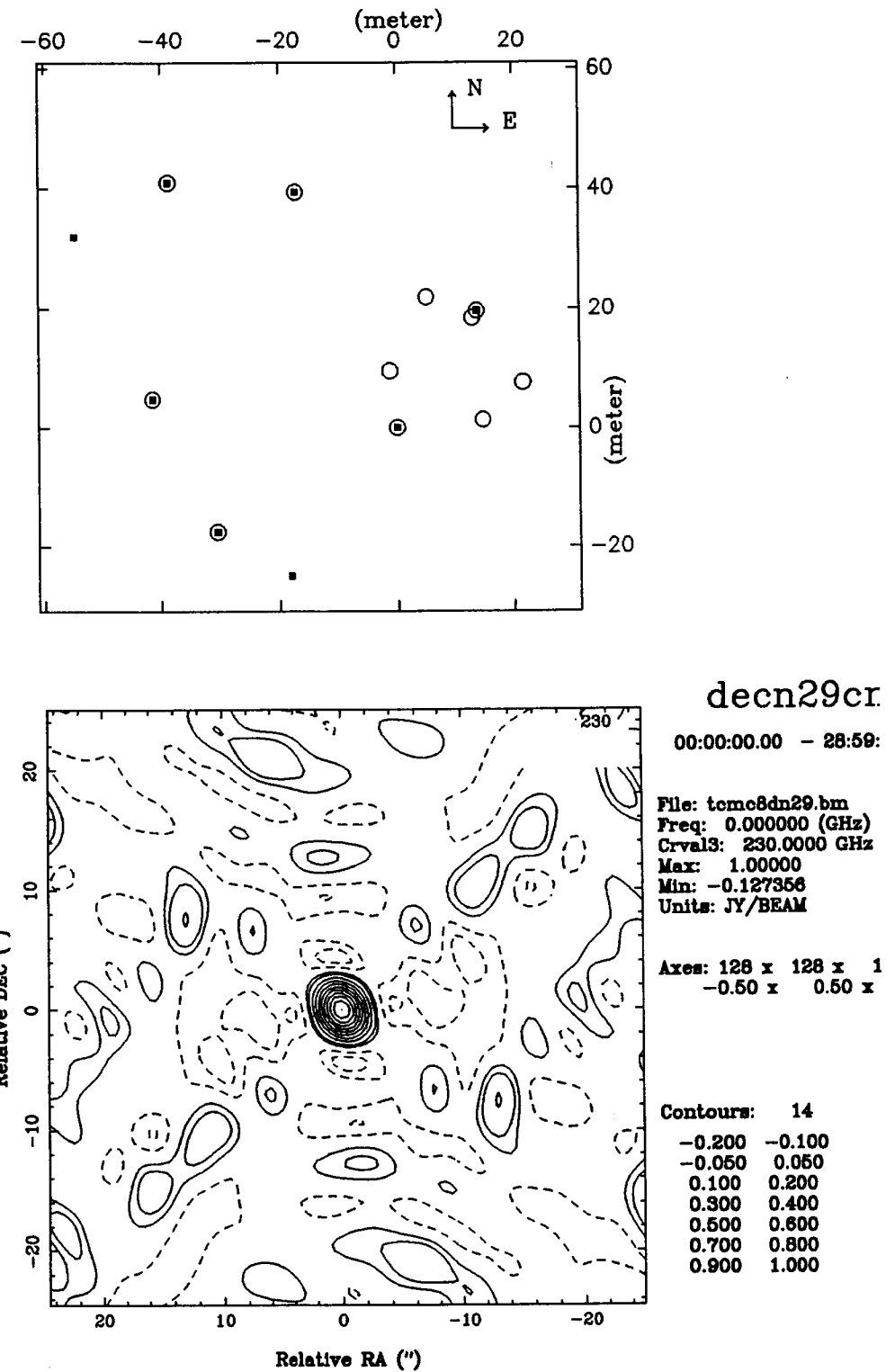
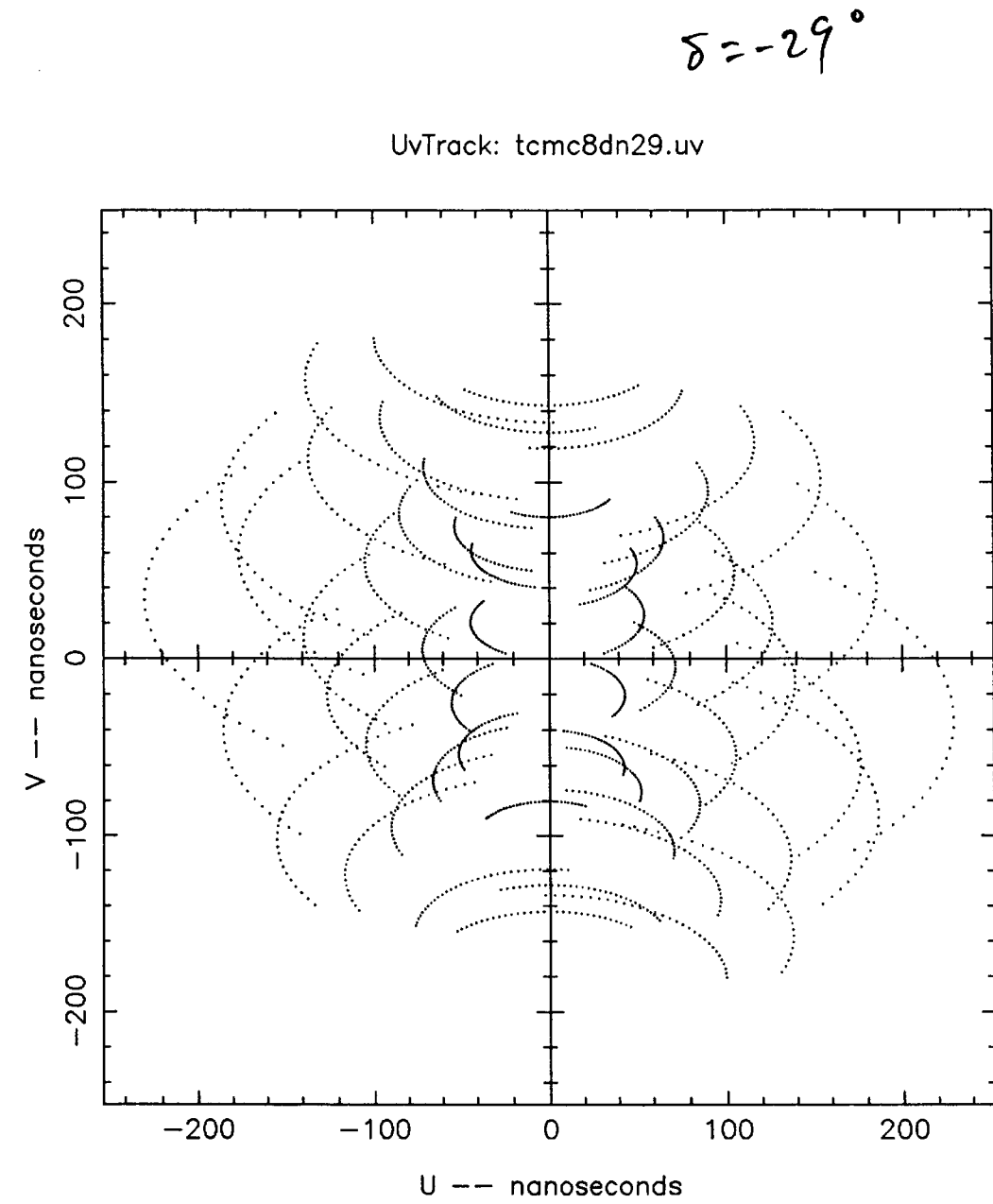


Fig. 6-2

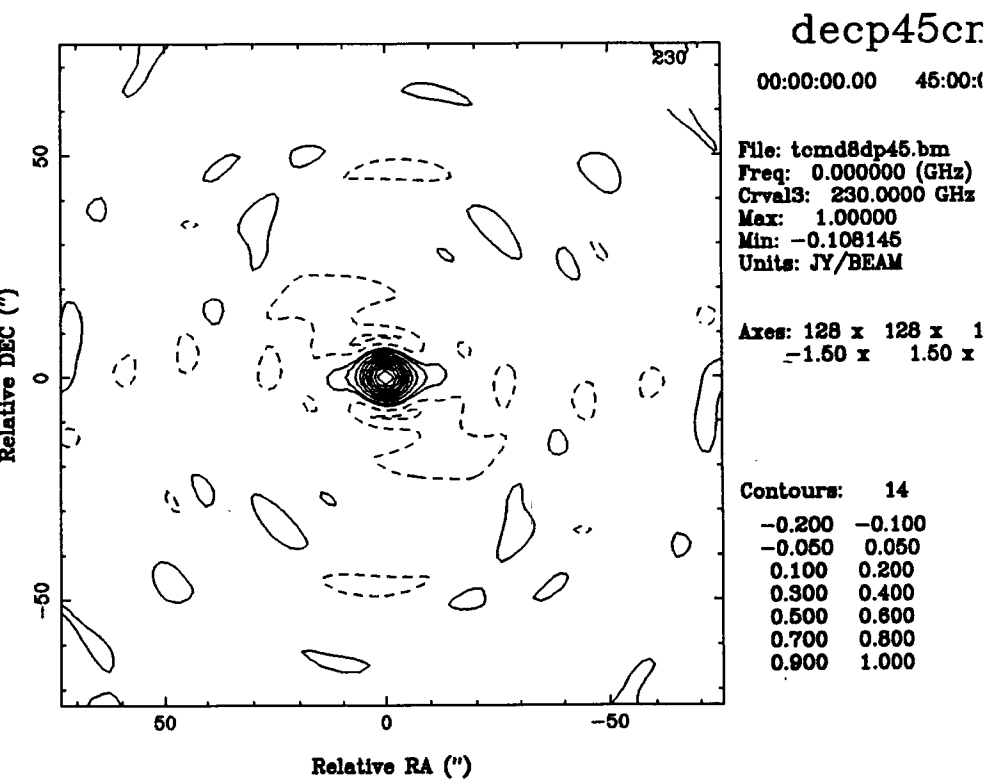
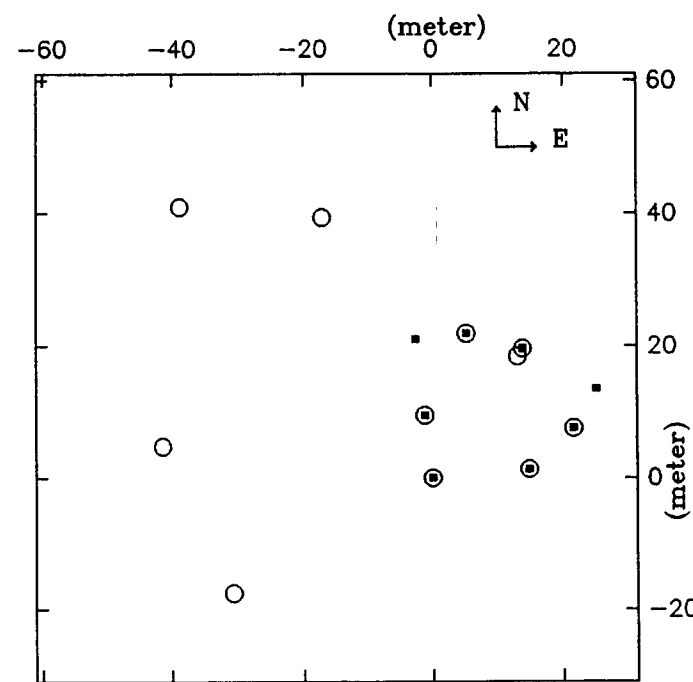
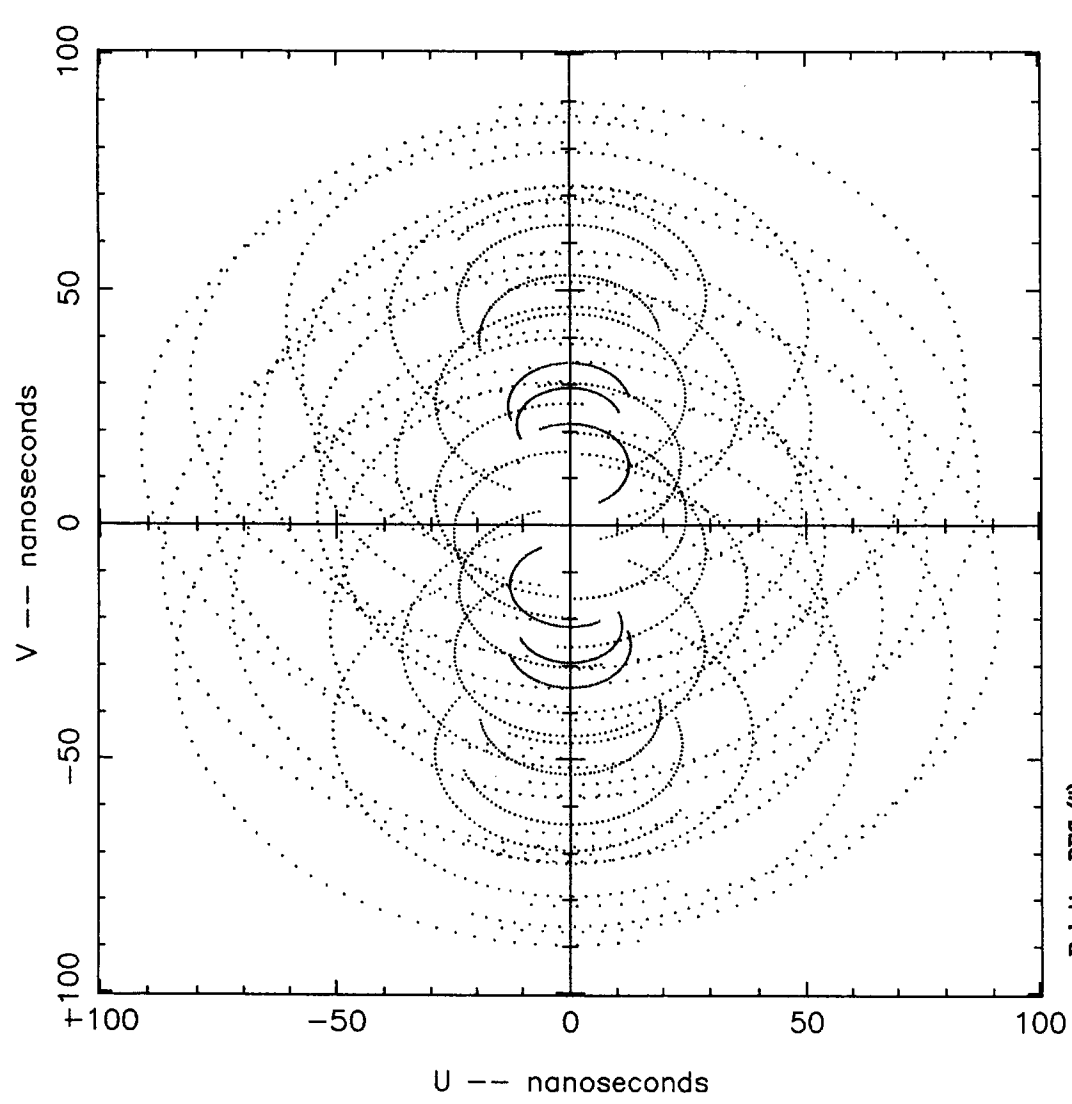


Fig 6-3

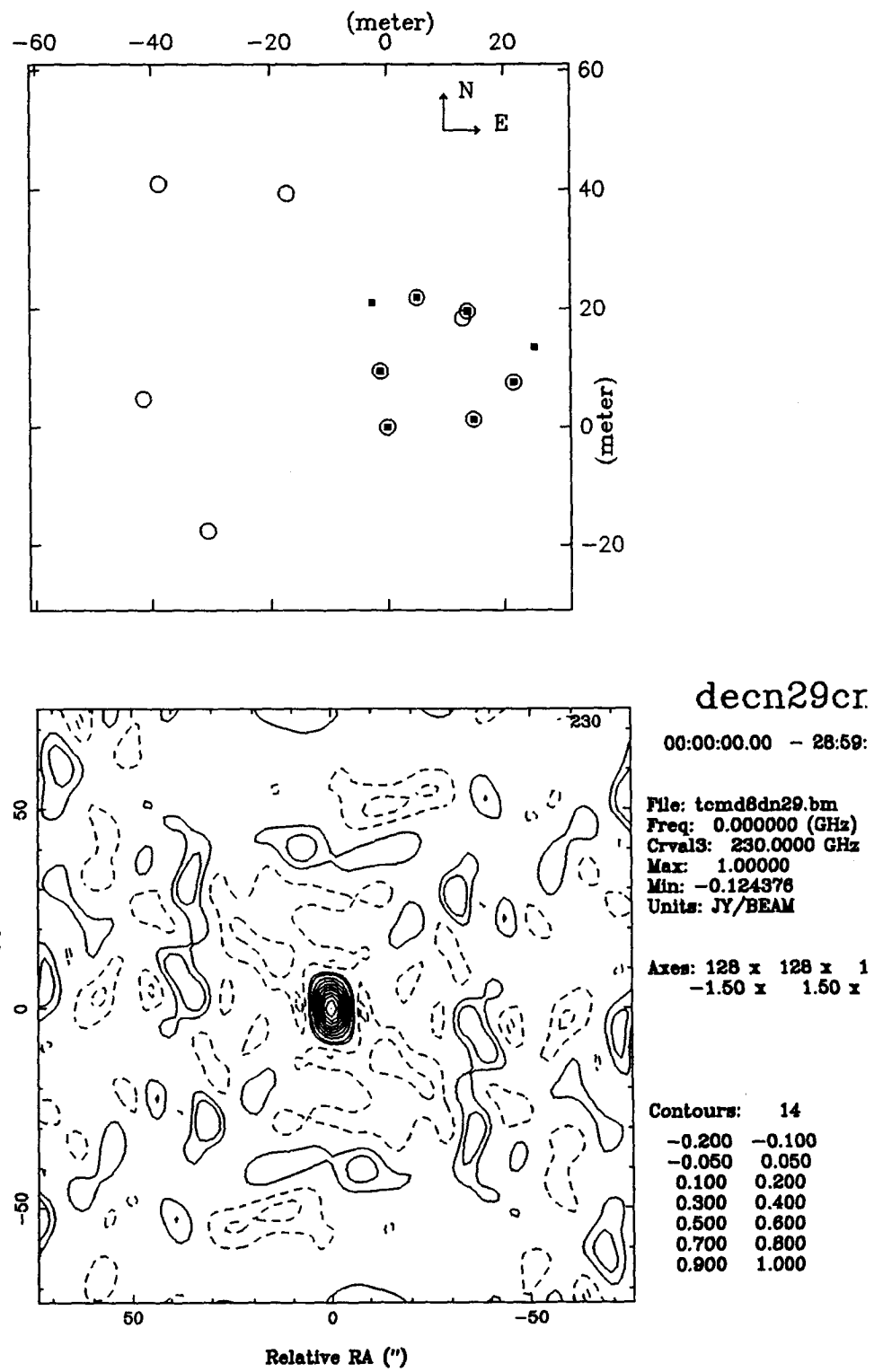
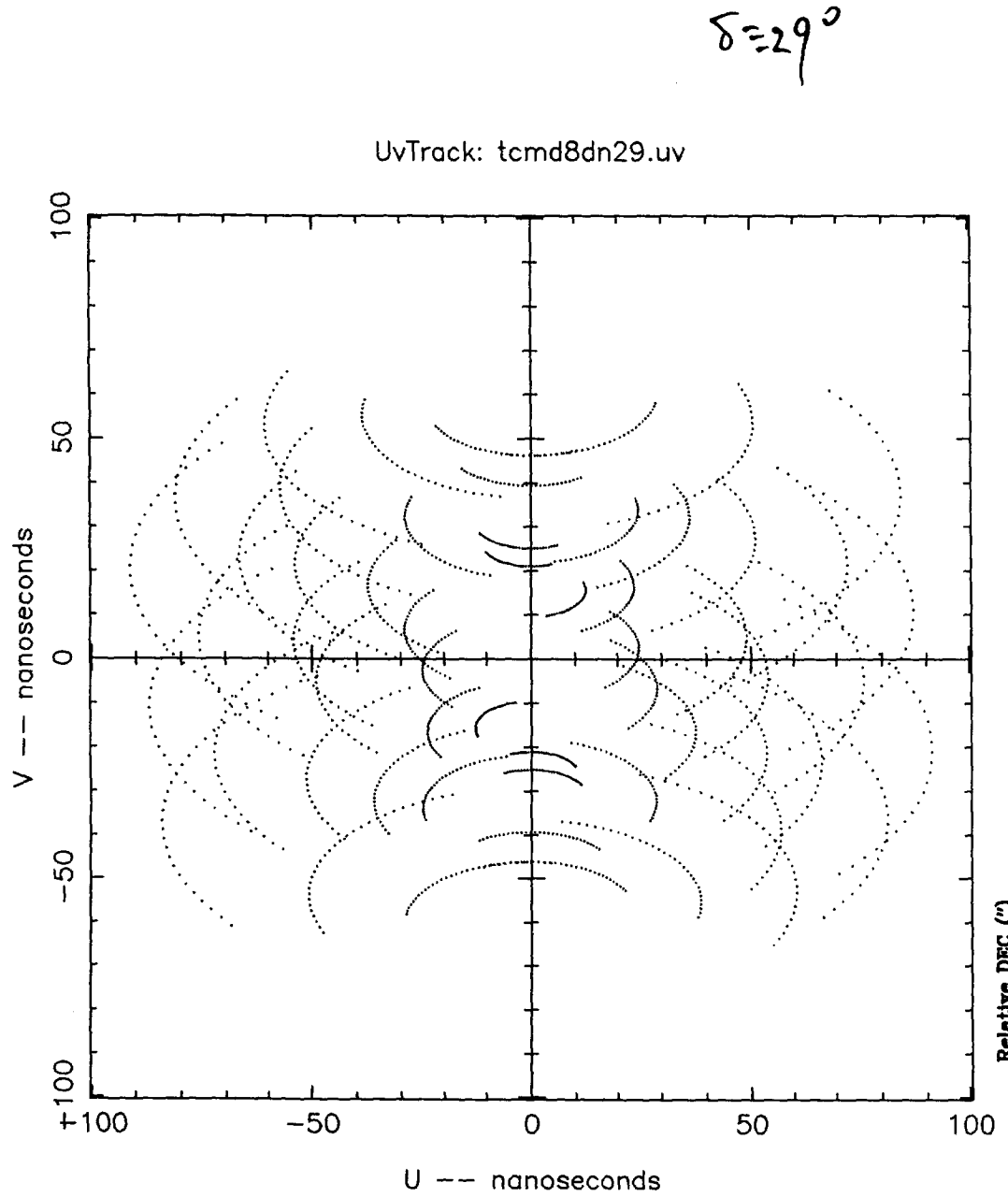


Fig 6-4